Mixed Magnetic Oxides

Dilipkumar V Meshram
Madhav N Rode

Mixed Magnetic Oxides

EMPYREAL PUBLISHING HOUSE

India | UAE | Nigeria | Uzbekistan | Montenegro

Mixed Magnetic Oxides

By:

Dilipkumar V Meshram

Madhav N Rode

First Impression: 2019

Mixed Magnetic Oxides

ISBN : 978-81-944069-6-9

Rs. 650/- ($18)

DISCLAIMER

Information contained in this book has been published by Empyreal Publishing House and has been obtained by the authors from sources believed to be reliable and are correct to the best of their knowledge. The authors are solely responsible for the contents of the articles compiled in this book. Responsibility of authenticity of the work or the concepts / views presented by the authors through this book shall lie with the authors and the publisher has no role or claim or any responsibility in this regards. Errors, if any, are purely unintentional and readers are requested to communicate such error to the authors to avoid discrepancies in future.

Published by:
Empyreal Publishing House

About The Authors

Dr. Dilipkumar V. Meshram is Associate Professor and Head of Department of Physics at Vaidyanath College of Arts, l. and Commerce, Parli-Vaijnath, Dist. Beed, having 28 years of experience in academics and research. He received M.Sc. and Ph.D. in Physics from Dr. Babasaheb Ambedkar Maratwada University, Aurangabad, Maharashtra. He has worked as a Vice-Principal at Vaidyanath College, Parli and also worked on different committees of university as well as UGC. He also awarded with teacher fellowship from UGC. He has published more than 15 research papers in various National and International Journals of high repute and conferences and also working as a Chief Guest Editor of International Journal of Advance and Innovative Research.

Email: dvmeshram1164@gmail.com

Dr. Madhav Namdev Rode is Associate Professor at Vaidyanath College of Arts, Science and Commerce, Parli-Vaijnath, Dist. Beed, with close to 20 years of experience in academics and research. He received M.Sc. and Ph.D. in Physics from Dr. Babasaheb Ambedkar Maratwada University, Aurangabad, Maharashtra State. He has also working as a Member, Board of Studies and Research guide in Physics, Dr. Babasaheb Ambedkar Maratwada University, Aurangabad, and his research is focused on Non-Linear optical crystals, Self frequency doubling crystals, NLO properties of Nano material's and optical biosensors, radiation effects and defects in materials, nuclear technology and radiation protection, low-z materials, polymer materials. Four research students working under his guidance and two students already awarded Ph.D. degree under his supervision. Two minor research projects sanctioned by UGC- New Delhi successfully completed. He has published more than 75 research papers in various National and International Journals of high repute and conferences.

Email: madhavrode1@gmail.com

Preface

The development of the magnetic oxides into useful materials has started by the pioneering work of J.L.Snoek. Mixed magnetic oxides have found increasing applications in successively developing technology specifically for telecommunication and data storage systems. The controllable and combined magnetic and electrical properties made these materials very useful and created research interests to explore the basic parameters which play role to tailor the materials for specific use. Though various technological developments are taking place in fine turning of these materials for specific applications that culminate into advanced technology, systematic attempts are still awaiting to explore the mysteries behind fascinating properties of magnetic oxides having spinel structure with specific stoichiometry and composition.

The book is a small attempt to introduce how to synthesis the mixed magnetic oxides and characterize the material in order to understand the role of property controlling parameters as well as to come across basic approach for tailoring useful material.

The book introduces the basic research approach for material with spinel structure to explore useful properties such as magnetic electrical and thermo electrical properties.

The materials with finely tuned electrical and magnetic properties became need for technological development where more efficient electronic devices, better performing hybrid electrical vehicles smarter data storage devices more efficient communication systems and sensors are being developed. Mixed magnetic oxides with spinel structure can be tailored to achieve fascinating properties. Natural spinel structure ($MgAL_2O_4$) is stable and as there is extremely large variety of oxides which adopt in fulfilling the conditions of overall cation to anions ratio 3/4. Coexistence of ferric and ferrous cation in coordination with other cations combinations can be able to form an extremely wide variety of total solid solutions. It indicates that composition and stoichiometry may strongly modify the properties with maintaining the same crystalline structure.

The book presents studies of two solid solution systems. Ni Al_2O_4 is partly inverse and $NiCr_2O_4$ is completely normal. NI^{2+} cation has a strong octahedral site preference but Nickel ferrite has reported to be 80% inverse. Therefore the systems Ni0.7Mg0.3AlxFe2-xO4, Ni0.7Mg0.3CrxFe2-xO4 are expected to exhibit variation in cation distribution on heat treatment in order to achieve fascinating properties.

Thus the book is intended for introducing the basic things to synthesis and characterization of the solid solutions of mixed magnetic oxides. The book will be useful for beginners and will be helpful to create interest for research in the area of materials development. The authors have tried to emphasize to explore properties that are structure and composition sensitive. The authors are grateful to their guides Dr. N.R.Shamkuwar & Dr. B.H.Pawar. The authors are also thankful to Dr. M.D.Sirsat. Valuable suggestions will be respectively considered for further process.

Dilipkumar V Meshram
Madhav N Rode

Acknowledgements

It is our first and for most privilege to express our deep sense of gratitude to research guides Dr. N.R.Shamkuwar in valuable guidance constant encouragement and motivation for present book. We are also grateful to Dr.M.D. Sirsat, Prof. Dr.Shankar Ambhore, and Prof.Dr. G.G.Muly whose guidance and motivation is always with us. We extend gratitudes to Jawahar Eudcation Society's Chariman Shri. Jugulkishor Lohyia, Secreatory Shri. Dattappa Itake and Deputy Chariman Dr.D.G.Munde for their Cooperation and encouragement. Thanks one due to our Principal Dr. R.K.Ipper for being very much helpful. We thank whole hearted the Librarian S.A. Dhande who always extend his cooperationa

Finally our acknowledgment would be incomplete if we fail to offer our heartiest gratitude to our family members Namdev Rode, Indubai N. Rode, Sadhana Meshram, Sanjay Rode, Avlokit, Sukeshini, and Kalyani for bearing home responsiblites and who patiently helped in the process of writing this book.

Lastly the auther extend their thanks to their teachers, colleagues, scientist for their valuable help. Finally thank are due to the publisher Dr. Akhter Alam and Empyreal Publication House for their support to print and publish this book in very short period of time.

Dilipkumar V Meshram
Madhav N Rode

Table of Contents

CHAPTER - 1

INTRODUCTION TO MIXED MAGNETIC OXIDES

1.1 INTODUCTION

The important innovations in the field of magnetic oxides took place after Second World War. The development of the magnetic oxides into useful materials has started by the pioneering work of late J.L. Snoek [1]. Since last five decades magnetic oxides have found increasing application in exacting technological requirements due to their controllable and combined magnetic and electrical properties [2].

Mixed magnetic oxides with spinel structure have wide technological applications. These are also known as ferrites if they have $M^{2+}Fe_2^{3}+0_4^{2-}$ composition where M^{2+} is divalent metal ion. These materials are most relevant. The wide usefulness of these materials fascinated the scientists, physicists and engineers to study their basic properties in order to know the controllable parameters to design the suitable material for desired applications [3]. The new findings with above approach may reveal the reality of controlling parameters and can lead to a break through in the ferrite technology, which may be the most useful development. Thus mixed magnetic materials have been gaining importance in recent times especially incontext of devices which can provide necessary infrastructure and flexibility for various human endeavors.Though various technological developments are taking place in fine-tuning of these materials for specific applications that culminate into advanced technology, systematic attempts are still waiting to explore themysteries behind fascinating properties of mixed magnetic oxides.

1.2 Phenomenon of Magnetism:

Magnetism was observed as early as 800 B. C. in a naturally occurring material called load stone (Fe_3O_4). According to the modern theories, the magnetism in material arises due to orbital and spins motion of electrons as well as spin of nucleus. The electron revolving around a nucleus possesses angular momentum and intrinsic spin. An atom has a specific electronic configuration obeying certain principles such as Pauli's exclusion principle and Hund's rule. The coupling of angular momenta and spins through interactions gives rise to magnetic moment. A number of such magnetic moments may align themselves in different directions to generate a net non-zeromagnetic moment. The atoms having completely filled shells have nonet magnetic moment. However, the atoms having partly filled shells have permanent magnetic moment. The nuclear spin contribution isnegligible to magnetizationin case of polycrystalline solids theorbital magnetic momentum is quenched by crystal field. Thus the Nature of magnetization produced depends on the number of unpaired valence electrons present in the atoms of the solid and on the relative orientations of the neighboring magnetic moment.

1.3 Types of magnetic material:

The magnetic materials are classified according to the magnetism present in the material. Magnetism in materials has been classified into five categories.

(1) Diamagnetism

(2) Paramagnetism.

(3) Ferromagnetism.

(4) Antiferromagnetism.

(5) Ferrimagnetism.

When a solid is placed in a magnetic field, it was magnetized. The magnetic moment per unit volume developed insidea solid is called magnetization and is denoted by M. Theimportant parameter called magnetic susceptibility which is a measure of the quality of the magnetic material, is defined as themagnetization produced per unit applied magnetic field.

$$\chi = M/H \quad \ldots\ldots\ldots\ldots\ldots\ldots\ldots\ldots\ldots\ldots..(1.1)$$

where H is the strength of the applied magnetic field (Also referred toas the magnetic field intensity). For isotropic media, M and H pointin the same direction and χ is a scalar quantity. The magnetic fluxdensity B produced inside the medium as a consequence of the applied field H is given by

$$B = \mu_0 (H+M) \quad \ldots\ldots\ldots\ldots\ldots\ldots\ldots\ldots...(1.2)$$

where, μ_0 is the permeability of the free space or vacuum and is equal to $4\pi\times10^{-7}$Hm. B can be expressed in terms of χ as,

$$B = \mu_0(1+\chi)H \text{……..(1.3)}$$

Thus M and χ decide the type of magnetic material.

(1) Diamagnetic material

The material for which χ is negative (that is M is in opposite to H) is known as diamagnetic material. If it is placed in amagnetic field it shows very weak magnetizing effect. The atoms of such material do not contain any permanent magnetic moments. The existence of small magnetic moment in this material is attributed to change in angular frequency of the orbital motion of electrons in magnetizing field (Larmor precession). This magnetic moment is always directed opposite to the applied magnetic field. The atoms of such material have completely filled shells (e. g. MgO)

(2) Paramagnetic material

The material for which χ is positive (i.e. Mis parallel to H) is known as paramagnetic material. The atoms of such material have partly filled shells. They have a permanent atomic magnetic moment.If such a material is subjected to magnetic field, it shows weak magnetic effect but unlike to that of diamagnetic material. The magnetic moment in this case is aligned in the direction of the magnetizing field

(e g. Gd_2O_3)

(3) Ferromagnetic materials

The magnetic susceptibility of ferromagnetic material may be very large ($10^5/cm^3$). If this type of material is subjected to a magnetic field it shows a very strong effect which arises when the adjacent magnetic moments align themselves in the same direction

(e.g. EuO).

(4) Antiferromagnetic material

The atoms of such material have the adjacent magnetic moments, which are equal and opposite to each other resulting incomplete cancellation of magnetic moments. (e. g. Cr_2O_3)

(5) Ferrimagnetic material

These materials are similar to anti-ferromagnetic one sexcept that the adjacent magnetic moments are unequal in magnitude and hence complete cancellation of moments does not take place

(e. g. Fe_3O_4.).

1.4 Forrimagnetism

The word 'ferrimagnetism' was coined by L. Neel [5] to describe the properties of those substances, which below a certain temperature exhibit spontaneous magnetization arising from a non-parallel alignment of atomic magnetic moments. Neel envisaged a partitioning of the moments into two sub lattices, which are alignedanti-parallel to each other because of their mutual interaction and produce a total magnetic moment equal to the difference between their individual magnitudes. This difference can arise in sever always. Ferrimagnetism is identical to anti-ferromagnetism except that the magnetizations of the two sub-lattices have different magnitudes, which result in a non-zero value of net magnetization. This type of magnetism occurs in materials such as ferrites, which are basicallythe oxides of various metal elements. The most common example is magnetite or ferrous ferrite. (Fe_3O_4). The ferrites crystallize into face centered cubic spinel structure. The spinel structure is similar tothe structure of the compound $MgA1_2O_4$. The ferromagnetic substances, often referred to as ferrites, are ionic oxide crystals whose chemical composition is of the form $Me^{2+}{}_1Fe_2{}^{3+}O_4{}^{2-}$, where Me^{2+} signifies a divalent metal ion. There are two sub-lattice sites which metal ion can occupy. In one site the metal ion is tetrahedrally coordinated to four oxygen anions and is known as tetrahedral or A-site. In another site the metal ion is octahedrally coordinated by six oxygen anions and is known as octahedral or B-site. The metal ions in the composition are distributed between these two sites as per their site preference energy and thermal history. The metal ions present at A-site and B-site constitute A and B sub-lattices respectively andhave opposite types of magnetization. The net magnetization of a unit formula of the composition is the difference of magnetization of A-site and B-site. Neel attributed the anti-

parallel arrangement of spins of A-site and that of B-site to the negative AB-interaction. Besidesthis, there exist the AA and BB interactions, which are much weaker than AB interaction. The behavior of ferrimagnetic material is primarily the function of the structure of the crystal i.e. inter-atomic distance and arrangement of cations as well as type of cations that determines the particular kind of magnetic interaction predominant.

The interesting and useful electrical and magnetic properties of the spinel ferrites are governed by the distribution of the iron and thedivalent metal ions among the octahedral and tetrahedral sites of thespinel lattice. A whole range of possible distribution is observed andthis can be represented in a general form by

$Me_{\delta}^{2+}\ Fe^{3+}_{1-\delta}\ [Me^{2+}_{1-\delta}\ Fe^{3+}_{1-\delta}]\ O_4^{2-}$ where the ions inside the brackets are located in octahedral sites and the ions outside the brackets are in tetrahedral sites. The limiting case, when $\delta=1$ is called normal spinel and the other limiting case, when $\delta=0$ is called inverse spinel. For a random distribution $\delta = 1/3$.

1.5 Development of ferrites

The first magnetic material known to human being is magnetite (Fe_3O_4), the ferrous ferrite. Hilpert [6] prepared the first ferrite (magnetite) in 1909 He carried out chemical synthesis of some ferrites but they had very poor magnetic moments and werenot useful as the magnetic components. After wards Hilpert, Kato,Takei [7] and Forestier [8] studied ferrites from electromagnetic,chemical and crystallographic point of view. Prof. Takie and Prof.Kato pioneered the first ferrite with promising magnetic and electricproperties. Their work was disrupted by the second world war butfortunately Dr. J. L. Snoek and his coworkers in Philips laboratory in Holland started investigation for magnetic properties of ferrites and they produced several ferrites with considerable magnetic properties, high electrical resistivity and low hysteresis loss. Thus Snoek'sferrites had considerable commercial values and this provided agreat stimulus to experimental and theoretical work.

The crystal structure of mineral $Mg^{2+}\ Al^{3+}O_4^{2-}$ was first determined by Bragg [9] and Nishikawa [10] and found to be face centered cubic with larger unit cell. The structure of ferrite was proved to be spinel similar to that of $Mg^{2+}\ Al_2^{3+}\ O_4^{2-}$. X-ray analysis of ferrite was carried out by Barth and Posnjak [11] in 1932.According to them it is necessary to assume that the divalent metal ion interchanges position in crystal structure. Thus they discovered inverted spinelstructure. L. Neel proposed fundamentals of thetheory of ferrimagnetism in 1948, which give insight to understand the properties of ferrites. Later on J. Smith , H.P.J. Wijn [12], K. J.Standley, and E.C. Snelling [13] expounded ferrites in details. W.Gorter [14], G. Blasse and other[15] have discovered the importance of mixed ferrites. Verwey et al [16] studied the electrical conductivity of ferrites and reported that the conductivity in ferritesis due to hopping mechanism. They proposed that the resistivity rises when ferrous ions are replaced by other metal ions in the lattice.

Yafet-Kittel [17] extended Neel's theory of magnetic sub-lattices in ferrites by postulating canted arrangement of magnetic moment of sub-lattices. When intra and inter interactions are comparable to one another due to substitution of a suitable cation which dilutes the A-B interaction then the spins of the A-Sub-lattice and that of B-sub-lattice are no longer collinear. There are two sub-lattices particularly at B-site depending upon the local magnetic environment and the magnetic moments of these two are canted. Koops [18] proposed a model to explain the dielectric dispersion in ferrites.

The observed Curie temperature from magnetization and cation distribution were connected by the formula suggested by Gellio [19] and Smart [20]. Gorter worked independently and correlated the cation distributions found by microwave resonance and magnetization. Philips Company in 1954 announced some ferrites as permanent magnetic materials. In 1954 E. Albers Schoenberg [21] in United States reported the application of ferrites or microwave devices as well as memory devices in computer. In 1989 Roes [22] proposed that a material of good compromise of high permeability, saturation magnetization and high curie temperature can be prepared substituting the cations such as Ti^{4+} and Sn^{4+}. Berger [23] found that discontinuous variations on a micro-scale resulted in high power losses. Thereafter people concentrate on reducing hysteresis losses. Ochiai [24] and Sano [25] suggested the uniform microstructure, fine grain size and high density are essential for low hysteresis loss. Due t these needs different methods of preparations came into use. Sano attempted to increase the density of material by hot pressing. Later on many methods such as coprecipitation and sole gel citrate precursor have been used. Leroux [26] suggested that the valence changes and cation

Vacancies are created in the spinel phase Fe_2O_3 precipitated due to oxidation reaction during the heat portion of the sintering step. The sintering in oxygen rich environment is found to enhance the properties. Thus the ferrites have been developed studied and are still subjected to unlimited advancement.

1.6 Applications of mixed magnetic oxides

Mixed magnetic oxides (which are also known as ferrites) have novel combined electronic and magnetic properties. The most important things about them are their high resistivity (from 10^{-3} Ωcm[e.g. $Fe^{2+}Fe_2^{3+}O_4^{2-}$] to 10^{11}Ωcm ([e.g.singlecrystal YIG.]) wide usefulrange of magnetization, permeability and coercivity.These the most useful materials in science and properties made them technology. The properties like permeability and magnetic loss factor of material are of prime importance. In development of materials one aims at the best compromise between a high permeability and a low loss level. This can be achieved by suitable chemical composition, method of preparation and processing techniques. Thus the materials of a vast range of promising properties have been developed and ferrites have become very usefulin every walk of life in the modern world. Ferrites are widely used ascore materials in transformers and in antenna of radio receiver's as well as transmitters. They are used in ultrasonic generators modulators, phase-shifters and, isolators [27]. Some ferrites exhibit aloop property. This rectangulartypical rectangular hysteresis hysteresis property and suitable coercivity are important factors touse ferrites in memory [28] and recording devices for digitalinformation [29]. Ferrites with small coercive force are used in magnetic amplifiers. Some hard ferrites are used in sound systems and in micromotors.

Ferrites with sharp and definite curie temperatures are used as sensors of temperature controls. The position and rotational angle sensors have also been designed using ferrites. Radio waves absorbing paint containing ferrites has been developed to render an aircraft or submarine invisible to radar. The precipitation of ferriteprecurs is used to scavenge pollutant materials such as mercury from waste streams. Pollutants can be magnetically separated. Thus ferrites play important role in controlling pollution. The ferrites have been used as electrodes due to their high corrosion resistance and the appropriate conductivity. Ferrites are widely used in radio and television circuits. The largest consumption of soft ferrtes is intele vision where half a kilogram is used for each set in the form of deflector, and yoke. High frequency applications of soft ferritesinclude a large number of microwave components such as circulators, isolators, gyrators, phase shifters, YIG tuned filters, and switches and substrates for microwave integrated circuits. Some ferrites are used in switch mode power supplies. Thus ferrites have covered a vast area of applications.

1.7 Review of literature and aim of the present investigation

Initially polycrystalline pure ferrites have been studied toknow the controlling parameters behind basic properties. It is foundthat controllable properties of ferrites provide a wide scope of their technical applications. By suitable mixture of metal cations, ferrites with virtually any specific properties can be prepared. Such mixed magnetic oxides are known as mixed ferrites. Many investigators like E. W. Gorter and G. Blass had discovered the importance of mixed ferrites. The magnetic and electrical properties of such mixed ferrites depend upon method of preparation, atomic number and valence of metallic cation, stoichiometry of composition and sintering process (Sintering process includes rate of increase ofsintering temperature, sintering temperature, rate of cooling after sintering for a certain duration and sintering duration).

The nickel ferrite ($NiFe_2O_4$) is an inverse spinel having acollinear ferrimagnetic order [30]. The addition of trivalent ion like$Al^{3+}$and Cr^{3+} for Fe^{3+} in $NiFe_2O_4$ influences the electrical and magnetic properties of the system (31-37). The investigations doneby various workers have shown that the micro-structure (38-40), electric [41-43], dielectric (44) and magnetic (45-48) properties ofthe basic nickel ferrite are greatly influenced when Ni^{2+}ions or Fe^{3+}ions are partially or completely replaced by tetravalent ions The most effective means to control saturation magnetization of nickel ferrite is through making substitution for trivalent iron. $NiAl_2O_4$ is a partially inverse spinel in which the ratio of Al^{3+} in the tetrahedraland octahedral site is about 2:3. $NiCr_2O_4$ is a normal spinel with acanted ferrimagnetic order at octahedral site [49].

The spinel structure seems to be particularly attractive as it allows a variety of magnetic orders from collinear to frustration. This is due to the fact that in spinels intra-sub-lattice interactions are weaker than the inter-sub-lattice interactions and as a result there areunsatisfied bonds in the ferrimagnetic phase. Because of the unsatisfied bonds increasing magnetic interactions accentuate the competition between the various

exchange interactions resulting in a variety of magnetic structure [50]. The negative super-exchangeinteraction exists in ferrites. The strength of the exchange interactionis specified by exchange integral [51]. The exchange integrals ofintra-sublattice interactions and inter-sublattice interactions follow the order $J_{AB}>J_{BB}>J_{AA}$ in collinear ferrimagnetic order. Thus the antiferromagnetic A-B super-exchange interaction is the main cause ofthe cooperative behaviour in ferrites [52]. The magnetic orders can be controlled by cation substitution [53). It is found that change in J_{BB}/ J_{AB} and M_A/M_B ratios modify the magnetic properties. This in spires to study the properties of ferrites with the substitutions of nonmagnetic and magnetic cations, K. Seshen et al [54] havereported the effect of cation distribution on the properties of some magnesium-nickel ferrites in which the migration rate of Mg^{2+} on tetrahedral site depends upon the cooling rate of heat treatment due tohigh diffusibility.

The substitution of non-magnetic and magnetic cations with different valences on tetrahedral and octahedral sites has been a subject of many researchers in order to get particular propertiesresulting from cation distribution in crystal lattice. The survey ofliterature shows that nickel ferrite is an inverse ferrite structure having collinear ferrimagnetic order where degree of inversion depends upon the rate of heat treatment in preparation. Pure nickel ferrite is characterized by excessive losses. Therefore severalhave proposed the substitutions of othercations. Aswith other ferrites, the most effective means to control saturation magnetization of nickel ferrite is through making substitution fortrivalent iron. Ni $Al_2 O_4$ is partly inverse, Ni Cr_2O_4 is completely normal. Ni $^{2+}$ cation has a strong octahedral site preference but nickeferrite has been reported to be 80% inverse. Thus the systemNi_{1-x} Mg x Fe $_2$ $O_4$is expected to show variation in cation distribution on heat treatment and there by the magnetization can bemodified. Keeping nickel and magnesium in specific ratio for which the magnetization will be maximum. The substitution of Alf as wellas the substitution of Cr^{3+} may enhance basic properties of yielded mixed nickel ferrites.

In reported works to our knowledge, there is no mention of the studies of basic properties of the mixed magnetic oxides of solid solutions like $Ni_{0.7}$ $Mg_{0.3}$ Al_x Fe_{2-x} O_4 and $Ni_{0.7}$ $Mg_{0.3}$ Cr_x $Fe_{2-x}O_4$.

Therefore the studies of the basic properties of these mixedmagnetic oxides with a view to study the effect of substitution of nonmagnetic and magnetic trivalent catins on the structural, electric and the magnetic properties have been undertaken for the present investigation.

REFERENCES

1. J.L. Snoek, Physica, 3 (1936) 463.
2. K. J. Standley,Oxide Magnetic MaterialClarendon press Oxford (1962)
3. Alex Goldman, Modern Ferrite Technology, VanNostrand Reinhold, New York (1990)
4. Kittle C. Phys. Rev. 70(1956) 965
5. L. Neel, Annales de Physique 39(1948)137.
6. S. Hilpert Ber. Deut. Cheem. 42(1909 2247.
7. Y. Kato and T. J. TakeiInst. Of Elect. .Engg. Japan 53 (1953) 408.
8. H. ForestierAnnales Chimie Xe series Tome 9 (1928)353.
9. W. H. Bragg Phil. Mag. 30 (1915) 305.
10. S. Nishikawa , Proc. Math. Soc. Tokyo, 8 (1915) 199.
11. Barth T. F. and Posnjak.E. Z. Krist, 82 (1932)325
12. Smith J. and Wijn H.P.J. Ferrites,John and Wiley and Sons New York (1959)
13. E. C. Snelling.Soft ferrite properties and application,liiffe, London (1969)
14. E. W. Gorter Nature 173 (1954) 123.
15. G. Blasse, Phillips Res. Rept. Suppl. Nn. 3 (1964).
16. Verwey E. J. W.F. de Boer, Van Santen,J. Chem. Phys., 16 (19480 109.

17. Yafet Y. and Kittle C. Phy. Rev. 78(1950)266.
18. Koops C. G. Phys. Rev. 83 (1951) 121.
19. M. A. Gellio, J. Chem. Phys. 24(1956) 306.
20. J. S. Smart Phy, Rev. 94 (1954) 847
21. Albers Schoenerg E.,J. Appl. Phys. 25 (1954) 152.
22. Roes E. Ferrites, Tokyo University Tokyo Press.(1971)
23. M. H. Berger et al . Advances in ferrites Vol.1New Delhi (India) Oxford &IBH Publishing Co.(1989) 619
24. T. Ochiai Advances in Ceramics 16, (1985) 447.
25. A. Sano, A. Morita, A. Matsukawa 1988b.Proc. HFPC., San Diego. Clif., May 1-5 (1989),
26. D. Leroux, P. Onno and P. Perriat,Advances in ferrites Vol. 195(1989)
27. R. F. Soohoo, Microwave magnetics,Harper & Row Publishers New York(1985).
28. R. S. Weiss, Phys. Rev. 96 (1954) 800.
29. I.Stein, J. Appl. Phys. , 34,7,1976 (1963).
30. J. M. Daniel A. Rosenwaig, Can. J. Phys.,48(1970) 381
31. T. Tsushima J. Phys. Soc. Japan 18(1963)1162.
32. J. J. Bara, A.T. Pedziwiatr, Z. M. Standnik,A. Szytwa, J. Todorovic, Z. Tomokowe,W. Zarek, Phys. Stat.sol. A44(1977) 325
33. L. R. Maxwell, S.J. Pickart Phys. Rev. 92 (1953) 1120
34. A. Hauet ,J. Teillet, B. Hannoyer,M. Lenglet,Phys. StatSol.A103 (1987)1257.
35. J. Chappert , R. B. Frankel,Phys. Rev. Lett.19(1967)570.
36. V. I. Nikoloev et al, Sov.,Phy. Solid State 13 (1971)317
37. V. I. Nikoloev et al,Sov.,Phy. Solid State 14 (1972)521
38. J. S. Baijal ,D.Kothari, S. Phanjaubn,Solid State. Commun. 69 (1989)277
39. D. C. Khan,M. Misra, A. R. Das, J. Appl. Phys. 5 (1982) 2722
40. B. V. Bhise, M. B. Dongare, S. A. Patil, S. R. Sawant,J. Mater. Sci. Lett. 10 (1991) 922.
41. B. L. Patil S. R. Sawant, S. A. Patil, R. N. Patil,J. Mater. Sci. 29 (1994)175.
42. M. G. Patil. V. C. Mahajan, S. D. Latke,B. V. Bhise& S. A. Patil,Solid State. Commun. 91 (1994)667.
43. C. Prakash, J. S. Baijal, P. Kishan,J. Less.Common.Met. 106 (1985)257.
44. C. Prakash, J. S. Baijal, P. Kishan,J. Less.Common.Met. 107 (1985)51
45. S. Unnikrishnan, D. K. Choudhary,Phys. State. Sol.(a) 121 (1990)265
46. H. N. Padys.R. G. Kulkarni,Solid State. Commun. 61 (1987)645.
47. C. Prakash, J. Mater. Sci. Lett. 6(1987)504
48. A. R. Das, V. S. Anathan, D. C. KhanJ. Appl. Phys. 57 (1985) 4181.
49. T. A. Kaplan ,K. Dwight. D. Lyons &N. Menuyk, J. Appl. Phys. 32(1961)135
50. N. N.Jani, B. S. Trivedi, H. H. Joshi, G. K. Bichile &
51. R. G. Kulkarni, Bull.Mater. Sci. Vol.21, No.3, June (1998) 233-239.

52. E.W. Gorter Proc.I. R. E. 43 (1955)1945.
53. P.W. Anderson, Phys. Rev. 79(350)350.
54. Y. Yfet &C. Kittel.,Phys. Rev. 87(1952)290.
55. K. Seshan, A. L. Shashimohan, D. K.Chakrabarty,&A.B. Biswas, Phys. State. Sol.(968,(1981)97-101

CHAPTER-2

THE SPINEL STRUCTURE AND FERRIMAGNETISM

2.1 Introduction

Although a magnetic domain is important in explaining cooperative magnetic phenomenon, the next larger physical magnetic entity after the magnetic ion, is the ferrite unit cell, which interestingly exhibits a variety of magnetic order [1]. The crystal structure of a ferrite can be regarded as an interlocking network of cations and anions. The cations may be either belonging to transition metal group or to rare earth group. For anions oxygen is preferred due to the large electro-negativity which prevails the ionic type of bonds in almost all oxide spinels and helps to acquire high resistivity [2]. The arrangement of the ions in the crystal structure of the ferrite plays an important role in determining the magnetic interaction [3].

2.2 Crystal structure of spinel ferrite

The spinel ferrites have the general chemical formula $Me^{2}Fe_{2}{}^{3}O_{4}$ where Me^{2} is divalent metal ion. In case of mixed ferrites a suitable combination of cations that fulfills electro neutrality requirement can be used instead of divalent andtrivalent cations. The spinel structure is called after the mineral spinel $MgAl_2O_4$. It is formed by closely packed face centered cubicarray of oxygen anions with holes partly filled by the cations. There are two kinds of holes differing in coordination: tetrahedral or A site and octahedral or B-site. The unit cell of this mineral containseight formula units. Bragg [4] and Nishikawa [5] first determined its structure. The unit cell of spinel structure with positions of theions in only two octants is as shown in figure (2.1).

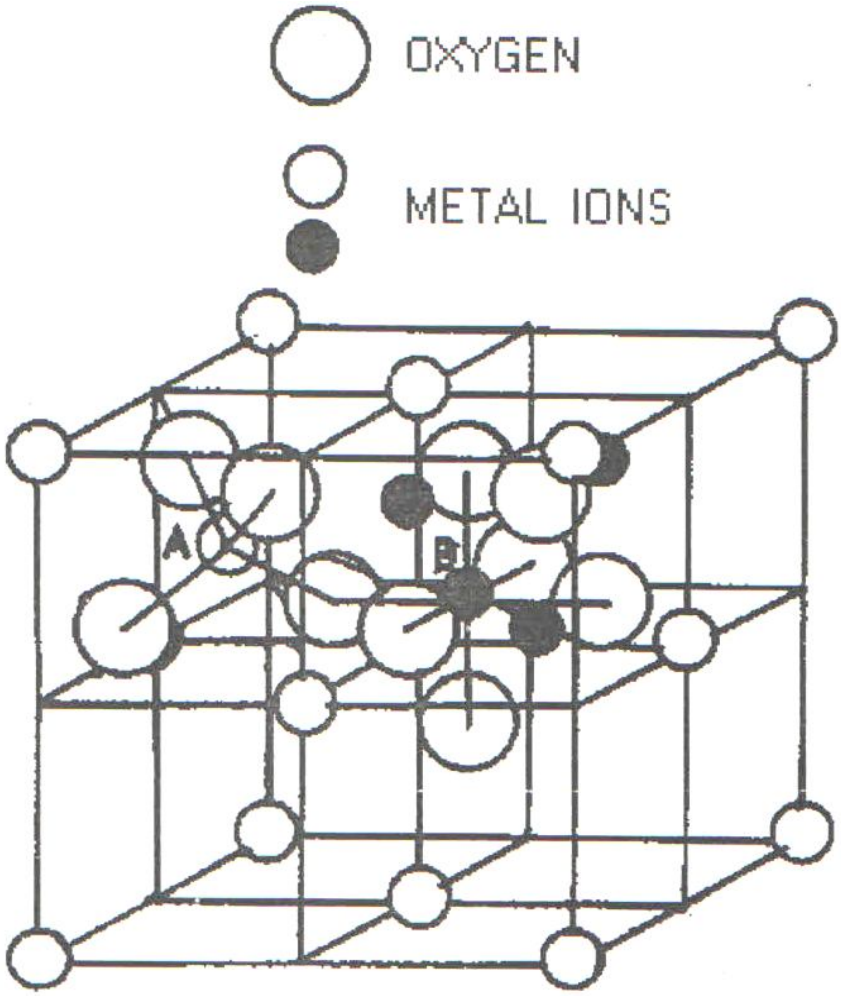

Fig. 2.1 Unit cell of spinel structure -
Positions of the ions in only two octants

In some interstices the cations are coordinated by four equidistant anionsand are called tetrahedral sites or A-sites. The tetrahedral site is asshown in figure [2.2]. In the remaining other interstices the cations are coordinated by six equi-distant anions and are called octahedral sites or B-sites. The octahedral site is as shown in figure [2.3]. In the unit cell of spinel ferrites, there are 64 tetrahedral sites and 32 octahedral sites available out of which only 8 and 16 are occupiedby metal ions respectively [6]. The crystal structure is best described by subdividing the elementary cube with edge a/2. Theanions (oxygen ions) are positioned in the same way in all octants.The surrounding of oxygen in spinel is as shown in figure 2.4.

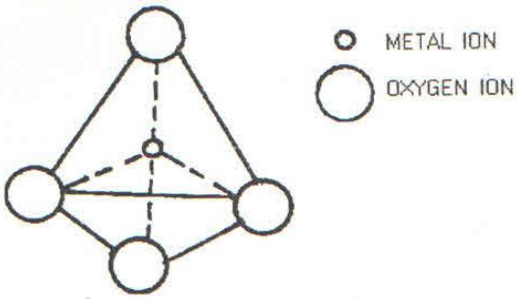

Fig. 2.2 Tetrahedral site

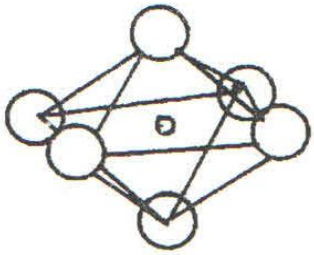

Fig 2.3 Octahedral site

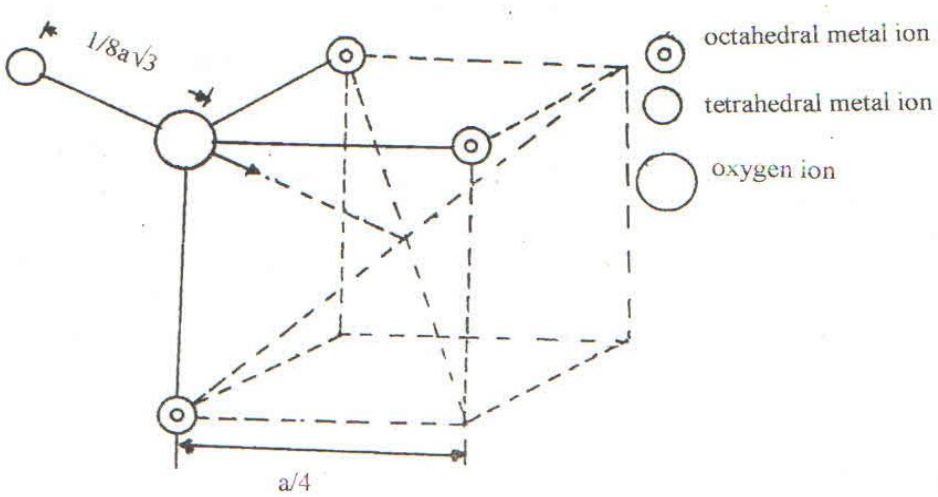

Fig. 2.4 Surrounding of oxygen ion in spinel

Each octant contains four oxygen ions, which form the corners of atetrahedron. The edge of the face centered cubic oxygen lattice is1/2a. Each oxygen is located at the distance equal to ¼ of length of body diagonal from alternate corners of octants. The array of oxygen ions as a whole in the crystal constitute a face centered cubic lattice with edge equal to a/2 and thus there are four such interpenetrating face centered cubic oxygen lattices. The surrounding of the oxygen ions and metal ions in two adjacent sites of the spinel is depicted in figure (2.5). The positions of metal ions are different in the two octants sharing a face and sharing an edge.Thus complete picture of the location of the metal ion can beobtained. The surrounding of B-site ions by other B-site ion in the spinel ferrite is shown in figure (2.6.).

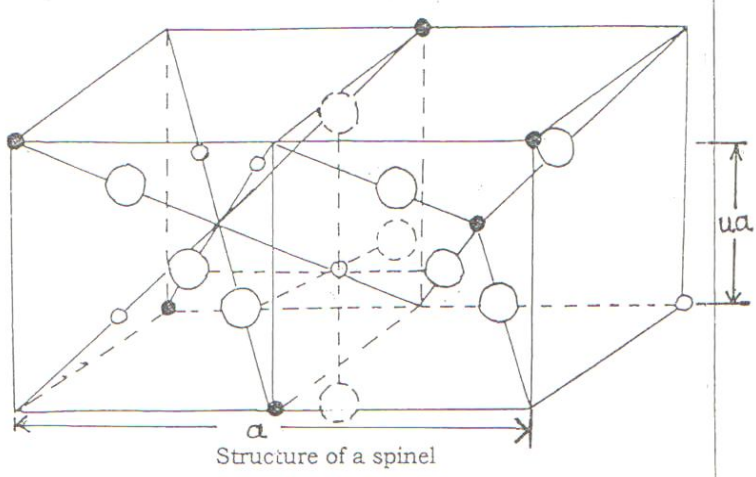

Structure of a spinel

Fig. 2.5 Surrounding of the oxygen ions and metal ions in two adjacent sites of the spinel

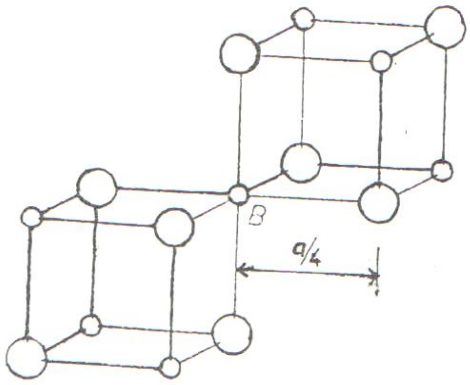

Fig. 2.6 Surrounding of B-site ions by other B-site ion in the spinel ferrite

In one of the octants an occupied tetrahedral site is located at the center and four more sites are located on the corner of the octants. In the adjacent octant, the central site is not occupied but owing to transition symmetry and half of the corner sites are occupied. Thus the occupied tetrahedral sites form two interpenetrating face centered cubic lattices having an edge 'a' which are displaced with respect to each other over adistance a. √3/4 in the direction of body diagonal of a cube. Each tetrahedral ion is surrounded by four other tetrahedral ions, which lie in the corner of regular tetrahedral. There are twelve nearest neighbor octahedral ions for every tetrahedral ion. Each octantcontains four octahedral metal ions and these are situated at site analogous to those of the oxygen ions, which is at one-quarter length of the body diagonal from the other ends of the four body diagonals of the octant. The octahedral metal ions form four interpenetrating face centered cubic lattices, with edge 'a', which are displaced with respect to each other over a distance $\frac{1}{4}a \times \sqrt{2}$in the direction of the face diagonals of a cube [7].

The symmetry of the environment of a tetrahedral ion by the neighboring ions has strictly cubic symmetry. The symmetry of the environment of an octahedral site by nearest metal neighbors islower than cubic. The local symmetry of the cation is cubic in the tetrahedral site and that is trigonal in the octahedral site. The trigonal symmetry is due to both the configuration of neighboring cations and the distortions of the an ion octahedron if oxygen parameter is not equal to 3/8. Each of the four body diagonals belongs to just one of the B-sites in the primitive cell. The local symmetry of the A-site remains cubic even if oxygen parameter is not equal to3/8. Both transnational and local symmetries corresponding to the O^7_h-F3dm space group strictly apply only ifeach sub-lattice contains only one kind of cations i.e. if all M ionsin $MFe_2^{3+}O_4$ are in tetrahedral and all Fe_2 3^+ in octahedral positions. The spinel is then called normal. Barth and Posnjak [8] using X-ray and Hastings and Corliss [9] using neutron diffraction proposed another cation distribution exiting in many spinels called inverse spinel. In the inverse spinel one half of the cations Fezarein A-site and the rest together with the Mions are randomly distributed among A-site and B-site. There are also many examples of inter mediate cases between normal and spinel (random spinel).Therefore in order to characterize fully the spinel structure a furtherparameter describing a degree of inversion is needed. The chemical formula may then be explicitly written as

$$M_\delta M'_{1-\delta}[M_{1-\delta} M'_{1+\delta}]\ O_4$$

The cations on B site are in brackets [10]. If 8 is equal to 1 the structure is said to be a normal spinel structure and if & is equal to zero, the structure is said to be aninverse spinel. When the value of 8 may be in between one and zero (mostly 1/3) then the structure is said to be random spinel structure. In case of soft ferrites & depends upon the method of preparations, sintering temperature, sintering time, the rate of cooling and quenching.

If there are different cations coexisting in equivalent interstices, (partially or fullyinversion of solid solution) the symmetry is perturbed. The symmetry of the spinel structure may also be changed by a spontaneous distortion due to the cooperative Jahn-Teller effect. It has been pointed out on the basis of far infrared spectra and calorimetric measurements [11-14] that somecations in the spinel which are octahedrally coordinated might be shifted a little out of the central positions (of center ions) and would also change the space group. Wycoff [15] proposed the spinel group as O^7_h [Fd_{3m}] and the ionic positions as follows anion (32b)

$$[u,u,u]\ ;\ [u\ \bar{u},\bar{u}];\ [\bar{u},\ u,\ \bar{u}];\ [\bar{u},\ \bar{u},\ u]\ ;$$

$$\left[\frac{1}{4}-u,\frac{1}{4}-u,\frac{1}{4}-u\right];\ \left[\frac{1}{4}-u,u+\frac{1}{4},u+\frac{1}{4}\right];$$

$$\left[u+\frac{1}{4},\frac{1}{4}-u,u+\frac{1}{4}\right];\ \left[u+\frac{1}{4},u+\frac{1}{4},\frac{1}{4}-u\right];$$

cation (16c) positions

$$(5/8,5/8,5/8);\ (5/8,7/8,\ 7/8);$$

$$(7/8,5/8,\ 7/8);\ (7/8,7/8,5/8).$$

cation 8f positions

$$[0,0,0];\left[\frac{1}{4},\frac{1}{4},\frac{1}{4},\right]$$

With the translations, for a face-centered lattice,

$$[0,0,0];\left[0,\frac{1}{2},\frac{1}{2}\right];\left[\frac{1}{2},0,\frac{1}{2}\right];\left[\frac{1}{2},\frac{1}{2},0\right]$$

The packing of the ions within the lattice is perfect when theoxygen parameter u is equal to$\frac{3}{8}$.

From the translations it is obvious that the unit cell (of cube edge =a) consists of the two different groups of four cubes with edge a/2(octants) with ideal ionic positions. The 8f and 16c positions with nearest neighbors in spinel structure are shown in figure [2.7]. However the cation substitution causes cell expansion. The expansion is along the diagonal of the cube as shown in figure (2.8).The projection of the spinel ionic positions to a cube face for anideal spinel system (for which u = 3/8) is shown in the fig.[2.9]

2.3 Oxygen parameter (u parameter)

In an ideal close packed structure of oxygen ions, the metalions having radius less than or equal to 0.30 ^{0}A can be in corporated in the tetrahedral site and the metal ions having radiusless than or equal to 0.55^{0}A can be incorporated in the octahedralsite. This results in a cell edge a= 7.47^{0}A.If we incorporate cations of higher radii, the lattice has to be expanded. In an ideal case tetrahedral and octahedral sites expand in the same ratio and the distance between the tetrahedral site (0, 0, 0) and oxygen anion site (3/8,3/8,3/8) is3/8 (u_{ideal}). However, practically the in corporation of metal ions in tetrahedral site moves the an ions from their ideal position in [111] direction away from the nearest tetrahedral ion and there is an expansion in the tetrahedral site at the expense of shrinkage of octahedral site [16). The difference in the expansion of octahedral and tetrahedral site is characterized by a parameter called oxygen parameter (u).

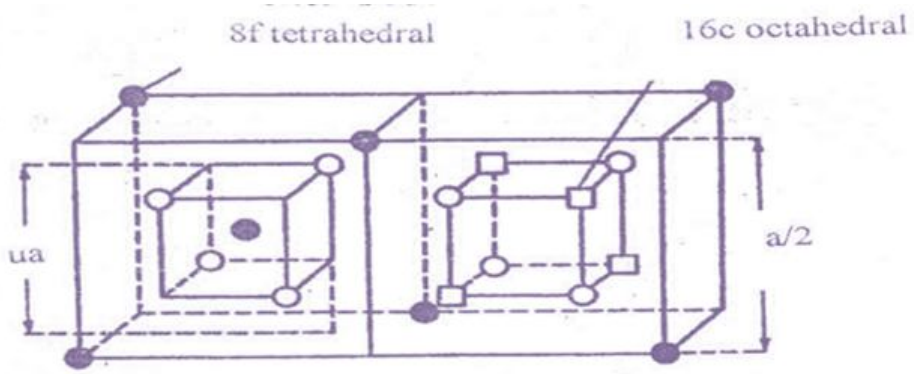

Fig. 2.7 8f 16c & nearest neighbors in spinel structure

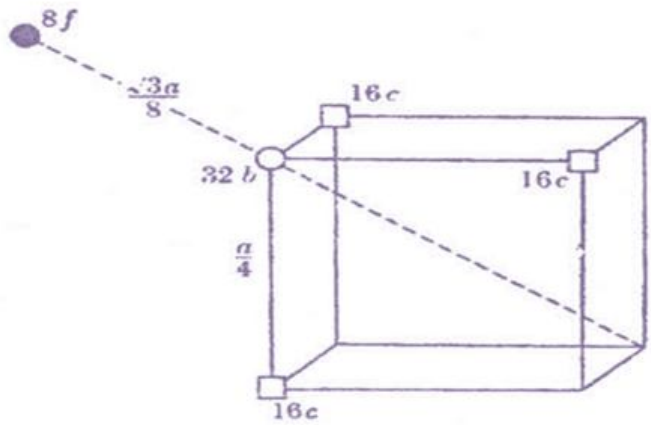

Fig. 2.8 Expansion of unit spinel cell

The tetrahedral site is expanded by an equal displacementof the four oxygen ions outwards the body diagonals of the cube,still occupying the corners of an expanded regular tetrahedron. The four oxygen ions of

the octahedral site are shifted in such a way that this oxygen tetrahedron shrinks by the same amount as the first expansion and as a result the oxygen surrounding of each B ion is no longer of cubic symmetry. The value of oxygen parameter can be determined with the help of X-ray diffraction or neutron diffraction. The $u_{obscrvcd}$ is always greater than u_{idcal} because of the stranger expansion of the tetrahedral interstices at the expense of shrink age of the octahedral interstices. For small displacement, radii of the Sons on tetrahedral site (A- Site) and Octahedral site (B-Site) ie. r_A & $r_B$can be determined using following relations,

$$r_A = \left(u - \frac{1}{4}\right) a\sqrt{3} - r_o^{2-} \quad \text{..... (2.1)}$$

$$r_B = \left(\frac{5}{8} - u\right) a - r_o^{2-} \quad \text{..... (2.2)}$$

Wherer$_A$ radius of tetrahedral site and r_B is radius of octahedral site, u is oxygen parameter, $r_o^{2-}$is radius of oxygen ions and a is lattice parameter. [17]

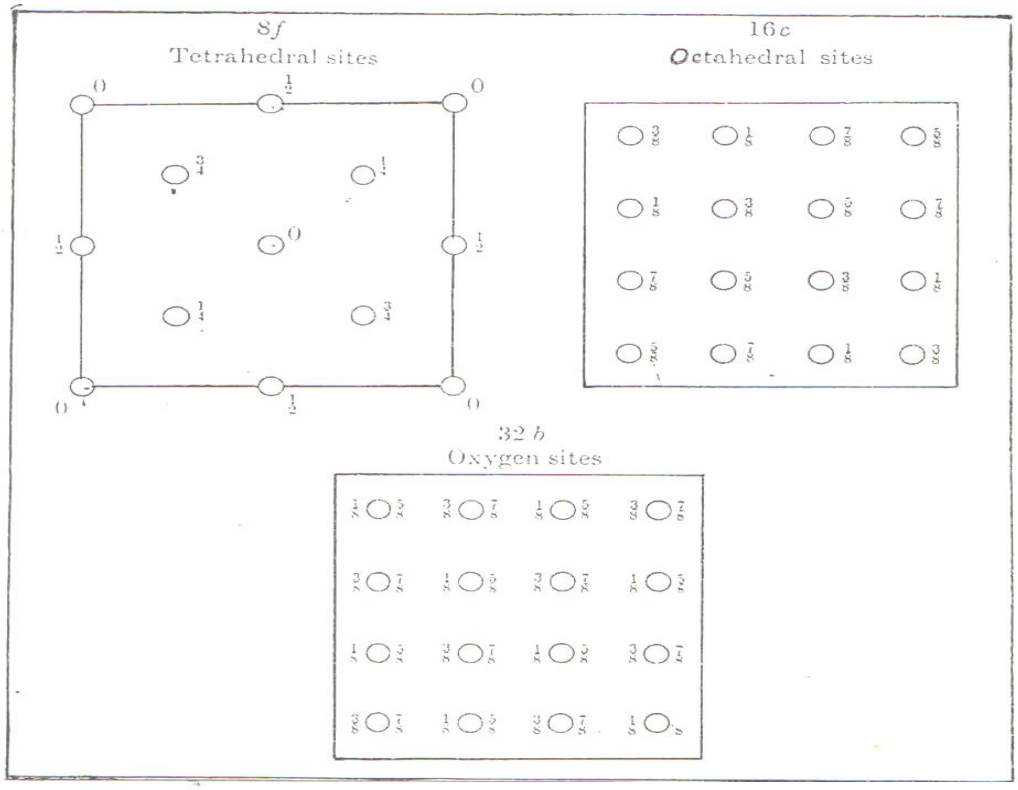

Fig. 2.9 Projections of the ionic positions in spinel structure.

2.4 Classification of ferrite

The ferrites are classified into four groups according to their crystal structure.

2.4.1 Spinel Ferrite

This is the simplest among the ferrites. Spinel ferrite has a face centered cubic structure. The general chemical formula of spinel ferrites is $Me^{2+}Fe_2^{3+}\ O_4^{2-}$ where Me^{2+} is divalent metal ion and may be belonging to the group of transitionelements [18].

2.4.2 Garnet ferrite

The garnet ferrite has a cubic structure (larger crystal ascompare to spinel crystal). The general chemical formula for agarnet ferrite is $Ln_3^{3+}Ln_5^{3+}O_{12}^{2-}$where Ln may be either of Y, Sm,Eu, Gd, Tb, Dy, Ho, Er, Tm & Lu.

2.4.3 Magnetoplumbite ferrite

The magnetoplumbite ferrites have a hexagonal structure. The general chemical formula of the magnetoplumbite ferrite is $Me^{2+}Fe_{12}^{3+}O_{19}^{2-}$ where Me^{2+} may be either of Ba or Pb.

2.4.4 Perovskite Ferrite

It has a typical Perovskite structure. It is with orthorhombic unit cell having general formula $MeFeO_3$, where Meis larger metal ion such as rare earth yttrium. g. Me + = Ca, Ba, Sr, Pb, Cd.The spinel ferrites are further classified on thebasis of cation distribution as.

2.4.5 Normal spinel ferrite

If 8 tetrahedral sites are occupied by divalent metal 10 and 16 octahedral sites are occupied by trivalent metal ion then the spinel is called normal spinel.

$$\text{e.g. } (Zn^{2+}) \wedge [\, Fe^{3+}\, Fe^{3+}]^B O_4^{2-},\ (Cd^{2+})^A [Fe^{3+}Fe^{3+}]^B O_4^{2-}$$

2.4.6 Inverse Spinel Ferrite

If half of the trivalent ions are occupied in tetrahedral sites and remaining half trivalent ions in addition to all the divalent metalions are occupied in octahedral sites, the ferrite is known as inversespinel ferrite.

$$\text{e.g. } (Fe^{3+})^A [Cu^{2+}\, Fe^{3+}]^B O_4^{2-}$$

2.4.7 Random Spinel Ferrite

In such type of spinel ferrite, both divalent and trivalentions are occupied in tetrahedral and octahedral sites randomly,

$$\text{e.g. } (Mx^{2+}Fe_{1-x}^{3+})^A [M_{1-x}^{2+}Fe_{1+x}^{3+}]^B\ O_4^{2-}$$

$$(Mn_{0.8}^{2+}Fe_{0.2}^{3+})^A [Mn_{0.2}^{2+}Fe_{1.8}^{3+})^B O_4^{2-}$$

The degree of in version and the type of cations that occupy octahedral site and tetrahedral sites play an important role in the magnetic properties of the spinel ferrites.

The electroneutrality considerations lead to three basic type of spinel (ordering)

(1) 2-3 Spinel e.g. $M^{2+}M_2^{,3+}O_4^{2-}$

(2) 4-2 Spinel e.g. $^{M4+}M2\ ,^{2+}O_4^{2+}$

(3) 6-1 Spinel e.g. $M^{6+}M_2^{,1+}O_4^{2-}$

The other combinations of mixed cations of different valency with suitable electroneutrality conditions of ions in thecomposition are also possible and arecalled as mixed ferrites [19].

2.5 Factors influencing cation distribution

The cation distribution in the ferrites over the tetrahedraland octahedral sites in spinel ferrite is found to be the function of temperature, pressure, chemical composition, ionic radius, electronic configuration, electrostatic energies (Madelung energy) and the polarization effects. In order to explain the site preference of transition metal ions two theories have been proposed, which differ in the chemical bonding in oxide. Dunitz and Orgel [20] have used crystal field theory which is based on purely ionic type of bonding where as G.Blasse [21-22] has proposed a simplified molecular orbital approach, taking into accounts the carrier bonding between oxygen and transition metal ions. According to the crystal field theory the ^{d3} ion has the highest octahedral site preference energy followed by d^4, d^8, d^6, d^9, ^{d2} and d^1. The ions with d^0, d^5, d^{10} configurations have no crystal field stabilization energy and, therefore no site preference. According to the orbital approach of B lasse, the ions with d^5, d^6, d^7, d^9 and d^{10}electronic configuration show a tetrahedral site preference,

The following factors influence the cation distribution,

1. Ionic radius

The tetrahedral sites are smaller than the octahedral sites and divalent ions are generally larger than the trivalent ions. Therefore it is quite obvious that smaller trivalent ion would go totetrahedral site and larger divalent would go into octahedral site. However, the large divalent ions tend to occupy tetrahedral sitesand

trivalent ions tend to occupy octahedral sites as this is favored by polarization effects. If the A-site ions have a lower valency and the B-site ions a higher valency, the intermediate O^{2-} ion becomes polarized towards B-sites. Thus the polarization favors normal spinel structure. If the trivalent ions partly occupy the B-sites then the inverse spinel is formed.

2. Electronic Configurations

Some cations have a special preference for a certain environment e.g. Cd^{2+} andZn^{2+} show a strong preference for tetrahedral site in which case the 4s, 4p and 5s, 5p electrons respectively can form a covalent bond with the six 2p electron of the oxygen ions. This produces four bonds oriented towards thecorners of a tetrahedron. Ni^{2+} and Cr^{3+} show strong preference for octahedral environment. It is due to the favorable fit of the charge distribution of these cations in the crystal field at octahedral site.

3. The Electrostatic Energy

The electrostatic energy gained when the ions, at first thought to be infinitely far apart, are brought together to form the spinel lattice is known as Madelung energy. The largest contribution to the crystal energy in oxide spinel is the Coulomb energy of the charged ions (Madelung energy). It is given as,

$$E_c = -\left(\frac{e^2}{a}\right) \times A_M \quad \ldots\ldots\ldots\ldots\ldots\ldots\ldots\ldots\ldots\ldots\ldots\ldots.. \quad (2.3)$$

Where e is the charge of electron, a is the lattice parameter and A_M is the Madelung constant. A_M may be expressed as a function of the mean electric charge q_A of the cations in A-site and of the oxygen parameter u. Thompson and Grimes [23] proposed a formula for Madelung constant incase of spinel as,

$$A_M = A_M(q_A,^{u}) = 139.8 + 1186_{\Delta u} - 6483_{\Delta}{}^{2}_{u} - (10.82 + 4132.2_{\Delta u} - 1903_{\Delta}{}^{2}_{u})qA + 2.609q2A \ldots\ldots\ldots(2.4)$$

Where Au = u-0.375. Am depends on qa for different values of the oxygen parameter (u). With increasing A_M the stability of the spinel increases. Therefore, owing to its dependence on q_A, the Coulomb energy generally plays an important role in the equilibrium distribution of cations among A and B sites. In normal arrangement the metal ions with the smallest positive charge are surrounded by four oxygen ions and the metalions with higher positive charge are surrounded by six oxygen ions which is eletrostatically the most favorable one. The normal structure has the lowest lattice energy when u >0.379. Verwey et al [24] Proposed that spinel consisting of divalent and trivalent metalions has the inverse structure and there is the lowest lattice energy when u < 0.379.

4. Method of preparation

The method of preparation also can influence the cation distribution over tetrahedral and octahedral site. The cation distribution is strongly depended on the heat treatment in the sintering process especially on the rate of increasing temperature and on the rate of cooling. In case of some ferrite cation distributionis found to follow the Boltzmann distribution which is given by thefollowing relation,

$$\frac{{}^{\delta}(1+{}^{\delta})}{(1+{}^{\delta})2} = \exp\left(-\frac{E}{K} = kT\right) \quad \ldots\ldots\ldots\ldots\ldots\ldots\ldots\ldots\ldots\ldots\ldots \quad (2.5)$$

Where $^{\delta}$ is distribution parameter, E is activation energy, k is Boltzmann constant and T is absolute temperature [25].

2.6 Origin of ferrimagnetism

The spontaneous magnetization in larger quantity such asin ferromagnetic material was attributed to the spin alignment of magnetic atoms by molecular field or acrystal field, which is supposed to be the consequence of the quantum mechanical exchange interaction between the nearest neighboring ions. This interaction arises due to the Pauli's exclusion principle according towhich any change in the relative orientation of the two spins would disturb the spatial distribution of charge or vice versa. The strength of exchange interaction between the adjacent atoms depends on the extent of overlap of their wave functions as well as the relative orientation of the electron spins but not on the spin magnetic moments. This exchange interaction is the main cause of the spinal ignment in the magnetic material. The following relation gives the energy of the two interacting atoms [26].

$$U_{jj} = -2J_e.S_iS_j \ldots\ldots\ldots\ldots\ldots\ldots\ldots\ldots\ldots\ldots\ldots\ldots\ldots \quad (2.6)$$

Where Je is an exchange integral, S_i and S_j are spins of the $i^{th}$and j^{th}atoms which are interacting.The value and sign of J_e decide the type of exchange interaction. Je is positive for large inter-atomicdistances.[D/d > 1.5 to 3 where D is distance between the interacting atoms and d is the radius of the atom] The exchange integral Je is negative for smaller inter-atomic distances. [$D/d \leq 1.5$]. If J_e is positive the spins are aligned in parallel way and if Je isnegative the spins are aligned in anti-parallel way. In case of ferritescations are distributed over two sub-lattices and the direct exchange interactions among metal ions are not possible because the metalions are coordinated by larger size of oxygen anions. There exists aspecial type of exchange interaction. The bonding in ferrites is a certain amount of admixture of ionic and covalent which results m the superposition of states. Thus there exists orbital overlap between oxygen ion and cation. In orbital overlap two electrons of oxygen spend a fraction of their time in the orbits of the adjacent atoms. Thus there is exchange interaction between the two cations via oxygen anion. This type of interaction is called super exchange interaction.Anderson [27] proposed the super exchange theory in which it is assumed that one of the electrons in the oxygen ion could interact with or exchange with the unpaired electron of themetal ions at A - site. To be able to pair with the spin of the metalion, the spin of the oxygen electron would have to be opposite to that on the metal ion. This would leave the other spin in the oxygen ion orbital free to pair with the unpaired spin of another metal ion.Since the spin of the first electron of the oxygen ion is opposite to that of the first metal ion the second electron of the oxygen is coupled in opposite way with the second metal ion and as a resultthe spins at A-site and B-site are anti-parallel. This is the reason forthe stability of the anti-parallel alignment of the two metal ions adjacent to the oxygen ion. In 1951 Zener [28] proposed an alternative mechanism to the super exchange which he called double exchange. In this case, the spins of the ions of the sameelements of two different valences simultaneously exchange electrons through the oxygen ion, there by changing the valences of both. Thus $Fe^{++}O_2^{-}$ Fe^{+++} can change to $Fe^{++}O_2^{-}$ Fe^{++} .In thisway super-exchange interaction is the main cause of the ferrimagnetism. This super-exchange interaction is the strongest when two cations and intermediate oxygen an ion are collinear andw eakest when the angle made by two cations with oxygen is a right angle.

2.7 Magnetic Interactions in Ferrites

There are three types of interactions in ferrite namely A-A interaction, B-B interaction and A-B interaction. A-A interaction isthe interaction between cation at tetrahedral site and B-B interactionis the interaction between the cation at octahedral site (A-A and B-B are known as intra-interaction). The A-B interaction is the interaction between cation at tetrahedral site and cation at octahedral site via oxygen anions (It is known as inter interaction).

The strength of interaction between magnetic moments on various sites (the negative interaction or exchanges force between the moments of two metal ions on different sites) depends on the distance between these ions and the oxygen ion that links them as well as on the angle (Me1-O-Me11) between the three ions. The interaction is the greatest for an angle of 180^o and also where the inter-atomic distances are shorter. The various possible configurations of the ion pairs in spinel ferrites with favorable distances and angles for an effective magnetic interaction as envisaged by Gorter [29] are as shown in fig.[2.10].

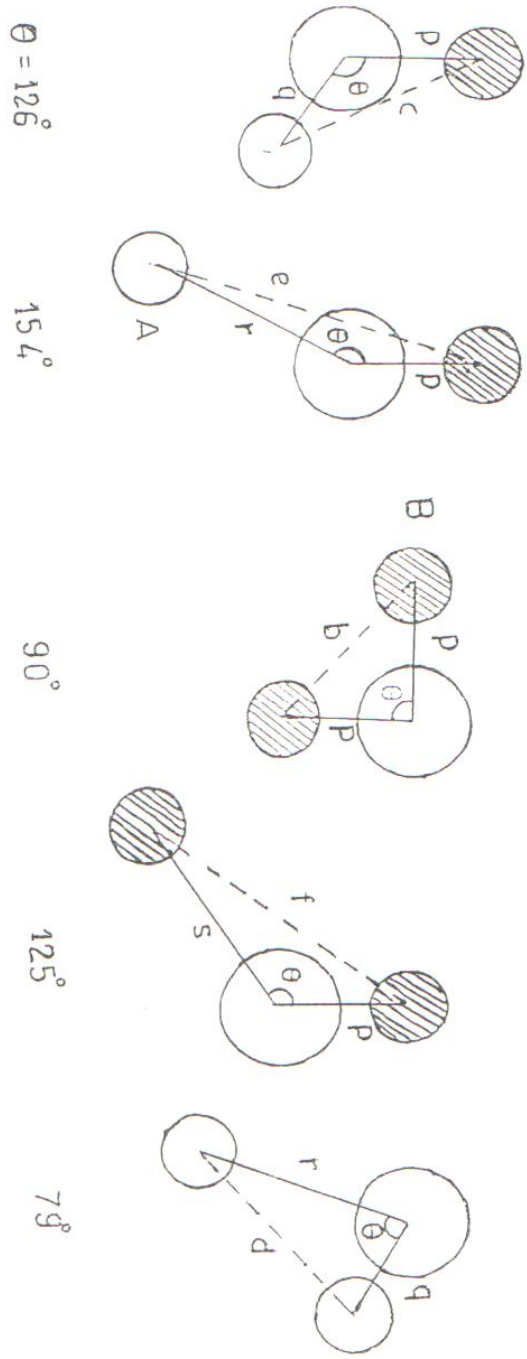

Fig. 2.10 Interaction angles for inter and intra

In the cases of A - A and the B-B interaction, the angles are too small or the distances between metal ions and the oxygen ions are too large. The best combination of distances and angles are found in the A-B interactions. For undistorted spinel, the A-O-B angles are about 125^0 and 154^0. The B-O-B angles are 90° and 125° and one of the B-O-B distances is large. A-A interaction is the weakest because of relatively larger distance and the unfavourable angle approximatelyof 80°. Thus the interaction between magnetic moments of the Asite and B sites is the strongest. The B-B interaction is much weakerand the most unfavorable situation occurs in the A-A interaction, which is weakest. The A-B interaction orients the unpaired spins of these ions antiparallel. An individual A-site interacts with a single B-site, but each A site is linked to four such units and each B site is linked to four such units. Therefore, to be consistent through out the crystal, all A site and all B site act as unified block and are coupled anti-parallel and the resultant magnetic moment is

equal to the difference between those of A and B ions. The value of magnetic moment for the B sub-lattice (M_B) is greater than that of the A sub-lattice (M_A) due tothe crystallographic difference as well as the more cations are occupied at the octahedral site.

The resultant saturation magnetization (Ms) may be written as,

$$M_s = M_B - M_A \quad (2.7)$$

The magnitude of exchange energies is affected by the deviation in oxygen parameter u from the value 3/8. If u > 3/8, the oxygen ions are displaced in such a way that in the A-B interaction the distance between A & O ions is increased and that between the B-ion and A-ion is decreased. The angle (0) A-O-B is decreased [30].

2.8 Magnetic order in spinel ferrites

The spinel structure seems to be particularly attractive as it allows a variety of magnetic orders from collinear to frustration.This is due to the fact that in spinels intra-sub-lattice interactions are weaker than the inter-sub-lattice interactions and as a result there are unsatisfied bonds in the ferrimagnetic phase. Because of the unsatisfied bonds, the increasing magnetic interactions accentuate the competitionbetweenthe various exchange interactions resulting in a variety of magnetic order [31].

The negative super-exchange interaction exists in ferrites. The strength of the exchange interaction is specified by exchange integrals [32]. If the exchange integrals of intra-sublattice interactions and inter-sublattice interactions follow the order $J_{AB}>J_{BB}>J_{AA}$ then there is acollinear ferrimagnetic order. [33]The magnetic order can becontrolled by suitable cation substitution. [34] It isfound that acertain cation (generally nonmagnetic) substitution can render thethat one of the intra sub-latticeinteractionin such a wayinteractions (J_{BB} or J_{AA}) is comparable with the inter-sub-latticeinteraction (J_{AB}) and a non collinear (canted) spin order comes into existence. A variety of magnetic orders are found by substituting a non-magnetic cation. A tentative phase diagram of the possible magnetic order has been suggested by Dormann [35]. The canted spins order like Yafet-Kittel configuration, localized canted spin order random canted spin order, spiral structure, spin glass (i.e. frustrated spin or frozen spin situation) type order and cluster sping lass type order have been observed.

2.9 Neel's theory of ferrimagnetism

In 1948, Neel [36-37] proposed a theory to explain the phenomenon of ferrimagnetism. He assumed that the crystal lattice could be divided into two sub-lattices.These are crystallographically different sites and are known as tetrahedral site(A site) and octahedral site (B site).With the help of Weiss field theory [38], Neel postulated the existence of negative intra and inter interactions among the spins of A site ions and that of B site ions. The magnetic moment of each A site ion is more or less antiparallel with that of each B site ion. There are three interactions namely A-B, A-A & B-B interaction and strength of the interactions follow the order $J_{AB}>J_{BB}>J_{AA}$.

The magnetic field acting upon an atom or ion is given inthe following form.

$$H=H_0+H_m \quad (2.8)$$

where H_0 is externally applied field , H_m is internal molecular field which a rises due to interaction with other atoms or ions within the material. Neel applied the Weiss field concept to two sub lattice spinel structure and deduced the relations which give the effective field acting on the cations residing at both the sub-lattices such as,

$$H_A= H_{AA}+H_{AB} \quad (2.9)$$

$$H_B= H_{BB}+H_{BA} \quad (2.10)$$

where H_A molecular field acting on an ion at A-sitem, H_{AA} is molecular field due to neighboring A ions, H_B is molecular field acting on an ion at B-Site. Thus the molecular filed components may be written as,

$$H_{AA}= \gamma_{AA} M_A;\ H_{AB} = \gamma_{AB} M_B \quad (2.11)$$

$$H_{BB} = \gamma_{BB} M_B;\ H_{BA} = \gamma_{BA} M \quad (2.12)$$

where γ's are suitable molecular field coefficients and M_A and M_B are the magnetic moments of the A and B sublattices.

It may be shown that $\gamma_{AB} = \gamma_{BA}$ but γ_{AA} is not equal to γ_{BB} unless the two sublattices are identical. Neel elucidated that $\gamma_{AB} < 0$ and favors anti-parallel arrangements of M_A and M_B, which give rise to ferrimagnetism. The net spontaneous magnetization is given by,

$$M_S = M_B - M_A \quad \text{.....(2.13)}$$

Where M_A is magnetization of A-sub-lattice and $M_A$is magnetization of B-sub-lattice. On application of the magnetizingwritten as,field H_O, the total magnetic field acting on each sub lattice may be

$$H_a = H_O + H_A \quad \text{.....(2.14)}$$

$$H_a = Ho + \gamma_{AA}M_A + \gamma_{AB}M_B \quad \text{.....(2.15)}$$

$$H_b = H_O + H_B \quad \text{.....(2.16)}$$

$$H_b = Ho + \gamma_{BB}M_B + \gamma_{AB}M_A \quad \text{.....(2.17)}$$

where H_a, is effective field acting on A site and H, is effective field acting on B-site. These effective fields ($H_a$and H_b) give rise to the saturation magnetization in the ferrites.

Neel determined various possible forms of the temperature dependence of magnetization curves giving a very satisfactory explanation of the magnetization observed in ferrites with spinel structure. Assume that $\alpha = \gamma_{AA}/\gamma_{BB}$ and $\beta = \gamma_{BB}/\gamma_{AB}$. The values of αand ß control the magnetic order in ferrites. If ß is large and α is small, i. e. the Weiss field constant in the B -lattice is small at T=0. The A-lattice has higher Weiss field constant and $M_{BO} > M_{AO}$. ($M_{AO}$and M_{BO} are magnetization of A-sub-lattice and B-sub-latticerespectively at T is equal to zero). The magnetization in the Blattice, therefore, begins to decrease faster than that in the A-latticeas if the curie point of the B-lattice were lower than that of the A– lattice. At certain critical temperature (Curie temperature) both sub-lattice magnetization vanishes. Consequently the M_A versus T curve is more convex than that for M_B and it is possible that below the curie temperature M_B-M_A is zero. If β is small and α is large then M_A decreases less rapidly than M_B.The temperature dependence magnetization for spinel ferrite is shown in figure [2.11]. Neel's theory can explain the magnetic properties of ferrites and helps to determine the cation distribution with the help of observed saturation magnetization.

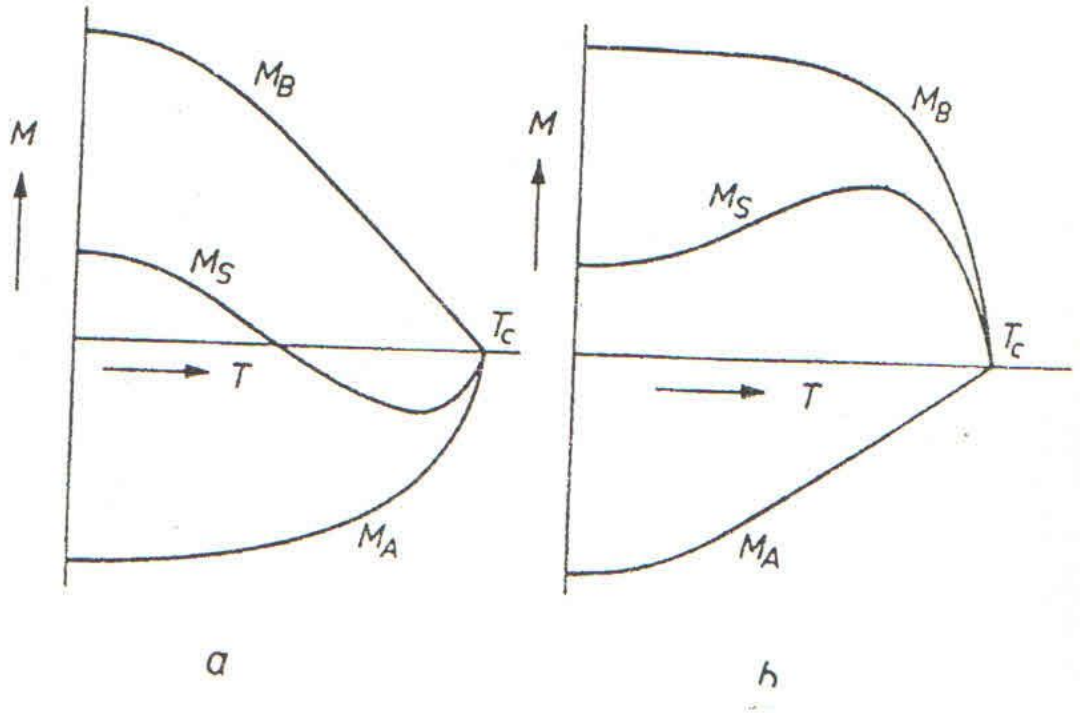

Fig. 2.11 Temperature dependence magnetization

2.10 Yafet-Kittel theory of ferrimagnetism

It was found that the magnetization per formula unit for some ferrites showed a significant departure from Neel's collinear model. Yafet and Kittel (1952) [39] were the first to argue that non-magnetic substitution on one sublattice could lead to a non collinear or canted spin arrangement on the other sub-lattice. They proposed a model after their names to explain the significant departure of magnetization from Neel's collinear order. They developed three – sublattice molecular field model. In Neel's model the magnetic ions on A and B have parallel spin arrangement and the A-B interaction is the strongest as compared to the AA and BB interactions. However when A-B interaction is diluted with respect top A-A and B-B interactions, the collinear two-sublinear model is not applicable. They assumed the triangular spin arrangement. In Yafet-Kittel model they considered the possibility of splitting of each sublattice depending on specific local magnetic environment. They found that when there is strong negative interactions within sub-lattice B, the two equivalent sub-structures B_1 and B_2 come into existence both spontaneously magnetized, but there magnetization are not exactly anti-parallel. Instead they are aligned at some angle other than 180^0. Thus there is resultant magnetization of the B lattice and it is this resultant magnetization which sets anti-parallel with the magnetic moment of A sublattice. This triangular spin arrangement within the lattice results in reduction of magnetization. The Y. K. model of spin arrangement is as shown in figure [2.12].

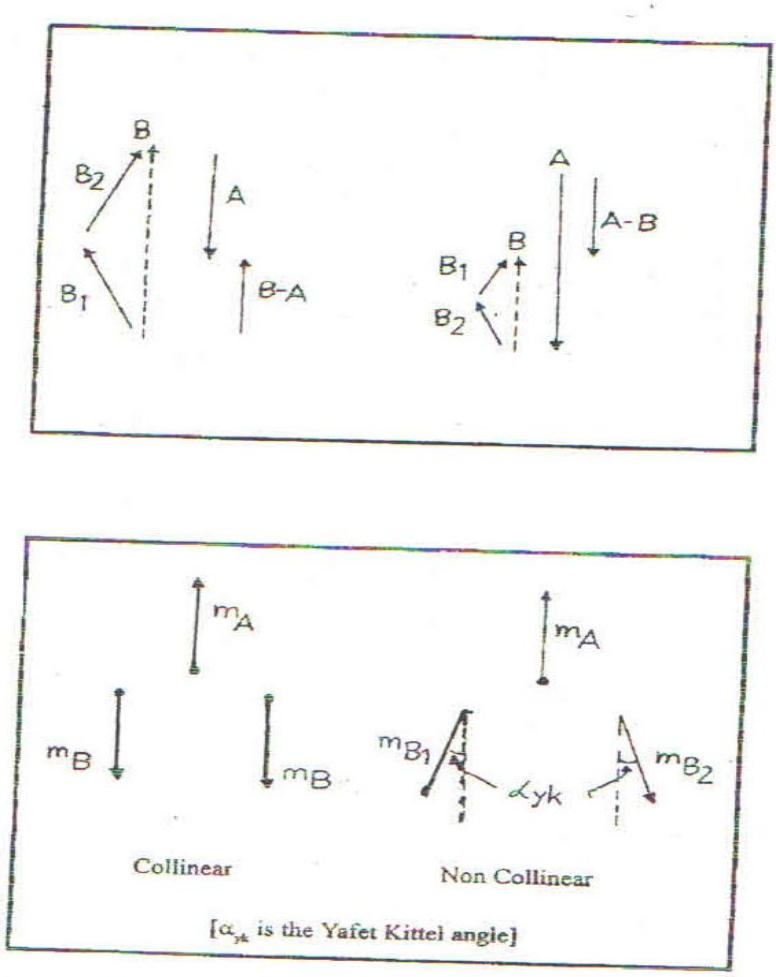

Fig. 2.12. Yafet Kittel three sub-lattice model

The theory of the triangular arrangement was further developed by Lotegering [40], which predicts triangular or canted, helical or screw type of possibilities for the spin arrangement. In this theory long range nature of interaction was assumed. However, Anderson [41] (1959) have argued that a Yafet-Kittel arrangement, if it exists at all, must be of a short-range nature. Geller and Co-Workers [43] developed a descriptive model of local random canting. The canting angle can be given as,

$$M_s = (M_B) \cos \theta_{YK} - (M_A) \quad \ldots\ldots\ldots\ldots\ldots\ldots\ldots\ldots\ldots\ldots (2.18)$$

2.11 Random Canting Model

In the random canting model it is proposed that the substitution in one sublattice of a ferrimagnet lead to spin canting in the other sub-lattice. Rosenwaig [44] assumed that the nearest neighbor of a B site can be considered to be canted with an average angle $<\alpha>$. The canting angle can be determined as,

$$\cos <\theta_B> = (M_A/M_B).(J_{AB}/J_{BB}) \quad \ldots\ldots\ldots\ldots\ldots\ldots\ldots\ldots\ldots\ldots (2.19)$$

Where M_A and M_B are spontaneous magnetization of sublattice A and B. J_{AB} and J_{BB} are exchange integrals. The saturation magnetization is given by,

$$N_B = M_B \cos <\theta_B> - M_A \quad \ldots\ldots\ldots\ldots\ldots\ldots\ldots\ldots\ldots\ldots\ldots\ldots (2.20)$$

It is called random because its existence may be on either site of the sub-lattice.

2.12 Local Canting Model

Geller [45] has proposed a localized canting approach in which individual moments on one sublattice are canted at different angles depending on the local magnetic environment. This concept was formalized by Dionee [46-48] in a refinement of the Neel molecular – field model. Rosenwaig presented a localized variant of the Yafet-Kittel calculations in which nearest neighbor exchange parameters were kept constant and the statistics for local nearest neighbor was used to obtain effective molecular fields and local canting angles. White et al [49] (1979) extended the procedure by using the Rosenwaig average canting angle.

2.13 Villain Model

Villain [50] proposed that the spinel structure gives rise to topological frustration that results in perturbed magnetic ordering. This perturbation depends on the dilution of the two sublattices. The frustration is due to the competition between the inter and intra –sublattice interaction. The non- magnetic substitution gives rise to high ground state degeneracy, which is due to the prevention of long range ordering. Such a system was termed as co-operative paramagnetic system. The degeneracy is reduced by the addition of non-magnetic impurities and a spin glass where phase is stabilized.

REFERENCES

1. S. Krupicka &P. Novak,Phys. Status Solidi 4 (1964) K117
2. S. Krupicka &P. Novak,J. Appl. Phy. 40 (1969) 872.
3. B. Vishwanathan V. R. K. Murthy,Ferrite MaterialsSpringer-Verlag (1990)
4. W. H. Bragg,Phil. Mag. 30 (1915) 305.
5. S. Nishikawa, Proc. Math.Soc. Tokyo ,8(1915) 199.
6. R. S. Craik and D. J. TabbleFerromagnetism & ferromagnetic domainAmsterdam:North Holland Publ. Co.(1965)
7. J. Smit &H. P.J. Wiijn, Ferrites John Wiley & Sons, NewYork.(1959)
8. T. F. W. Barth, Z. Posnjak, Krist 82 (1932) 325-334.
9. J. M. Hastinggs and L. M. Corliss,Rev. Mod. Phys. 25 (1955) 114
10. J. Smit &H.P.J. WijnFerrites John Wiley & Sons, New York.(1959) 141
11. N. W. Grimes Philos. Mag.26 (1972) 1217
12. N. W. GrimesSpectr. ACTA 28a (1972) 2217
13. N. W. Grimes, Proc. Roy. Soc. A338 (1974) 223
14. N. W. Grimes, T.J. O'Connor and P. Thompson, J. Phys. C11 (1978) L505.
15. RW.G. Wyckoff,Crystal structures, Vol.1&2 Interscience New York.
16. J. Smit &H.P.J. WijnFerrites ,John Wiley & Sons, New York.(1959) 139

17. J. Smit &H. P. J. Wijn, Ferrites John Wiley & Sons, New York.(1959)140
18. B. Vishwanathan V. R. K. Murthy,Ferrite MaterialsSpringer-Verlag (1990)2
19. E. W. Gorter, Nature 165 (1950) 4202
20. J. D. Dunitz, L.E. Orgel ,J. Phys. Chem. Solids (1957)
21. G. Blasse Philips Res. Rep. Suppl. No.3 (1964)
22. G. Blasse Philips Res. Rep. 20 (1965) 528.
23. P. Thompson, N. W. Grimes,Philos. Mag. 36 (1972) 501.
24. E.J. W.Verwey and E. L. Heilmann, J. Chem. Phys. 15 (1947) 174.
25. B. Vishwanathan V. R. K. Murthy, Ferrite MaterialsSpringer-Verlag (1990)2
26. R.K. Puri ,V. K. Babbar,Solid state physics, S. Chand &Comp. (India) (1997)
27. E. E. Anderson Phys. Rev. 134(1964) A1581.
28. C. Zener Phys. Rev. 81(1951a) 440.
29. E. W. Gorter Philips. Res. Rep. 9 (1954)321
30. E. W. Gorter ibd. 9 (1954b) 403
31. N. N.Jani, B. S. Trivedi, H. H. Joshi, G. K. Bichile &R. G. Kulkarni,Bull.Mater. Sci. Vol.21.No.3 June (1998) 233-239.
32. E.W. Gorter Proc. I. R. E. 43 (1955)1945.
33. P.W. Anderson, Phys. Rev. 79(350)350.
34. Y. Yfet &C. Kittel.,Phys. Rev. 87(1952)290.
35. Dorman, J.L. and Nogues M. J.J. Phys., Condens Matter 2 (1990)
36. L Neel, Ann. Phys. 3 (1948)
37. K. J. Standley ,Oxide Magnetic MaterialClarendon press Oxford (1962)
38. P. Weiss J.Phys. d (1907) 667
39. Y. Yafet., C. Kittle Phys. Rev. 87(1952) 210
40. F. K. Lotegering, Philip. Res. Rep. 11(1956) 190
41. P.W. Anderson Phys. Rev. 102(1956) 1008.
42. T. A. Kaplan Phys. Rev. 116 (1959)888.
43. S. Geller et al ,Bell. Syst. Tech. J. 63(1964) 565.
44. A. Rosenwaig Can. J. Phys.48 (1970) 2857.
45. S. Geller et al J. Appl. Phys. 335 (1962) 1195.
46. G. F. Dionne, J. Appl. Phys. 41 (1970) 4874.
47. G. F. Dionne, J. Appl. Phys. 45 (1974) 3621.
48. G. F. Dionne, J. Appl. Phys. 63 (1970) 377.
49. G. O White, C.A. Edmondeson , R. B. Goldfarb &C. E. Patton J. Appl. Phys. 50 (1979) 2381.
50. Villain J. Phys. B. 33 (1979) 31.

CHAPTER – 3

EXPERIMENTAL TECHNIQUES FOR INVESTIGATION

3.1 Introduction

The properties of mixed magnetic oxides are sensitive to the synthesis technique and to have precise quantitative as well as qualitative information of the properties of material, the sophisticated instrumentation for characterization is essential. The high purity ofreacting oxides is the prime need to have a good material formation.The most important thing for mixed magnetic oxide is the formation of the appropriate crystal structure. The analytical grade high purity oxides have been used for the synthesis of the systems for present investigation and the following experimental techniques have been used for synthesis and characterization,

1) Ceramic method

2) X-ray diffraction

3) Infrared spectroscopy

4) Hysteresis loop tracer

5) Double setup coil for low field susceptibility

6) Two probe method for d.c. Resistivity

7) Dielectric properties using two probe methods along with L-C-R-Q Meter

3.2.1 Techniques of Synthesis

Mixed magnetic oxides can be synthesized by using the following different methods.

1). Ceramic method

2). Co-precipitation/wet chemical method

3). Precursor method

4). Sol-gel method

5). Combustion method.

(1). Ceramic method: The solid state reaction is brought about at an elevated temperature through double sintering process in this method.

(2). Co-precipitation / wet chemical method: The cations in thecomposition are co-precipitated from common medium generally from hydroxides, carbonates, oxalates or formates. The starting solids in decided stoichiometry are dissolved and mixed in deionized water and highly concentrated NaOH is added to it in order to get precipitate. This precipitate is digested in boiling water and it is then filtered and washed. The powder thus obtained is heated in furnace. [1-3]

(3). Precursor method: In this method analytical grade nitrates are taken in required proportion and the mixer is dissolved in distilled water. The solution so obtained is heated at 40-50°C for about halfan hour. The dried citrate mixture is calcinated for two hours at about1000^{o}C.[4-6]

(4). Sol gel method: The sol gel method involves the forming of a concentrated sol of the reactant oxides or hydroxides and conversion of sol into a semi-rigid gel by removing the solvent .The gel is crushed and sintered in a furnace [7-9].

(5). Combustion method: The nitrates in required proportion are mixed and dissolved in deionized water to get precursor solution. The precursor is concentrated in a hot porcelain crucible for water evaporation. This dried precursor solution under goes spontaneous combustion or ignition within a second [10-13].

3.2.2 Ceramic method

Ceramic method is based on solid state reaction mechanism and is the most commonly used technique. It is known as double sintering ceramic method. It comprises the two stages; one is presintering and another is final sintering. Before pre-sintering the high purity analytical grade oxides are taken in the required stoichiometric proportion and then are mixed well in order to get the homogenous mixture. The small crustal size is essential for the good contact of reacting oxides. The smaller particle size can be achieved with the help of grinding by using ball- mill or agate mortar and pestle for sufficiently longer time. The second thing

is the higher density of the homogenous mixture for good reaction which also minimizes the porosity level. The pellets are made of the homogenous mixture (in powder form) by applying a suitable pressure to achieve high density. Sometimes hot pressing is used to make the pallets. The suitable binder like polyvinyl alcohol or acetone may be used. These pallets are pre-sintered at the elevated temperature (950^0C). The purpose of pre-sintering is to decompose the higher oxides and to assist in homogenizing the material as well as to reduce the effect of variations in the compositions of the raw materials [14]. The pre-sintering also reduces or controls the shrinkage of the material, which occurs otherwise during the final firing.

The pre-sintered pellets are ground again by using ball – mill or agate mortar and pestle for sufficiently longer time. Solids don't react together at room temperature over normal time scales.The nucleation in case of solid state reaction is difficult because ofthe following factors.

(a) The considerable differences in structure between reactants and product.

(b) The large amount of structural reorganization is involved informing the product: bonds must be broken and reformed and atomsmust migrate over considerable distances. Therefore only at high temperatures such ions do have sufficient thermal energy to jump outof their normal lattice sites and diffuse through the crystal to yield final product [15]. Therefore it is necessary to heat them at elevated temperature usually 1000° c to 1500° in order to bring about there action at an appreciable rate.

The inter-diffusion of cations through the final product layer is indeed the rate-controlling step. In the simple case of lattice diffusion through a planner layer, parabolic rate law of the followingform governs diffusion.

$$Dx/dt = k.\ x^{-1} \text{ or } x= (k^{/}\ t)^{1/2} \quad \ldots\ldots\ldots\ldots\ldots\ldots\ldots\ldots\ldots\ldots(3.1)$$

Where x is the amount of reaction (i.e. thickness of the growingspinel layer), t is time and k. K are rate constants.

The reaction occurs much more quickly with increasing temperature. The final sintering brings about the nucleation of product in solid state reaction. The nucleation of the product involves some reorganization of the oxide ions at the site of the potential nucleus together with the interchange of cations of reactants across the interface between reactants. There are some subsequent stages involving growth of the product layer. When growth tends to thicker layer, a counter diffusion of cations occurs through the exiting product layer and at this stage there are two reaction interfaces. This mechanism is known as Wagner reaction mechanism. The final sintering is done for longer period (From 24to 48 hours). Finally thesample is cooled either at certain rate or at the natural rate after switching off the furnace. The sample may be quenched to room temperature to get desired phase. Thus the compound is synthesized by ceramic method.

3.2.3 Synthesis of the systems

The base system was synthesized to study its magnetization.The maximum saturation magnetization was considered to select the proportion of nickel and magnesium. The eleven samples of the system $Ni_{1-x}Mg_xFe_2O_4$ were prepared with x = 0.0 to 1 in the step of 0.1 using double sintering ceramic technique.

The starting materials were of analytical grade high purity oxides such as NiO, MgO and Fe_2O_3 (MERCK). They were taken instoichiometric proportion by weighing with sensitive balance and were ground thoroughly. The pre-sintering is carried out using a programmable furnace namely Thermolyne (Model-1500,U.S.A.made) at 900°C for 24 hours. The samples then were cooled slowlyto room temperature. Pellets of 1 cm diameter of the powder have been made by cold pressing, applying the hydraulic pressure of 5tones/inch? The good quality pelletes have been obtained by usingPVA as binder and maintaining the pressure for about ten minute seach time. The presintered pellets were again ground to fine powder. Then the powdered samples were pelletized again using hydraulic pressure machine by applying pressure of 5 tones/ inch and polyvinyl as a binder. The pellets were finally sintered at 1050°C for 30 hours. Then they were cooled to room temperature at its natural rate.

The systems $Ni_{0.}7Mg_{0.3}Al_{xFe}2\text{-}xO_4$ and $Ni_{0.7}Mg_{0.3}Cr_xFe_{2-x}O_4$ have been synthesized by the same ceramic technique. Six samples of each systems were prepared where x= 0.0 to 0.5 in step of 0.1. Here also AR grade oxides were used. The rest preparation process was similar to that of the base - system,

3.3.1 X-ray Diffraction

The crystalline material consists of atomic or molecular arrays. In crystals the atoms or molecules are arranged in one of the Bravice lattices. The various techniques, such as x ray diffraction, neutron diffraction, Mossbauer-spectroscopy, can be used for the structural characterization of such material.

X-ray diffraction plays a very important role for obtaining the structural information of a crystalline material. Both qualitative and quantitative measurements of various parameters can be obtained by using X-ray diffraction method [16]. Each crystalline solid has its own characteristic x-ray powder pattern, which may be used as a finger print for its identification. X-rays are electromagnetic radiations of wavelength in the range of 0.5 -2.5 °A. The interplaner distance in the solid crystalline material lies within the range of x-ray wavelength, which is suitable for diffraction. Laue and Bragg suggested x-ray diffraction technique. When a crystal is exposed to the x-rays, the atoms in the crystal are excited by absorbing x-ray radiation and re-emit them in a specific way. The X-ray diffraction is based on the constructive interference of x-rays scattered from atomic planes of the crystal. [17] The condition of diffraction proposed by Bragg is given by

$$2d\sin\theta = n\theta \quad \ldots\ldots\ldots\ldots\ldots\ldots\ldots\ldots\ldots\ldots.. (3.2)$$

where d is inter-planer distance, θ is the angle of diffraction , n is an order of diffraction and 2 is wave length of incident x-rays. The intensity of each x-ray diffraction line is the total effect of scattering by electrons, scattering by nuclides and scattering by unit cell (scattering due to atomic array in the cell) of the crystal [18].

In scattering phenomenon particularly electric field is concerned. A beam of x-rays carries energy and the rate of flow of this energy through unit area perpendicular to the direction of motion of the wave is called intensity. The average value of the intensity is proportional to the square of the amplitude of the wave. In absolute unit the intensity is measured in ergs/cm^2/sec, but practically intensity is measured on a relative basis.

[i] Scattering by electron

The scattering intensity by electron is given by Thomson equation as,

$$I = \frac{I_0 e^4}{r^2 m^2 c^4}\left(\frac{1+cos^2 2\theta}{2}\right) \ldots\ldots\ldots\ldots\ldots\ldots\ldots\ldots\ldots\ldots..(3.3)$$

where , I. is intensity of incident beam, e is charge an electron , r is distance from electron to the point where intensity is measured, m is mass of electron, c is velocity of light and 0 is angle of diffraction. The intensity of the scattered beam is only a minute fraction of the intensity of the incident beam. The intensity decreases, as the inver sesquare of the distance from the scattering atom and the scattered beamis stronger in forward or backward directions than in a direction at right angles to the incident beam. The factor $\frac{1+cos^2 2\theta}{2}$ is called the polarization factor and it enters in equation because the incident beam is unpolarized. The Compton modified radiation occurs due to Compton Effect. In Compton Effect the scattering is in backward direction. There is an increase in the wavelength, which depends only on the scattering angle. The radiation so scattered is called Compton modified radiation but its phase has no fixed relation to that of the incident beam. It is incoherent radiation. It cannot take part in diffraction due to phase mismatch. Compton modified scattering cannot be prevented and it has the undesirable effect of darkening the background of diffraction pattern [17].

[ii] Scattering by atom

Nucleus of atom bears a charge and is capable to oscillate under the influence of the incident beam. However, nucleus is extremely heavy as compared to electron and it cannot be made too scillate to any appreciable extent. The net effect is coherent scattering by an atom. The waves scattered in forward direction are in phase where as the waves scattered in the rear direction have certain phase difference. Consequently the amplitude of the wave scattered in forward direction is more. The efficiency of scattering of a given atom in a given direction is known as atomic scattering factor. It is defined as a ratio of amplitudes.

$$f = \frac{\text{Amplitude of the wave scattered by an atom}}{\text{Amplitude of the wave scattered by one electron}} \ldots\ldots\ldots\ldots\ldots\ldots\ldots\ldots\ldots\ldots\ldots..(3.4)$$

f = z (atomic number) for any scattering in the forward direction. As θ increases, however, the waves scattered by individual electrons become more and more out of phase and f decreases. The atomic scattering

factor also depends on the wavelength of the incident beam. For a fixed value of θ, f is smaller for shorter wavelength.

[iii] Scattering By Unit Cell: There is a coherent scattering due to atomic positions in a unit cell and if Bragg's law is satisfied, the diffraction occurs in certain directions. Since the crystal is merely are petition of the fundamental unit cell, it is enough to consider the way in which the arrangement of atoms within a single unit cell affects the diffraction intensity [19]. The phase of the waves scattered by individual atoms of a unit cell depends on the arrangement of the atoms. The resultant wave scattered by all atoms of the unit cell is called the structure factor F which is defined by [20]

$$f = \frac{\text{Amplitude of the wave scattered by all the atoms of a unit cell}}{\text{Amplitude of the wave scattered by one electron}} \quad \ldots\ldots\ldots\ldots\ldots\ldots \text{(3.5)}$$

The scattered wave by a unit cell can be expressed in complex exponential form as given below,

$$Ae^{i\phi} = fe2^{\Pi i(hu+kv+lw)} \quad \ldots\ldots\ldots\ldots\ldots\ldots\ldots\ldots\ldots\ldots\ldots\ldots\ldots\ldots \text{(3.6)}$$

where, A is amplitude, f is atomic scattering factor ,ϕ is angle related to phase , uvw are co-ordinates of atom and h, k, 1 are integers.

The resultant wave is obtained by simply adding together all the waves scattered by the individual atoms. If a unit cell contains atoms 1,2,3...,N,with fractional coordinates $u_1v_1w_1$, $u_2v_2w_3$,$u_3v_3w_3$,… and atomic scattering factors $f_{1,}f_{2,}f_{3,}$ then the structure factor for the hkl reflection is given by

$$F=f_1e^{2\Pi i(hu1+kv1+lw1)}+f_2e^{2\Pi i(hu2+kv2+lw2)}{}_{+} \ldots\ldots\ldots\ldots\ldots\ldots\ldots\ldots\ldots\ldots\ldots\ldots \text{(3.7)}$$

This can be written in more compact form as,

$$F_{hkl} = \sum_1^N f\ n\, e^{2\Pi i}(hu_n + kv_n + lw_n) \quad \ldots\ldots\ldots\ldots\ldots\ldots\ldots\ldots\ldots\ldots \text{(3.8)}$$

Which indicates the summation extending over all the atoms of theunit cell [21].

The intensity of diffracted beam by all the atoms of the unit cell in a direction predicted by Bragg's law is proportional simply to$|F_{hkl}|2$. Thus the knowledge of atomic positions is essential for determining the scattering factor to calculate X-ray intensity of reflecting plane. The structure factor is independent of the shape and size of the unit cell. The reflections occur for unmixed indices or mixed indices depending upon the structure of the crystal.

For present investigation powder method is employed for x- ray diffraction. There are six factors affecting the relative intensity of the diffraction lines on a powder pattern:

1. Polarization factor
2. Structure factor
3. Multiplicity factor
4. Lorentz factor
5. Absorption factor
6. Temperature factor

(i) Polarization factor

The beam received from x-ray tube is unpolarized. A focusing monochromator is used to get a beam of monochromatic xray. The beam received from the focusing monochromator is partly polarized before it reaches the specimen and it also gets polarized partially by diffraction process. Thus polarization factor depends on the type of monochromator and the angle of diffraction

(ii) Structure factor

The structure factor depends on the atomic positions in acrystal cell as well as the type of the atoms in it.

(iii) Multiplicity Factor

The relative proportion of planes contributing to the reflection enters in the intensity equation as multiplicity factor. It is defined as the number of different planes in a form having the same spacing. Multiplicity factor depends upon the crystal system.

(iv) Lorentz factor

This factor is related to intensity distribution of reflection within certain range of angle around the exact Bragg angle. The intensity is the greatest at the exact Bragg's angle at which the Bragg's Law is exactly satisfied. If all the diffracted beams sent outby the crystal as it rotates through the Braggs angle are received in acounter, the total energy of the diffracted beam can be measured.This energy is called the integrated intensity of the reflection and isgiven by the area under the curve-plotted intensity versus diffraction angle.

The maximum intensity in diffraction depends on theangular range of crystal rotation over which the energy diffracted in the direction ϕ_B is appreciable. The maximum intensity is large at low scattering angles and small in the back-reflection region and dependson $1/\sin\phi_B$. Polarization factor and Lorentz factor are combined to get Lorentz polarization factor.

(V) Absorption

Absorption of x-ray takes place in specimen that decreases the diffracted intensity. Backward reflected beams undergo very little absorption but forward-reflected beams have to pass through whole specimen and are greatly absorbed. Absorption and temperature effects are ignored.

In the powder method monochromatic X-ray beam is made incident on the specimen. Each particle of the crystal specimen (i.e.in the form of powder) is oriented at random with respect to the incident beam. Some of the particles are correctly oriented and can reflect the incident beam while other will reflect for other planes.

When a beam of monochromatic x-rays falls on a crystal, each atom becomes a source of scattering radiation. In crystal there are certain planes which are particularly rich in atoms. The combined scattering of x-rays from these planes can be looked upon as reflections from these planes. The Bragg scattering is regarded as Bragg reflection. Hence the planes showing Bragg reflections are known as Bragg planes. At certain glancing angles, reflections from these sets of parallel planes are in phase with each other and hence they reinforce each other to produce maximum intensity. For other angles, the reflections from different planes are out of phase and consequently they reinforce to produce either zero intensity or extremely feeble intensity.

There are three different methods such as Lau method, rotating crystal method and powder method for X-ray diffraction.

3.3.2 X-Ray diffractometer

The X-ray diffraction is brought about with the help of diffractometer. The essential features of a diffractometer are shownin figure [3.1]. The powder specimen C in the form of flat plate is supported on a table H, which can be rotated about an axis O perpendicular to the plane of the drawing. S is the x-ray source. The position of the source is in such a way that it is suitable to bring about the focusing of the beam at the target. (Line focal spot). The source is also normal to the plane of the drawing and therefore parallel to the diffractometer axis O. The x-rays diverge from thissource and are diffracted by the specimen to form a convergent diffracted beam, which comes to a focus at the slit F and then enters the counter G. A and B are special slits which define and collimatethe incident and diffracted beams.

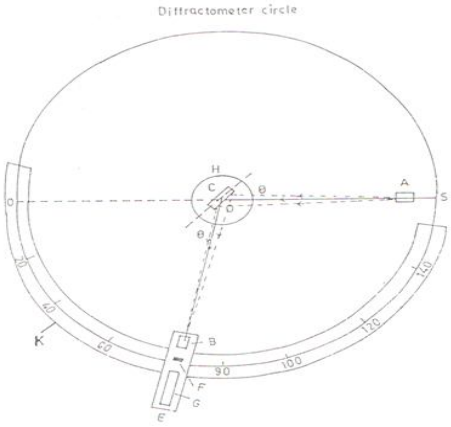

Fig 3.1 Schematic diagram of x-ray diffractometer

The receiving slits and counters are supported on the carriage E, which may be rotated about the axis O and whose angular position 20 may be read on the graduated scale K. The E and H are mechanically coupled so that a rotation of the counter through 2x degrees is automatically accompanied by rotation of the specimen through x degrees. This coupling preserves focusing conditions.The counter is power-driven at a constant angular velocity about the diffractometer axis. The succession of current pulses is converted into a steady current, which is measured on a rate meter called a counting rate meter, calibrated in such a count (pulses per second). Such circuit gives a continuous indication of x-ray intensity. The counter is set at 2θ and is connected to a counting rate meter. The sample table and counter are simultaneously rotated. Thus the sample is scanned.

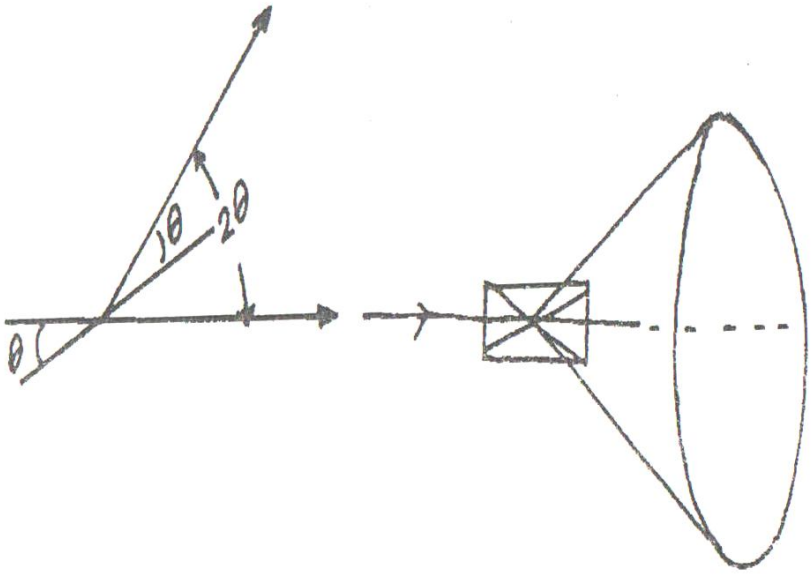

Fig 3.2 Bragg's angle and cone of diffraction

The powder method is employed for present investigation to study structural aspect of the specimen. The specimen used was inthe form of a fine powder. The powder contains tiny crystallites with random orientations with respect to the incident beam and almost all the possible θ and d values are available. Consequently every set of lattice planes are capable of reflection. The mass of powder is equivalent, in fact, to a single crystal rotating about all possible axes. The reflected beam from certain plane (hkl) makes the correct Bragg such a way that angle. If this plane is rotated about the incident beam as an axis in is kept constant, then the reflected beam travel sover the surface of a cone as shown in fig [3.2]. The axis of the conecoincides with the transmitted beam. The hkl reflection from a stationary mass of powder has the form of a cone of diffracted radiation and a separate cone is formed for each of differently spaced lattice planes.

Phillips diffractometer (model-3710) at USIC, Shivaji University Kolhapur is used for X-ray diffractogrammes. The X-ray diffraction is taken with following considerations

1). Target Cuka

2). Scanning rate 1° per minute

3). Rang of 20 is 20° to 70°.

4). Count rate of 4x108 counts/sec.

Lattice parameter, X-ray density and particle size have been determined using X-ray diffraction pattern. For spinel ferrite having cubic structure the inter-planer spacing d_{hkl} is obtained using the following relation

$$d_{hkl} = \frac{a}{\sqrt{h^2+k^2+l^2}} \quad \text{.....(3.9)}$$

where a is lattice constant and (hkl) are Miller indices.

Using Bragg's Law the Miller indices for cubic system are given as

$$h^2 + k^2 + l^2 = 4a^2 \frac{sin^2\theta_{hkl}}{\lambda^2} \quad \text{..... (3.10)}$$

Where λ is wavelength of incident x-rays, $(h^2 + k^2 + l^2)$ is always an integer while $4a^2/\lambda^2$ is constant for any one pattern.

The lattice parameter 'a' can be determined using the following formula,

$$a = \sqrt[d]{N} \quad \text{..... (3.11)}$$

where $N = h^2 + k^2 + l^2$) and d is inter-planer distance. The X-ray density (dx) can be computed using the following relation.

$$d_x = \frac{8M}{Na^3} \quad \text{.....(3.12)}$$

where M is Molecular Weight of sample and N is Avogadro's number (6.023 x 10^{23})

The cation distribution amongst the tetrahedral (A) site and octahedral (B) site can be calculated using the X-ray intensity ratio.

The intensity of any reflection can be calculated by using the relation given by Burger (22-24),

$$I_{hkl} = |F_{hkl}|2P\ L_P \quad \text{..... (3.13)}$$

where,

$$L_p = \frac{1+cos^2 2\theta}{sin^2\theta.cos^2\theta} \quad \text{..... (3.14)}$$

And is called Lorentz Polarization factor, P is multiplicity factor and F_{hkl} is structure factor.

In the intensity calculations for different planes the absorption and temperature factors have not been taken into consideration because absorption factor decreases the intensity of diffracted beam and temperature factor is negligible due to high melting point of (spinel ferrite) mixed magnetic oxides. The amplitude of the vibrations of the atoms does not vary as compared to the amplitude at absolute zero temperature.

The structure factor is F is a function of oxygen parameter uand the distribution parameter y. The formulae for the structure factors for the planes (hkl) are taken from those repeated by Furuhashi et al [25-27]. The multiplicity factor and Lorentz polarization factor are taken from the literature [28-30]. The structure factors for spinel structure are given as,

$$F_{220} = 8f_a + 16f_0(1 + cos2\Pi 4u) \quad \text{.....(3.15)}$$

$$F_{311} = 4f_a + \frac{8}{\sqrt{2}}f_b + 32f_0(cos6\Pi u.cos^2 2\Pi u - .sin^2 2\Pi u) \text{.....(3.16)}$$

$$F_{400} = 8f_a - 16f_b - 32f_0(cos8\Pi u) \text{.....(3.17)}$$

$$F_{422} = 8f_a + 0f_b + 32f_0(cos8\Pi u.cos^2 4\Pi u) \text{.....(3.18)}$$

$$F_{440} = 8f_a + 16f_b + 32f_0(cos^2 8\Pi u) \text{.....(3.17)}$$

where F_{hkl} are total structure factors for hkl plane, f_a, and f_b are the atomic scattering factors for tetrahedral and octahedral site respectively, f_o is atomic scattering factor of oxygen and u is an oxygen parameter (ideal value is 3/8). The single phase formation forthe present systems have been confirmed by using X-ray diffractograms. The intensity calculations have been carried out for both the systems. The structure sensitive plane ratios have been considered to decide the cation distribution.

3.4 I R-Spectroscopy

The atoms in solids vibrate at frequencies of approximately 10^{12} to 10^{13} Hz. The vibration modes involving pairs or groups of bonded atoms can be excited to higher energy states by absorption ofradiation of appropriate frequency. The electromagnetic radiation whose wavelength lies in the range 0.72μ (micron) to approximately 10004 μis known as infrared radiation. The entire infrared regioncan be divided into three regions.The region of electromagnetic radiation whose wavelength lies from 0.72μto 15μis called near infrared region

The second region of the radiation whose wavelength lies from 1.5μ to 20μ is called middle infrared region. The third region radiation whose wavelength lies from 20μ to 1000μ is called farinfrared region. The near infrared and far infrared regions are leastused for spectroscopic purpose because absorption of organic molecules in these regions is very small. The middle region is foundto be very useful for studying the symmetry of molecules.

When a molecule (or atom) interacts with electromagnetic radiation of the proper frequency (10^{12} to 10^{13} Hz) , it absorbs energy and the molecule is set into vibrations. If the transmission energy is plotted as the function of radiation frequency the energy distribution shows absorption at certain frequency.

The IR spectroscopy is used to determine the local symmetry in crystalline & non-crystalline solids. It helps to study the ordering phenomenon in ferrites, deformation of cubic spinel and force constant. Four IR bands v_1, v2, v3, v4 are observed in case of spinel ferrites. These are attributed to local symmetry of tetrahedral and octahedral sites in the unit cell.

Waldron [28] is the first to report the infrared spectra ofspinels. He found the four infrared active modes. Two of them, having the higher frequency, were supposed to arise from the motionof the oxygen ions, and the remaining two were assigned to the motions of the cations only. Later on White, De Angelis and Lutzusing group theory and considering the full cubic crystallographic unit cell(whereas Waldron considered rhombohedral unit cell) confirmed the four modes but the origin of the modes was found to be more complex. Very thorough investigation of infrared spectra of normal spinels was done by Preudhomme and Tarte [29]. They assigned the higher frequency band (600 cm^{-1}) to tetrahedral site andthe lower frequency band (400 cm^{-1}) to octahedral site.They also noticed the gradual increase in the absorption of higher frequencies. Hafher, Trate and others [30-31] applied IR spectroscopy to investigate the absorption bands in many normal as well as inverse spinel.

The third mode of vibration has been observed by Braberset al [32] in case of $MnFe_2O_4$ at 335 cm^{-1}. The bands in the region300 - 700 cm^{-1} are assigned to the fundamental vibrations of the ionsof the crystal lattice.
Thus infra-red spectroscopy is useful to understand the structure-based properties of the specimen. In case mixed magnetic oxides, which crystallize in face centered cubic spinel structure, the electric and magnetic properties of these materials are decisively dependent on the precise cationic & anionic positions inthe crystal. In such cases the vibration, electronic and magnetic dipole spectra can give information about the position & valency of the ions in the crystal lattice. The frequencies of the vibration dependon the cation mass, the lattice parameters, the cation oxygen bonding force and its bond length. IR - spectroscopy is used, to study cationic order, coordination number and deformation produced due to the accommodation of cations in the spinel structure.

The IR spectra in the range of 200-800 cm^{-1} were recorded at room temperature on the infrared spectrometer (mode1783, Perk inElmer). For recording IR spectra, powders were mixed with KBr inthe ratio 1: 250 by weight to ensure uniform dispersion in the KB_rlet. The mixed powders were then pressed in a cylindrical die to obtain clean discs of approximately 1- mm thickness.

The force constants K_t, and k_o, have been determined from IR absorption data using analysis of Bruesch et al [33], Lutz et al [34]and Lauwers et al [35]. The force constants of tetrahedral (k_t) and octahedral (k_t) complexes have been determined by using thefollowing relations.

$$k_t = (0.04416)(\upsilon_1^2)(M_2)\left[\frac{V}{V+3}\right] \quad \ldots\ldots (3.19)$$

$$k_o = (0.94218)(\upsilon_2^2)(M_1)/[M_1 + 32] \quad \ldots\ldots (3.20)$$

in which

$$V = 64 - \lfloor 2 \times M_1 \times U \rfloor / M_2 \ldots\ldots (3.21)$$

And

$$U = \frac{2k_0}{\upsilon_1^2 M_1 - 2k_0} \quad \ldots\ldots (3.22)$$

where, M_1 is molecular weight of cations at A-site , M_2 is molecular weight of cations at B-site, v_1 and $_{v2}$ are absorption bands attributed to tetrahedral and octahedral sites respectively. (Higher frequencyband corresponds to tetrahedral and lower frequency band corresponds to octahedral complexes.The molecular weights attetrahedral (M_t) & molecular weight at octahedral (M_0) have been calculated by using X-ray diffraction and magnetization data.

The values of bond lengths R_A and R_B have been computed using the formula given by Jan Smith [36] as,

$$R_A = (\delta + \tfrac{1}{8})a\sqrt{3} \quad \ldots\ldots (3.23)$$

$$R_B = (3\delta^2 - \tfrac{\delta}{8} + \tfrac{1}{16})1/2_a \quad \ldots\ldots (3.24)$$

where a is lattice parameter and 8 is equal to the difference between observed oxygen parameter and ideal oxygen parameter (U_{obs}.-U_{ideal}).

3.5.1 High Field Magnetization

The hysteresis loop study furnishes the information aboutthe magnetic properties such as saturation magnetization, coercivity, retentivity, energy loss, magnetic stwiching states of the materials, magnetic hardness & softness of the material. Hysteresis loop tracer technique is powerful device to study the saturation magnetization. If we apply magnetic field, the average magnetization perunit volume may take any value between zero to its saturation magnetization. When a magnetizing field is small enough, the induced magnetization varies linearly with the field and is reversible. When the field is steadily increased, however, the magnetization process becomes irreversible. With increasing field, the magnetization steadily increases and attains a saturation value for aparticular value of the applied field.(Magnetizing field). This maximum value is called saturation magnetization.[37] When the field is decreased after reaching the saturation magnetization, the decrease of magnetization follows another path and when the field is reduced to zero, a certain amount of magnetization is still retained by the sample. This is called remanent magnetization. The demagnetizing field to remove the remanent magnetization is called coereive force. If the field is further increased in the opposite direction, the sample gets saturated in the opposite direction. Thus for a complete cycle of magnetization a hysteres is loop is obtained as shown in figure3.3. The hysteresis loop property can be explained using the domain theory. According to Weiss theory [38], the exchange interactions between neighboring dipoles in materials containing permanent atomic magnet generate an internal exchange field, which align them in a particular direction. Thus in material there are regions which are spontaneously magnetized by such exchange field [39].These spontaneously magnetized regions are called domains magnetic moment vectors of different domains are randomly oriente so that no net magnetization is produced in the material as a whole (The magnetization may vary domain to domain). However, in the presence of an

external magnetic field, the effective magnetic moment in the domains gets aligned in the direction of the field and the domain begins to grow at the expense of those pointing in other directions, which results in some non-zero magnetization in thematerial [40].

When a small magnetic field is applied across a ferrimagnetic material, the domains pointing almost along the direction of the field grow at the expense of the domains having opposite orientation thus resulting in a small magnetization as indicated by the initial portion (OA) of the hysteresic curve. Such displacements of domain boundaries are mostly reversible and hence the portion OA of the curve is also reversible. As the field increases a large number of domains grows favorably which results in a large increase in magnetization (portion AB). The boundary displacements in these regions are often large and irreversible. The growth of domains continues until the favorable domains grows up to the maximum extent with their magnetization vectors still pointing along the socalled easy directions of magnetization. As the field increases further the domains rotate from there; the magnetization increases slowly (Portion BC) and finally attains a saturation value Bs when all the domains point along the direction of the field. On decreasing thefield, the magnetization does not follow the same path because the aligned domains do not regain their random state of orientation easily. There exists some non-zero magnetization even after removing the field altogether. This magnetization is called the remnant magnetization or remanence (B_r). The magnetization can be reduced to zero by applying a reverse magnetic field known as the coercive field. . A similar variation in the reverse magnetization is observed as the reverse field is first increased and then decreased.The closed loop CEFGC is called hysteresis loop, the line CI in this curve is never parallel to the field axis.

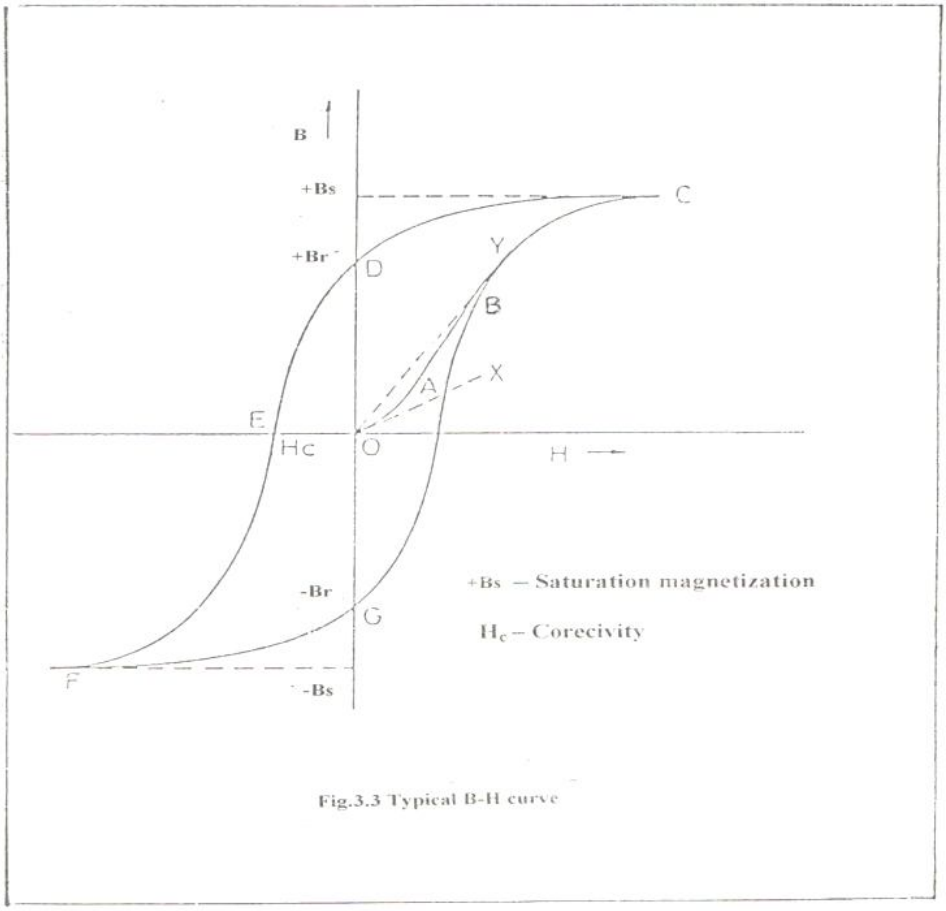

Fig.3.3 Typical B-H curve

Thus the hysteresis loop reveals the saturation magnetization which is the quality of magnetic material. The hysteresis loop also gives information about magnetic losses. The rectangular shape of a hysteresis loop gives the information about the switching magnetic states of magnetic material.

3.5.2 Hysteresis Loop Technique

The values of saturation magnetization (σ_s) & magneton number (η_B), the saturation magnetization per formula unit in Bohrmagneton, of all the samples are carried out using the high field hysteresis loop technique at room temperature. The experimental setup is shown in figure 3.4 .The experimental setup consists of an electromagnet, pick up coil, phase correcting network, integrating network, amplifier and cathode ray oscilloscope.

(1) Electromagnet

It is an U shaped yoke made up of high permeability iron A copper wire is wound on it. This yoke produces magnetic field between the pole pieces. The magnetic field thus produced can bevaried up to 5 Koe with the help of varying the alternating current.The magnetic intensity is calibrated as 100 mA current is equal to1Koe.

(2) The pick up coil

The pick up coil consists of two coils with equal areas and turns of copper wire. The pick up coil is interposed between the poles of electro-magnet. There is a gap in the middle of the coils and the sample in form of pellet is inserted in one of the coils. The terminals of the pick up coil are connected to the cathode ray oscilloscope.The field between the pole pieces changes continuously with the change in the alternating current. This makes the magnetic flux of the magnetic sample to change. This result in developing a voltage in the pick up coils, which gives magnetizing cycle to the sample inserted.

With the help of phase correcting network, integrated network, amplifier and C. R. O. the hysteresis loop is traced on the C.R. O monitor. First of all the calibration is done using the standard sample of Ni powder with the help of which magnetization values for other samples are determined. Ni pellet has saturation magnetization of 54.39 emu/gm. The magnetization is noted on the Y-axis of CRO.

The saturation magnetization can be determined with the help of theloop appeared on the CRO.

The calibration factor for Ni sample is given by

$$CF = \frac{Standard\ magnetization\ for\ Ni \times mass\ of\ Ni}{Vertical\ displacement \times volt\ per\ div.on\ C.R.O.} \quad \ldots\ldots\ldots\ldots\ldots\ldots\ldots\ldots\ldots\ (3.25)$$

The vertical displacement (h) in terms of mV is taken at roomsample and saturation magnetization calculated using the following relation,

$$\sigma = \frac{h \times volt\ per\ div.on\ C.R.O. \times CF}{mass\ of\ pallet} \quad \ldots\ldots\ldots\ldots\ldots\ldots\ldots\ldots\ldots\ldots\ldots\ldots\ldots\ldots\ldots (3.26)$$

The magnetic moment per formula unit in Bohr magneton (n_B) is given by

$$n_B = \frac{\sigma \times molecular\ weight\ of\ the\ sample}{5585} \quad \ldots\ldots\ldots\ldots\ldots\ldots\ldots\ldots\ldots\ldots\ldots\ldots\ldots\ldots\ (3.27)$$

The measurement of saturation magnetization is carried out by usingthe above method and formulae.

3.6.1 Low field ac susceptibility

The measurement of low field ac susceptibility of magnetic material is indispensable to extract information regarding physical, chemical & magnetic state of the substance. If a magnetic material issubjected to magnetic field, it gets magnetized. The magnetization is measured in terms of magnetic moments per unit volume. This magnetization depends on the magnetization field.

$$M \propto H\ i.e. M = \chi H$$

Or

$$\chi = M/H\ emu/cm^3 \ldots\ldots\ldots\ldots\ldots\ldots\ldots\ldots\ldots\ldots\ldots\ldots\ldots\ldots\ldots\ (3.28)$$

where M is magnetic moment per unit volume,H is magnetizing field and χ is susceptibility (volume susceptibility). The volume susceptibility (χ) is defined as the ratio of the magnetization M produced in a substance to the magnetizing field to which it is subjected. The mass susceptibility is related to volume susceptibility by following relation,

$$\chi_m = \frac{\chi}{\rho} emu - gm^{-1} \quad \text{.....(3.29)}$$

where ρ is density of the material.

The mixed magnetic oxides exhibit a substantial spontaneous magnetization at room temperature like ferromagnetic materials.They consist of self- saturated domains and exhibit the phenomenon of hysteresis. The saturation magnetization is temperature dependent.The ferrites show the paramagnetic behavior after Curie temperature.The susceptibility is temperature sensitive and its variation gives the information about magnetic structure of the sample. The susceptibility of ferrites becomes infinite at Curie temperature.

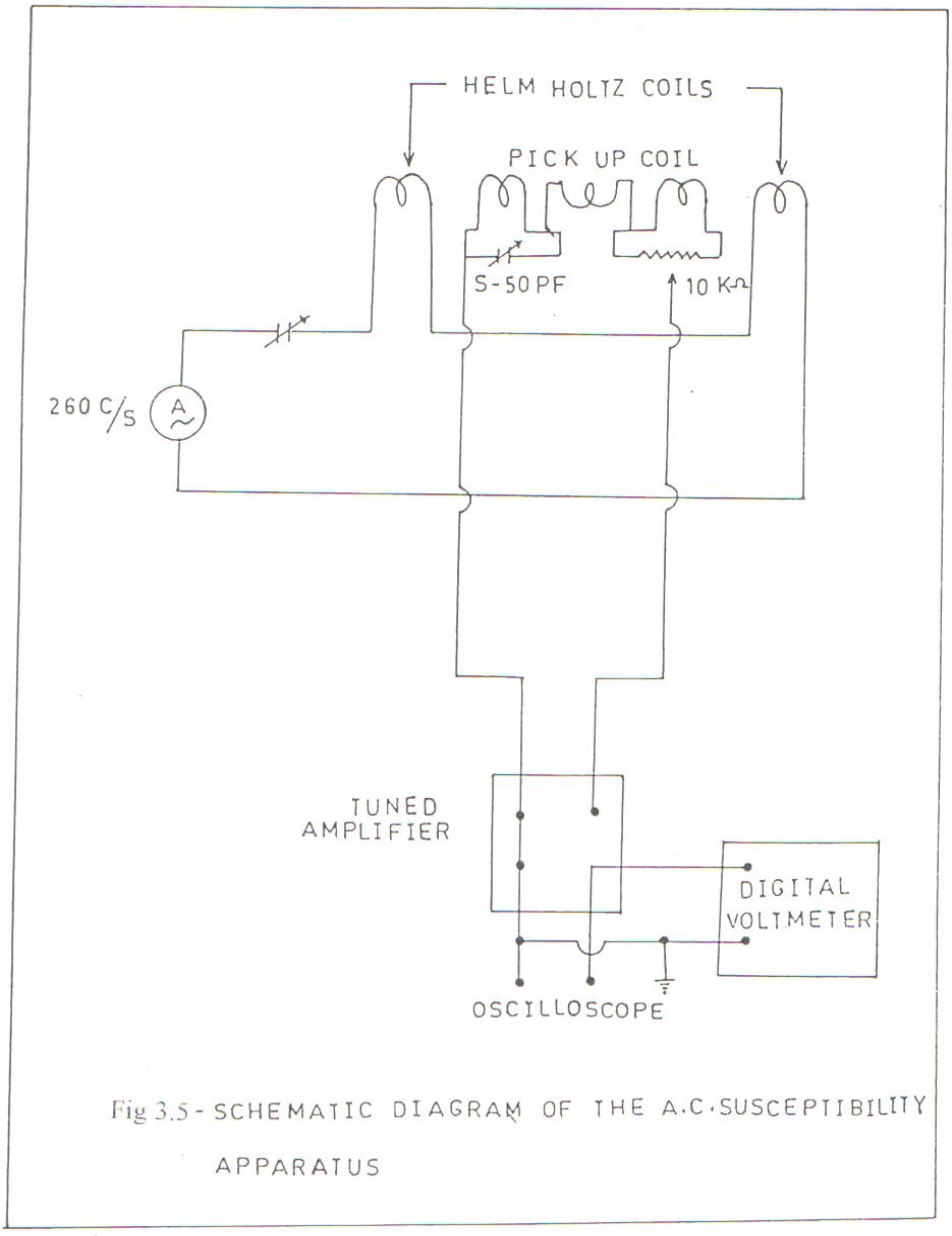

Fig 3.5 - SCHEMATIC DIAGRAM OF THE A.C. SUSCEPTIBILITY APPARATUS

The susceptibility variation with temperature gives information about whether the material consists of single domain,multi-domainor super-paramagnetic domain. A tailing effect is observed when sample shows transition from ferrimagnetic to paramagnetic state. The tailing effect is due to short range spin ordering. The susceptibility is directly proportional to magnetic moment & inversely proportional to coercivity of the material. When thermal energy is equal to volume energy the single domain (SD) particle becomes super paramagnetic (SP) and its magnetic moment spontaneously fluctuates between easy directions which gives zero coercivity and as a result the peaking effect is observed in the nature of χ versus T plot.[41-43]

3.6.2 Double Coil Setup

The measurement of susceptibility with respect to temperature is done with the help of double coil setup. The schematic diagram of the double coil setup is shown in figure 3.5. It consists of Helmoltz coil, pickup coil, and furnace and sample holder.

(1) Helmoltz coil

The two coils are made up of 100 turns of 175WG enameled copper wire wound on wooden stool of mean diameter 74cm. The two coils are fixed on wooden base such that a distance equal to their radius separates them.

(2) Pickup coil

The pick up coil consists of two coils. These are connectedin series and wound in opposite directions. The turns are in such away that e.m .f. induced in them, nullify each other. Third winding is of 10 kΩ from which a variable voltage of either polarity could be obtained. The voltage of right polarity and magnitude is fed in series with the main windings. This voltage is not balanced. An e. m. f. is produced due to small phase difference arising from the self-capacitance of the small windings. The e. m. f. induced in the coil is proportional to the magnetic moment of the dipole. It is preferable touse a higher frequency of the magnetic field for better sensitivity.The use of higher frequency is limited by resonance effect in the double coil. A signal of 260Hz frequency is used.

(3) Furnace

The furnace is made of 24SGW platinum wire wound in a non-inductance way. The coil is kept inside a multiple tube of diameter which is insulated properly on the outside by asbestos sheets. It is surrounded by glass jacket through which water can be circulated. This prevents overheating of the coils when the furnace is kept on. The temperature of the furnace is measured with the help of Pt-Rh thermocouple.

(4) Sample holder assembly

The sample holder is a quartz tube of about 30cm long and 1.5cm in diameter.The thermocouple is inserted into the tube in sucha way that it touches the sample. The sample placed inside thesample holder is heated gradually and at various temperatures the signals corresponding to the magnetic moment are recorded. The measurements are carried out from the room temperature upto Curietemperature (TC).

3.7.1 D. C. Resistivity

The ferrites have high resistivity up-to $10^{11}\Omega$-cm.The conventional band theory cannot account for such a high resistivity. An extensive investigation into the origin of the electrical conductivity of spinels has been carried out by Verwey et al [44] and later by Van Uitert [45] and Jonker[46]. In spinel ferrites the ionictypes of bonds are prevalent. The electrostatic interaction between conduction electron (or holes) and near by ions may result in apolarization and the carrier becomes situated at the center of polarization potential well which is deep enough to trap the carrier ata lattice site. Thus the charge carriers are localized. However due to the thermal excitation that causes the lattice vibrations the ions occasionally come close enough together and there is a considerable high probability of jumping of electrons to neighboring sites. Such aprocess of jumping electrons at thermal excitation is called hopping mechanism. Thus only the lattice vibrations induce the conduction by thermal energy and the resistivity ρdc becomes temperature dependence. It decreases with increase in temperature and is given by

$$\rho_{dc=\rho_0 exp\left(\frac{\Delta E}{k_B T}\right)} \ldots\ldots\ldots\ldots\ldots\ldots\ldots\ldots\ldots\ldots\ldots\ldots\ldots\ldots\ldots (3.30)$$

where p is the temperature dependent constant and AE is activation energy. The d.c. resistivity shows the kinks at the Curie temperature of the ferrites. The activation energy can be determined with help of plots of log ρ_{dc} versus 1000/T as

$$\Delta E = 0.198 \times slope\ of\ \log\log \rho_{dc} versus\ \frac{1000}{T}\ (eV) \ldots\ldots\ldots\ldots\ldots (3.31)$$

In ferrites the possibility of changing the valence of a considerable fraction of metal ions and especially that of iron ions exists. An appreciable conductivity in these systems is found to bedue to the presence of iron with different valence states at crystallographically equivalent lattice points. The conduction is dueto

exchange of localized 3d electrons from Fe^{3+} to Fe^{2+}. Generally charge carriers are of the order of 10^{22} /cm3 in ferrites but due tovery small mobility there is low conductivity.Various theories have been proposed to account for the electrical resistivity. Band polaron approach based on electron transition between localized shells was also suggested which is based on the fact that the ferrites being ferrimagnetic materials their magnetic properties would influence their electrical properties. Small polaron model has been introduced by Haubn reisser [47]. Lorentz and Ihle [48] have explained the electrical properties on the basis of thermally activated motion of electrons. Srinivasan et al [49] have reported the phonon induced tunneling. A small polaron is a defect created when an electric carrier becomes trapped at a given site as a consequence of the displacement of adjacent atoms or ions. The entire defect (chargeplus distortion) then migrates by an activated hopping mechanism.

The small polaron formation can take place in materials whose conduction electrons belong to incomplete inner (d or f) shells which due to small electron overlap, tend to form extremely narrow bands .The migration of small polaron requires the hopping of both the electron and the polarized atomic configuration from one site toan adjacent one.

The hopping probability is given as

$$P = \upsilon_0 exp\left(\frac{-W_H}{k_B T}\right) \text{..... (3.32)}$$

where $\upsilon_o$is lattice vibration energy, $W_H$is hopping energy.

The activated mobility is given as,

$$\mu = \left(\frac{e a_0^2 \upsilon_0}{k_B T}\right) \exp\left(\frac{-W_H}{k_B T}\right) \text{..... (3.33)}$$

where a_o is hopping distance , υ_o is lattice vibration frequency. The temperature dependence can be characterized by activation energy.

The activation energy does not belong to the energy picture of electron but to the crystal lattice around the site of electron.

It is reported by Mazen et al [50] that resistivity is affected due to structural phase information. Some cations like Mn^{3+} and Cu^{2+} create the tetragonal distrotions in cubic spinel structure. This distortion in the spinel structure affects the distance between the neighboring Fe^{2+} and Fe^{3+} ions and hence the conduction process of the hopping electron is also affected. Thus resistivity is controlled by ratio between Fe^{2+} and Fe^{3+} ions, (and also with valency variation of other cations like Ni^{2+}) which can be varies with the help of oxygensupply at the time of sintering as well as by suitable cation substitution, magnetic order and structural phase.

3.7.2 Two probe method

Two-probe method is wad for the measurement of d.c. electrical resistivity. The schematic diagram of experimental setup is shown in the figure 3.6. It consists of sample holder, furnace, temperature controller, ac and dc power supply and micrometers.

Sample holder

The sample holder is designed and fabricated specially forresistivity measurement.

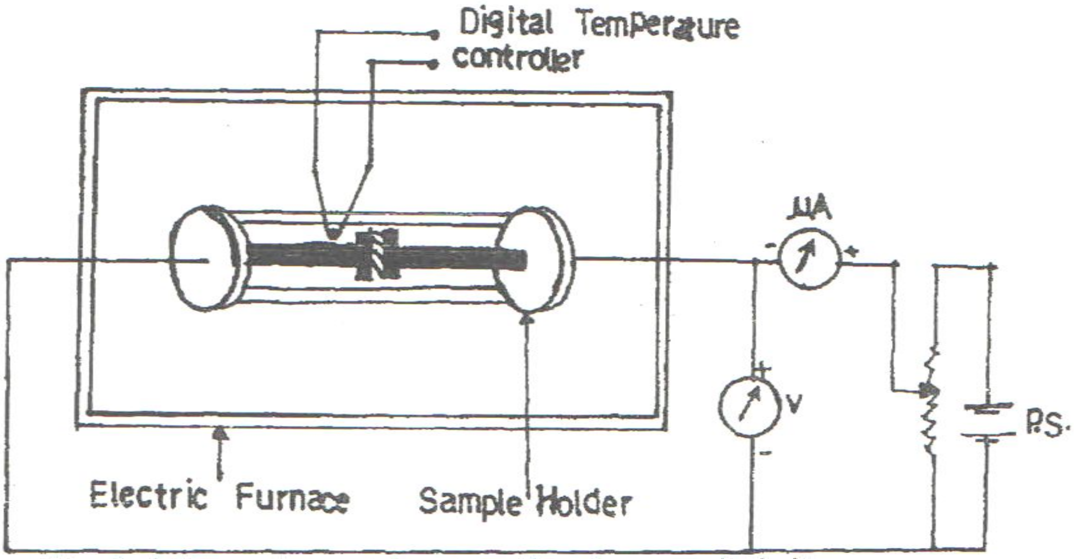

Fig 3.6 Experimental set up for d. c. resistivity

It consists of two ceramic beads with supporting stainless steel rods. The spring loaded stainless steel rod (E_2) is introduced into the ceramic beads and it presses the surface of the pellet. The stainless steel rod (E_1) is fixed at the other end.The sample in form of pellet is placed in the sample holder. The sample holder with pellet is placed in the furnace. A low voltage de issupplied to the probes of sample holder, which connects the endsurfaces of the pellet.Digital temperature controller, controls the temperature ofthe furnace. The temperature is varied at the slow rate of change throughout the experiment. The temperature is measured by using chromel-alumel thermocouple in contact with the surface of the sample. The surfaces of the pellets have made smooth and silver paste was applied on the surfaces. Each pellet was subjected to the thermal cycle before taking the readings of resistivity. In this way the precaution for good ohmic contact was taken. The temperature variation of d.c. resistivity is carried outadopting simple principle of voltage current characteristics.

The resistivity of the material is given by

$$\rho_{dc} = \left(\frac{\Pi r^2}{t}\right) \times R \, \Omega - cm \ldots\ldots\ldots\ldots\ldots\ldots\ldots\ldots\ldots\ldots \quad (3.34)$$

where r is radius of the pellet ,R is resistance of the pellet in Ω and tis thickness of the pellet.

3.8 Thermoelectric power measurement

The thermoelectric power arises due to the migration of charge carriers when there is a temperature gradient in a material from one region to another region. The temperature gradient leads to different carrier concentration. At hot end the carrier concentration is more and also the carriers acquire more kinetic energy. At cold end the carrier concentration is less. (However, some of the top energy carriers acquire energy even at the cold end and can migrate). These two situations lead to much stronger driving force for the out flow of carriers from the hot end towards the cold end. This gives rise to the thermoelectric power. The generation of the thermoelectric power depends upon the diffusion of the charge carriers, phonon drag and phonon scattering. In crystal the mobility is governed by the lattice vibrations scattering which is temperature dependent as well ascrystal direction dependent. Thermoelectric power is reliable probe to furnish the information about the nature of predominant charge carriers in the conduction process of a material. The ferrites are the high resistive material due to lonic type of bonds present in them. The temperature dependent charge transport phenomenon is due to hoppingof the electrons and the whole transfer.Thus the thermoelectric power measurement is essential to know about the transport properties of the ferrites. The iron excess ferrites show n type conductivity while iron deficit compositions show p- type conductivity.

Thermoelectric power studies were carried out over atemperature range from 350 °K to 850°K by differential method. The sample holder for measuring thermo e, m. f. consists of two non- magnetic copper electrodes

between which the sample is firmly fixed. An auxiliary heating coil is fixed to the upper electrode for additional heating in order to maintain a temperature gradient of about 10 °K between the two sides of the samples. The temperature of the two faces of the sample was measured by two chromel-alumel thermocouples, which are kept very close to the sample.

Thermo- e. m. f. was measured with the help of a digital voltmeter. Seebeck coefficient, charge concentration and drift mobility have been determined.

3.9.1 Dielectric constant measurement

The polarization is the main cause of dielectric properties.The capacitance of a capacitor increases when it is filled with dielectric material. The increase in the capacitance depends on the dielectric constant ($\varepsilon^{/}$). An ideal capacitor C_P (with loss freedielectric) in parallel with a resistor R_P is taken as the equivalent circuit of a capacitor with a dielectric having certain conductivity. The temperature dependent behavior at low frequency and the frequency dependent behavior for high frequency are generally considered.

Koops[51] showed that the ac resistivity and dielectric constant of the material exhibit dispersions due to the MaxwellWagner interfacial polarization which can be explained by a simple model. There are well conducting grains separated by layers of lower conductivity. A multilayer model in conjunction with an asymmetric distribution function is capableof accurately describing the relaxation spectra resulting from the Maxwell Wagner interfacial polarization. The origin of the interfacial polarization was attributed to the distribution of electrical resistivities in the oxides which was considered to be caused by the non-uniform distribution of oxygen ions in the oxides induced by the sintering process. The variation of $\varepsilon^{/}$ can be understood with the mechanisms of dielectric polarization and the electronic exchange which results in the displacement of the electrons in the direction of the electric field. The electron exchange in conduction is the main cause for polarization in ferrites.

The dielectric constant dispersion at higher frequency is dueto the presence of low conducting surface layers on the grains of the ferrites and may be distributed as per Koops's explanation. The frequency dependence of dielectric constant may be given as

$$\varepsilon^{*} = \varepsilon_{\infty}^{/} + \left(\frac{\varepsilon_{sk}^{/}}{1+j\omega T_k}\right) + \left(\frac{\varepsilon_{sk}^{/}}{1+j\omega T_t}\right) - j\left(\frac{\sigma_{dc}}{\varepsilon^{*}\omega}\right) \quad \text{(3.35)}$$

where ε_{sk} and E_{st} are static dielectric constants (at $\omega \rightarrow 0$) due to structural non uniformity of ferrites. T_k and T_t are relaxation times and ε_{∞} is dielectric constant as ω tends to ∞.

Using Koop's model the values $\varepsilon^{/}_{sk}$and T_k can be determined by considering $\overline{D} \gg h \; and \; \frac{\sigma_1}{\sigma_2} \gg \frac{\overline{D}}{h}$ condition.

$\varepsilon^{/}_{sk}$ and $T_k$may be given as,

$$\varepsilon_{sk}^{/} = \varepsilon_2^{/}\frac{\overline{D}}{h} \; and \; T_k = \varepsilon_0^{/}\frac{\varepsilon_2^{/}}{\sigma_1 h} \quad \text{(3.36)}$$

where, $\varepsilon^{/}_2$, σ_2 , h are the dielectric constant, conductivity and the thickness of the oxidized layer of the grain, o, is the conductivity of the grain bulk which according to Miroshkin et al[52] may be determined in the range of high frequency saturation and $\overline{D}$ is themean diameter of the grains.

Kramar et al. [53] suggested taking into account the variation of dielectric constant with respect to grain's size at each frequency. They further proposed that the contribution of grains with diameter D_i to $\varepsilon^{/}_{sk}$ depends on their relative quality (probability P_i).

The ogygen diffusion in the surface layers of grain with different sizes occur upto the depth h and then the Koop's formula can be modified as

$$\varepsilon^{/} = \frac{\varepsilon_2^{/}}{h} . \sum_{i=1}^{n} P_i D_i \quad \text{(3.37)}$$

Koop's relaxation depends on the distribution of grain size in the specimen. For materials in which hopping electronic or ionic chargesmake a significant contribution to polarization, low frequency dispersion of

dielectric constant bears Maxwell Wagner machanism.The effect arises from the interaction of capacitive barriers with high polarization due to migration of charges through larger but limited paths.

3.9.2 Temperature dependent dielectric constant

Both the dielectric constant and electric conductivity are basically electrical properties and it has been recognized that the same mechanism of exchange electrons between Fe^{2+} and Fe^{3+} is responsible for both the phenomenon. Iwauchi (54) and Rezlescu etal [55] have established a strong correlation between conductionmechanism and the dielectric behavior of ferrites. The electron exchange between Fe^{2+} and Fe^{3+} results in the local displacement of charges that causes polarization in ferrites. The magnitude of exchange, which also controls the conduction in ferrites, depends upon the concentration of Fe^{2+} and Fe^{3+} ions present on B-site. The concentration of Fe^{2+} and Fe^{3+} ions in ferrites can be varied with help of the method of preparation and suitable cation substitution. Some amount of Fe^{2+}ions is also formed due to possible evaporation. Man yearlier workers have stressed the importance of microstructure in controlling electrical resistivity of ferrites. Kramer and Larganteau etal [56] also reported the relation between grain structure and dielectric constant. In polycrystalline ferrites the grain boundaries, avoids and the inhomogeneous grain structure result in higher values of dielectric constant.

The dielectric constant varies with temperature. The temperature dependence of dielectric constant is carried out using two-probe method with L-C-Q-R-Meter. Experimental set up is as shown in fig 3.7. The measurement of ac resistance and capacitance were measured with the help of HP meter (4284A) at 1 KHz frequency for various temperatures. The dielectric constant is calculated using the following relation,

$$\varepsilon^{/} = \frac{cd}{\varepsilon_0 A} \quad \text{..... (3.38)}$$

where C is capacitance , d is thickness of pellet, A is cross sectional area of the flat surface of pellet and €, is perimittivity of free space(8.854×10^{-12} Fm^{-1}).

The dielectric loss tangent (tan) is calculated using the relation,

$$tan\,\delta = \left(\frac{1}{2\Pi\varepsilon_0 f}\right) \times \frac{\sigma_{AC}}{\varepsilon^{/}} \quad \text{..... (3.39)}$$

Where σ_{AC} is a.c. conductivity and f is frequency of applied signal.The variation of $\varepsilon^{/}$ with temperature at 1kHz frequency was carried out. The tanδ was obtained by using the following relation,

$$tan\delta = (17984600) \times \frac{\sigma_{AC}}{\varepsilon^{/}} \quad \text{..... . (3.40)}$$

The dielectric loss is given as,

$$\varepsilon^{//} = \varepsilon^{/} \tan\delta \quad \text{..... (3.41)}$$

The dielectric constantincreases with increase in temperature it reaches amaximum peak value and the loss tangent exhibits the similar trend with temperature. The dielectric loss initially increases slowly and then it increases rapidly.

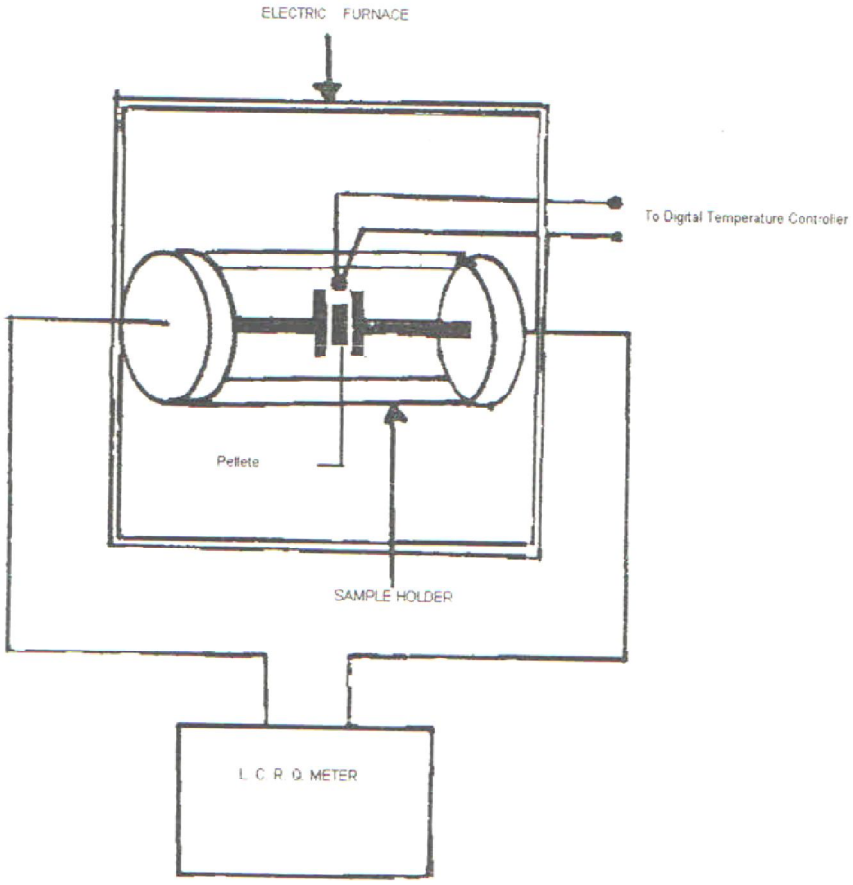

Fig 3.7 Experimental set up for dielectric constant

REFERENCES

1. Qi Chen, Adam J. Rondinone, Bryan C. Chakoumakos,Z. Johng. J.Mag &Magnetic Mater.194,(1999)1-7
2. H.H. Joshi, P. B. Pandya, K. B. Modi , N. N. Jani, G. J. Baldha & R. G. Kulkarni Bull. Mater. Sci. 20 No1,(1997) 93. K. M. Jadhav,
3. V. B. Kawade ,K. B. Modi, G. K. Bichile and R. G. Kulkarni, Physica B. 291 (2000)379383.
4. A. Vrma , T.C. Goel, R. G. Mendiratta &R. G. Gupta, J. Mag. & Magnetic Mater.192,(1999)271-276.
5. A. Wold J. Chem. Ed.57, (1980) 531.
6. Johnson Jr.,D. W. Amer. Ceram. Soc. Bull. ,60(1981)221
7. JAEGwang JEE. J.Mater. Sci. 33(1998)3965-3968.
8. Adriana S. Albuquerqe, Jose D.,Ardisson, Waldemar, A. A. Macedo,J. Mag. & Magnetic Mater.192,(1999)277-280.
9. C. H. Yan, Z. G. Xu F.X. Cheng Z.M.,Wang L. D. Sun, C.S. Liao J. T. Jia.Solid State Commn. 111(1999) 287-291.
10. A. G. Merzhanov, I. P. Borovinskaya(1972) Dokl. Akad.Nauk. SSSR (Engl.. Trans.)204,429
11. A.G. Merzhanov (1993)in Chemistry of Advanced Materials. (Ed. C. N. Rao),Blackwell, Oxford.
12. M.M. Sekar &K. C. Patil,Mater. Res. Bull.,28,(1993)485.
13. R. Mahesh ,R. Pavate , V. A. Prakash andC. N. R. Rao ,5 (1992)174
14. Swallow,D.and Jordon, A. K. (1964)Proc. Br. Ceram. Soc. 2,1.
15. Anthony R. West, Slid State Chem. and it's Appl.John Wiley & Sons.(1984)
16. L. Cervinka&Z. Sisma, Czech J.Phi's sect B (Czechoslovakia) 20, (1970)470.
17. B. D. Cullity, Elements of x-ray diffraction,Addison-Wesley Publishing Co.,(1956)
18. International Tables for X-ray crystallography, Vol. I Kynoch Press, Birmingham (1968)210
19. Han, G. Frank, W. Kinglor, A. Meyer and C. Stronger Z. Anorg. Chemi.271 (1953) 153
20. D. R. Gow, Prin. & Appl. Of electrochem.Champan and Hall London(1947)
21. M.J. Buerger Crystal Structure AnalysisWiley New York (1960)
22. H.S. Peiser , H. P. Rooksloy ,A. J. C. WilsonSX-ray diffraction by polycrystalline materials(The Inst. Of Phys.London)
23. A. Taylor , X-ray Metallography(John. Wiely &Sons Inc New York (1945)
24. P. Harold ,Klug and Leroy E. Alexander,SX-ray diffraction Procedures (John. Wiely & Sons Inc New York(1945)
25. H. Furuhashi, M. Inagaki, and S. Naka.J. Inorg. Nucl. Chem. 35(1973) 3009.
26. P. Porta ,F. S. Stone R. G. TurnerJ.Sol. Stet. Chem. 11(1974)135
27. Compt. Rend,International Tables for determination ofcrystal structure 230(1950) 213[24]
28. R. D. Waldron , Physical Rev. 99 No.6,(1955)1727.8
29. Preudhomme, J. and P. Tarte, Spectrochim.Acta 28A (1972) 69.
30. S. T. Hafner Z. Fur. Krist. 115, (1961)331.
31. P.Tarte Spectrochim Acta. 19, (1965)49

32. Brabers, V. A. M. and J. Klerk.Solid State Commu. 14 (1974) 613.
33. Bruesch, P. and F. D'Ambrogio,Phys. Status Solidi 50 (1972) 513.
34. Lutz, H. D. and H. Haeuseler, Ber. BunsengesPhys. Chem. 79(1975) 604.
35. Lauwers, H. A. and M. A. Herman.J. Phys. Chem. Solids 41 (1980) 223.
36. J. N. Smith, Magnetic Properties of Materials,McGraw-Hill, New York..Phys. Stat. Vol(A)12(1972) 623.
37. C. Kittel AND J. K. Galt ,Solid state phys. 3(1956) 437
38. P. Weiss, J. Phys. d 6(1907) 667
39. L. Neel, Ann. Phys. 3(1948) 137.
40. Alex Goldman ,Modern Ferrte Technology, VanNostrand Reinhold, New York(1990)
41. J. Crangle, Solid State Magnetism Arnold (1991)
42. R. Nagrajan & C. KrishnamurthyBull. Mater. Sci.,12,(1981)217.
43. K. Sheshan, A. L. Sashimohan,D. A. Chakrabarty,A. B. Biswas NP, SSP 19A, (1976)196.
44. E.L. W. Verwey, P. W. Haajman and F. C. Romeyn, LChem.Phys. 15,(1947) 181-187.
45. L.G. van Uitert, Proc. IRE,44,(1956) 1294.
46. G. H. Jonkar J. Phys. and chem of solids , 9 (1959) 165.
47. W. Haubenreisses. Phys, Stat. Solid. 21 (1961) 3905.
48. B Lorentz and D. Ihle Phy. State ,solidi, 69 (1975) 451
49. G. Srinivasan &C.M. Srivastav, Phys.
50. Stat. Solidi, 108 (1981) 665. S. A. Mazen ,M. A. Ahmed and B. A. Sabrah, Phys. Stat. Sol.,70 (1982) k71.
51. Koops C. K. ,Phys. Rev.83, (1951)121 \
52. Miroshin V. P., Ya.I. Panova, V.V. Passynrov, Phys. Stat. Sol. (a),66 (1981) 779.
53. G. P. Kramer, Ya. I. Panova, V.V. Passynkov, Phys. Stat. Sol. A76 (1983) 95.
54. K. Iwauchi, Jpn. J. Appl. Phys., 10,(1971) 1520.
55. Rezlescu N. & Rezlescu E., Phys. Status Solidi (a).23,(1974) 575.
56. A. Larganteau, J. P. Bonnet, P. Dorder, Phys. Stat. Sol. A. 122 (1990) 371.

CHAPTER – 4

RESULTS AND DISCUSSION FOR $Ni_{0.7}Mg_{0.3}Al_xFe_{2-x}O_4$ SYSTEM

4.1 X-ray Diffraction

The single phase formation of all the samples was confirmed from X-ray diffraction pattern as shown in fig. (4.1-4.6).the values of the lattice parameter 'a', have been determined byusing X-ray data with an accuracy of $\pm$0.002 A^0 for the sampleshaving x=0.0 to x = 0.5 and are listed in Table (4.1). The variationof lattice parameter with increase of Al^{3+} concentration in thecomposition is as shown in figure (4.7). It decreases with increase of Al^{+3} concentrations in the composition. There is co-relation betweenthe ionic radius and the lattice parameter. The ionic radii r_A and $r_B$have been estimated by considering the cation distribution. Thevalues of theoretical lattice parameters have been determined by using the following relation [1]

$$a_{th} = \frac{8}{3\times\sqrt{3}}[(r_A + R_0) + \sqrt{3}(r_B + R_0)] \quad \text{...} \quad (4.1)$$

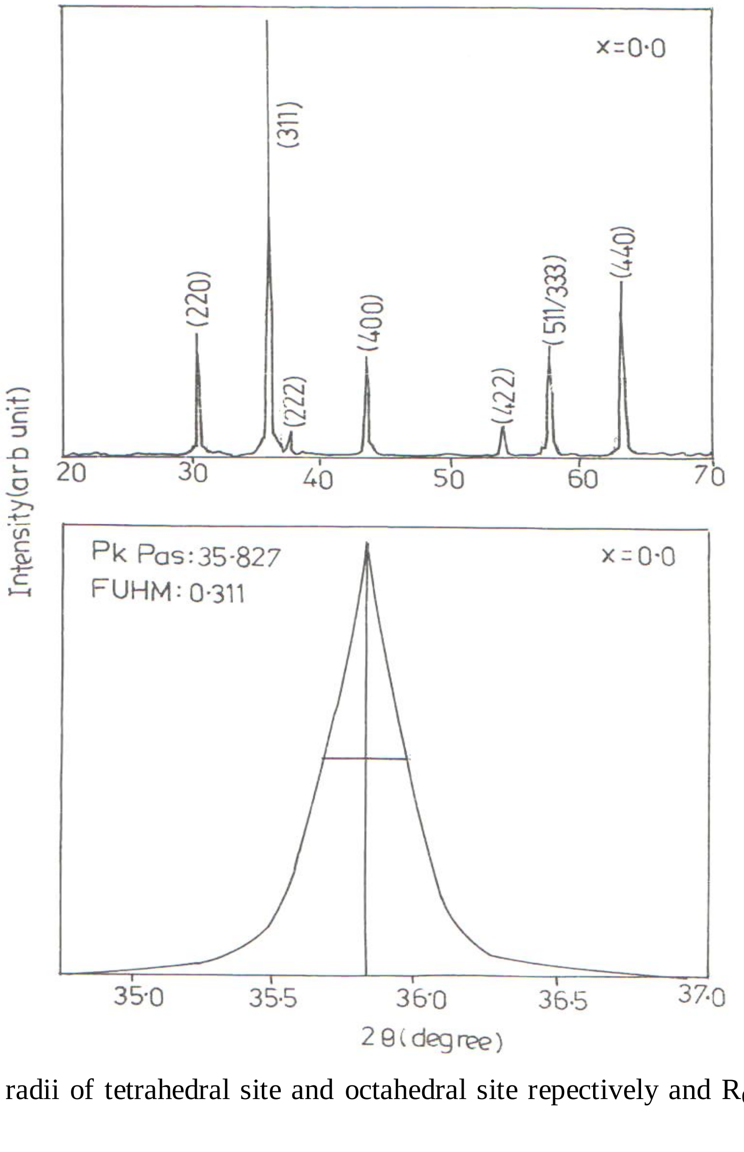

Wherer$_A$ and r_B are ionic radii of tetrahedral site and octahedral site repectively and R_0 is theradius of the oxygen ion [2].

The decrease in r_B with increase in $A1^{3+}$ suggests the replacement of larger Fe^{3+}(0.64 A ^{0}) by smaller $A1^{3+}$(0.51 A ^{0}) [3] B- site. The octahedral site plays a dominant role rather than the tetrahedral site in influencing the values of lattice parameter. The average ionic radii decrease slowly with increase in Al^{3+} content, which is reflected in the decrease in lattice parameter with (x). Thus the decrease in lattice parameter may be attributed to the replacement of larger Fe^{3+} (0.64A^0) by smaller ions Al^{3+} (0.51 A^0). The values of the theoretical lattice parameter and the observed lattice parameterare listed in the table (4.2). The values of lattice parameter are found to be comparable with the reported values in the literature [4-5].

Composition (x)	Lattice Parameter		X-ray density dx.gm/cm^3	Particle size t.A^0	Porosity %
	a.$_{obs.}$A^0	a.$_{cal.}$A^0			
0.0	8.333	8.334	5.175	315.61	30
0.1	8.331	8.332	5.081	313.38	10
0.2	8.329	8.330	5.015	323.66	20
0.3	8.326	8.327	4.950	326.86	28
0.4	8.324	8.326	4.869	313.15	13
0.5	8.321	8.321	4.813	239.72	21

Table-4.1: Variation of lattice parameter, x-ray density, particle size and porosity for $Ni_{0.7}Mg_{0.3}Al_xFe_{2-x}O_4$ system

Composition (x)	r_A A^0	r_B A^0	a_{th} A^0	$r_{obs.}$ A^0
0.0	0.64015	0.669425	8.323065	8.333
0.1	0.63742	0.66429	8.305169	8.331
0.2	0.68264	0.65982	8.286998	8.330
0.3	0.63120	0.65500	8.268971	8.328
0.4	0.66576	0.65078	8.250697	8.326
0.5	0.62280	0.64560	8.232819	8.319

Table-4.2: Variation of ionic radii and lattice parameter [theoretical and observed], for $Ni_{0.7}Mg_{0.3}Al_xFe_{2-x}O_4$ system

The x-ray densities of all the samples were calculated by using the formula [6]

$$dx = \left(\frac{ZM}{Na^3}\right) gm.cm^{-3} \quad \text{.....(4.2)}$$

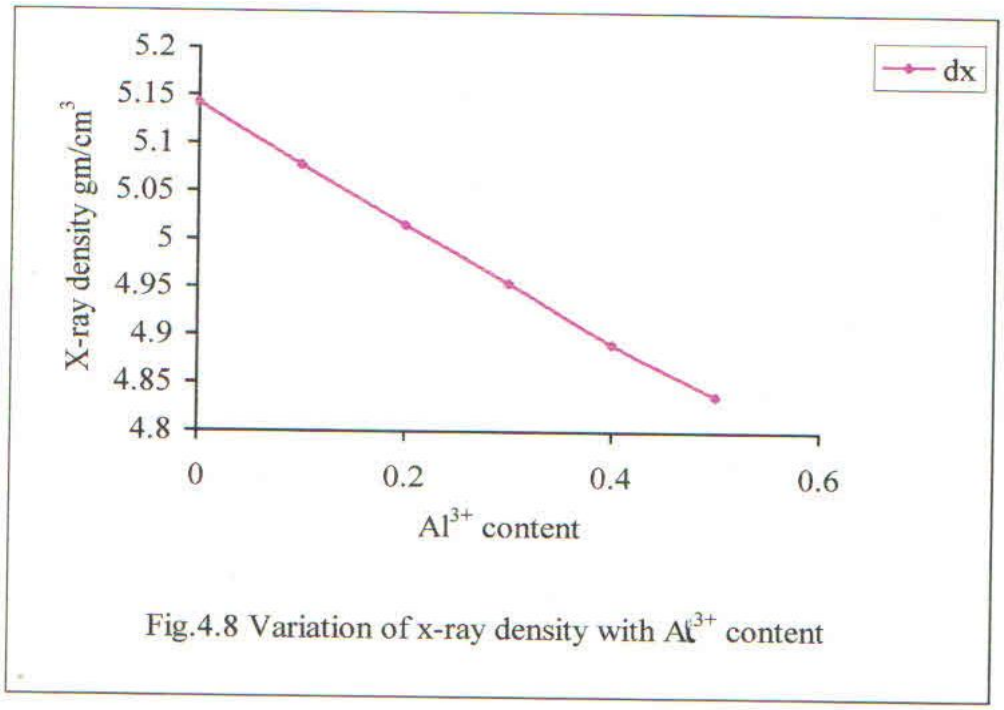

Fig.4.8 Variation of x-ray density with Al^{3+} content

where a is lattice parameter, Z is number of molecules per unit well (For spinel ferrite Z=), M is the molecular weight of the sample and N is the Avagadro's number. The variation of x-ray density (dx)as a function of All content (x) is as shown in figure (4.8). All thevalues of X- ray density are listed in the table (4.1). X-ray density is found to be decreasing with increase of AP in the system and bulk density reflects the same trend. This decrease in density may be ascribed to the density and atomic weight of Al^{3+} (27, 2.79gm cm^{-3}) which is lower than that of Fe3+ (55.8, 7.87gm cm^{-3}).

The particle size of all the samples was determined by Scherr's formula [7]

$$t = \frac{0.9\lambda}{B.Cos\theta} \quad \text{..... (4.3a)}$$

Where t is particle size, 2 is the wavelength of the target used (here CuKα=1.5418),B is the full width at half maximum of diffracted intensity line which is obtained by resolving (311) reflection line. The resolved peaks for all the samples are depicted inthe fig. (4.1-4.6). the values of particle size for the samples are listedin the table (4.1). The particle size is observed to be in the range 300A° to 400A^{o} and the mean particle size is estimated as 314.401 A^{0}. This is appreciably comparable value with that observed inceramically prepared powders.

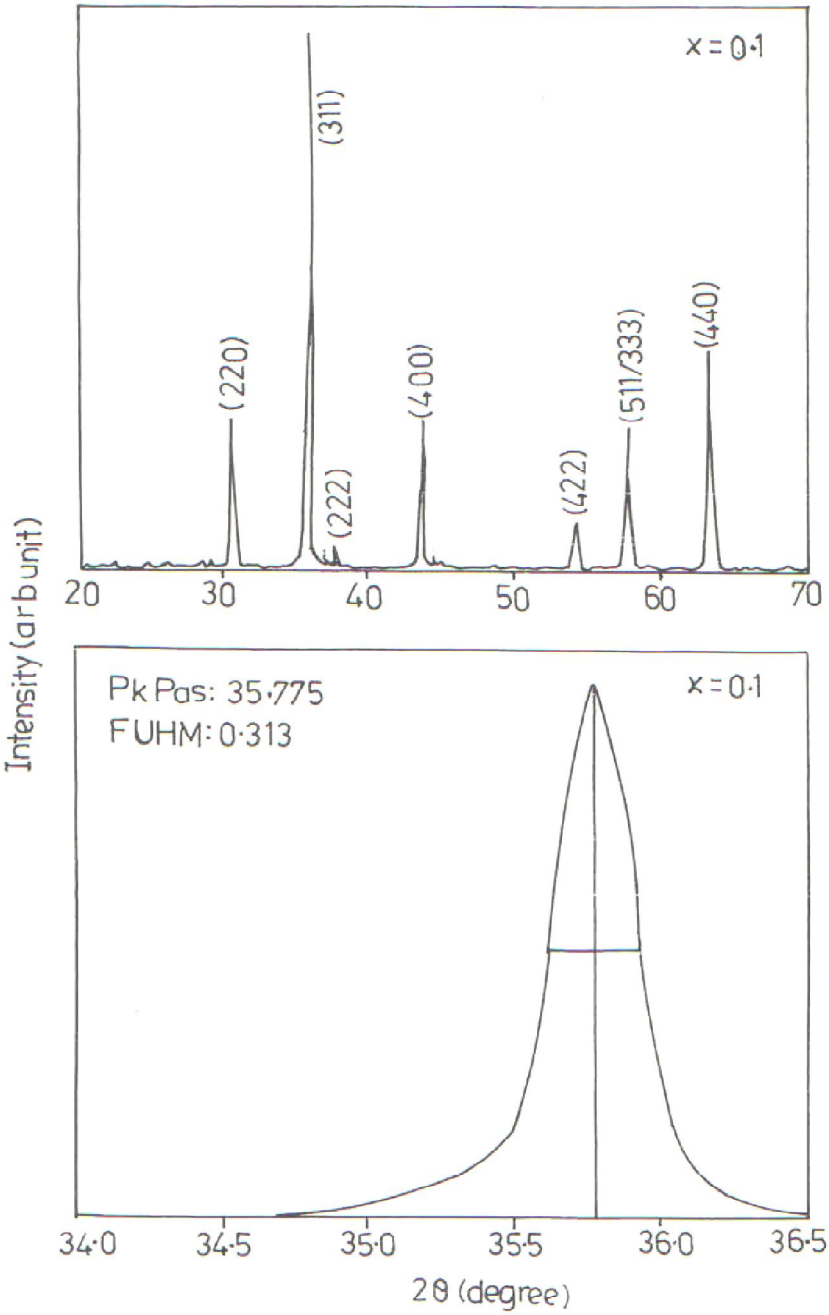

Fig.4.2 Typical X-ray diffractograms of $Ni_{0.7}Mg_{0.3}Al_xFe_{2-x}O_4$ for x = 0.1

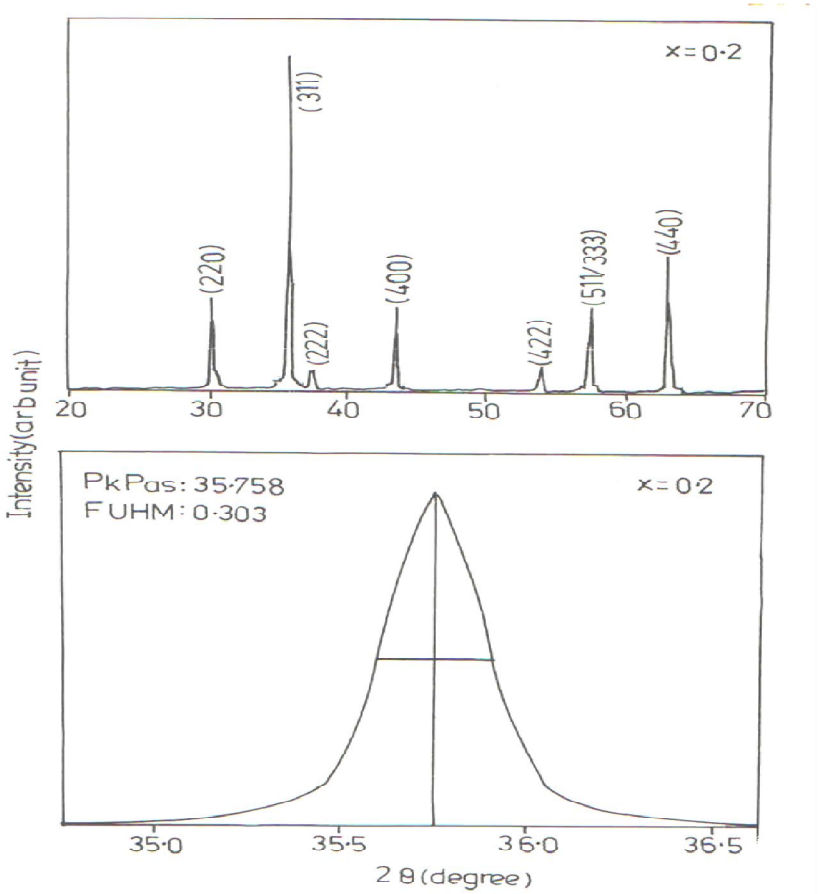

Fig.4.3 Typical X-ray diffractograms of $Ni_{0.7}Mg_{0.3}Al_xFe_{2-x}O_4$ for x = 0.2

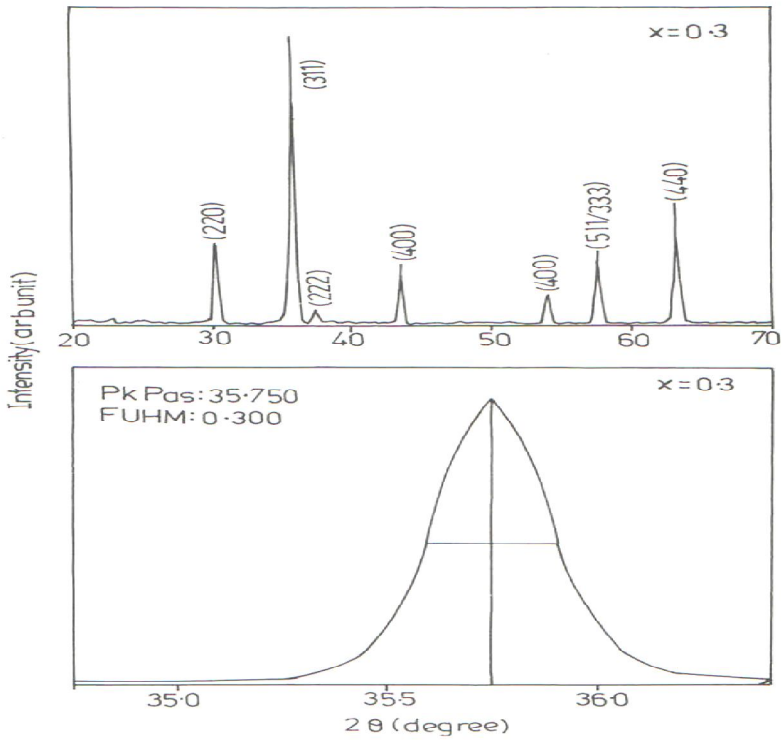

Fig.4.4 Typical X-ray diffractograms of $Ni_{0.7}Mg_{0.3}Al_xFe_{2-x}O_4$ for x = 0.3

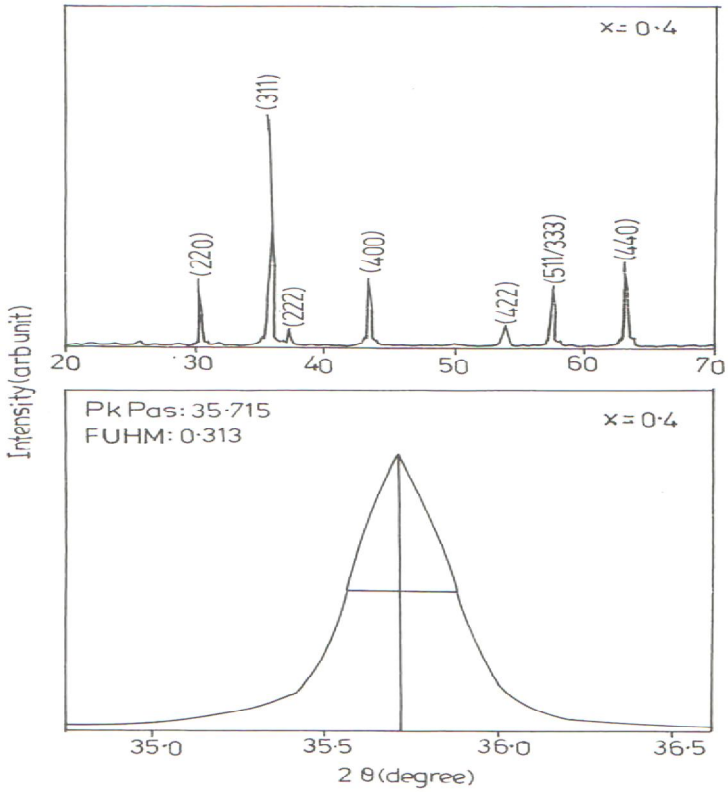

Fig.4.5 Typical X-ray diffractograms of $Ni_{0.7}Mg_{0.3}Al_xFe_{2-x}O_4$ for x = 0.4

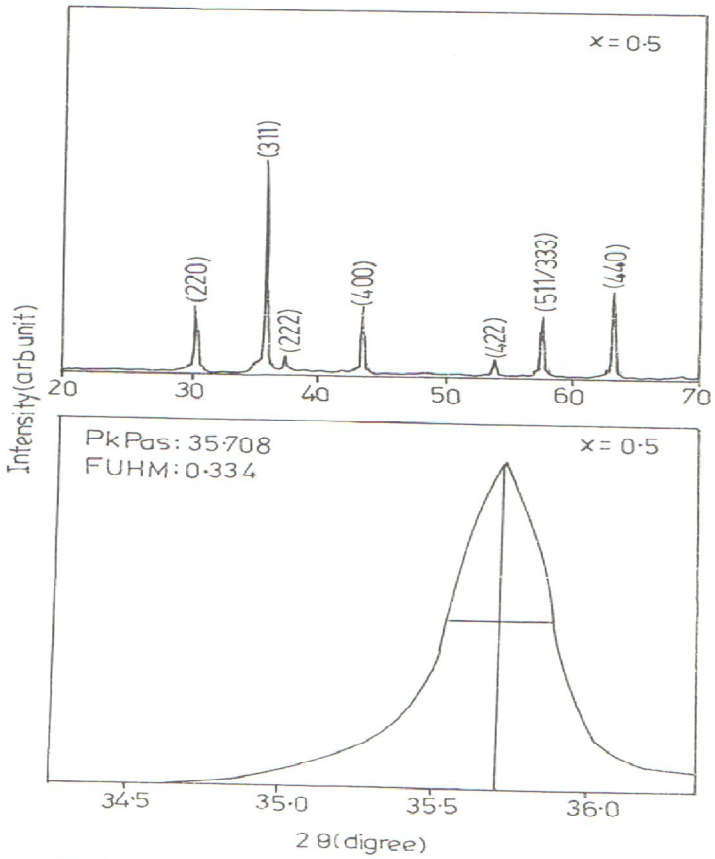

Fig.4.6 Typical X-ray diffractograms of $Ni_{0.7}Mg_{0.3}Al_xFe_{2-x}O_4$ for x = 0.5

The percentage porosity (% P) of all samples have been determined with the help of following relation, [8]

$$\%P = \left[1 - \frac{d}{dx}\right] \times 100 \quad \text{.. (4.3b)}$$

where d is bulk density , dx is -ray density. The values of % P are listed in the table (4.1). The porosity level is found to be 10 % to 30%.

The X-ray intensities have been calculated by using the formula given by Burger [9]

$$I_{hkl} = |F_{hkl}|2\ P.L_P \quad \text{.................................. (4.4)}$$

where F_{hkl} is structure factor, P is multiplicity and L_p is Lorentzpolarization. The cation distributions are determined by considering the ratios of intensities for the structure sensitive planes [10-13]. According to Ohnishi and Teranshi [14] the intensity ratios of the planes $I_{220}/I_{(400)}$ and $I_{(422)}/I_{(400)}$ are structure sensitive. The ratios $I_{220}/I_{(400)}$ and $I_{(422)}/I_{(400)}$400 have been taken into consideration to determinecation distribution be sides the saturation magnetization. The intensity ratios are listed in the table (4.3). The cation distribution based on theX-ray intensity ratio has been estimated and it is given in table (4.3).

(x)	Cation distribution		Intenisity Ratios					
	A-Sites	B-Sites	I_{220}/I_{400}		I_{422}/I_{400}		I_{440}/I_{422}	
			Cal.	Obs.	Cal.	Obs.	Cal	Obs.
0.0	$(Mg^{2+}_{0.015}\ Fe^{3+}_{0.985})$	$[Ni^{2+}_{0.7}\ Mg^{2+}_{0.285}\ Fe^{3+}_{1.015}]$	1.32	1.1	0.50	0.27	4.97	5.66
0.1	$(Mg^{2+}_{0.028}\ Al^{3+}_{0.022}\ Fe^{3+}_{0.95})$	$[Ni^{2+}_{0.7}\ Mg^{2+}_{0.272}\ Al^{3+}_{0.078}Fe^{3+}_{0.95}]$	1.36	0.90	0.5	0.27	4.56	4.76
0.2	$(Mg^{2+}_{0.038}\ Al^{3+}_{0.054}\ Fe^{3+}_{0.908})$	$[Ni^{2+}_{0.7}\ Mg^{2+}_{0.262}\ Al^{3+}_{0.146}Fe^{3+}_{0.892}]$	1.26	1.07	0.47	0.27	4.47	5.68
0.3	$(Mg^{2+}_{0.053}\ Al^{3+}_{0.081}\ Fe^{3+}_{0.866})$	$[Ni^{2+}_{0.7}\ Mg^{2+}_{0.247}\ Al^{3+}_{0.219}Fe^{3+}_{0.834}]$	1.21	1.08	0.46	0.31	4.55	4.44
0.4	$(Mg^{2+}_{0.065}\ Al^{3+}_{0.117}\ Fe^{3+}_{0.818})$	$[Ni^{2+}_{0.7}\ Mg^{2+}_{0.235}\ Al^{3+}_{0.283}\ Fe^{3+}_{0.782}]$	1.14	1.00	0.43	0.24	4.69	5.53
0.5	$(Mg^{2+}_{0.015}\ Al^{3+}_{0.138}\ Fe^{3+}_{0.788})$	$[Ni^{2+}_{0.7}\ Mg^{2+}_{0.226}\ Al^{3+}_{0.362}Fe^{3+}_{0.712}]$	1.13	1.04	0.43	0.17	4.17	6.94

Table-4.3: Cation distribution intensity ratios for $Ni_{0.7}Mg_{0.3}Al_xFe_{2-x}O_4$ system

4.2 IR spectra

The IR spectra of$Ni_{0.7}$ $Mg_{0.3}$ $A1_x$, Fe_{2-x}, O_4 with x = 0 to 0.5 in step of 0.1 systems are shown in the figure (4.9-4.11). The IR spectra of all samples have been used to locate the band position in order to determine the absorption frequency. The high frequency band v_1 is in the range 600 to 610 cm^{-1} and the lower frequency band v_2 is in therange 300 to 430 cm^{-1} [15-16]. The absorption bands obtained in the present investigation are found to be in the expected range of wavenumber. The difference in band position is expected because of the difference in the Fe^{3+}-O_2 distances for the octahedral and tetrahedral complexes. Waldron[17] and Hafner[18] attributed the v_1 band to the intrinsic vibrations of the tetrahedral groups and v2 to the octahedral groups. The force constants have been calculated using the Waldron analysis. The bond lengths R_A and R_B have been determined using the formulae given Smith J.N. [19]. The values of K_t, K_o, R_A and R_B are listed in the table [4.4). The molecular weight at tetrahedral (M_t) and that at octahedral (M_o) site have been calculated using the cation distribution obtained from X-ray diffraction and magnetization measurements. The values of V_1, V_2, K_t, K_o, R_A and R_B are found to bein good agreement with the reported ones. The force constant K decreases with the increase in R_A and the force constant K_o decreases with decrease in the R_B. The slight variations in v_1, and v_2 indicate that the method of preparation, grain size, and sintering temperature can influence the band positions. The decrease in bond lengths is attributed to the decrease in lattice parameters. A slight splitting ofsome bands indicates valence variations of F_e (i. e, presence of $Fe2^+$ion). Normally the force constant for tetrahedral site is higher than that for octahedral site due to the stretching bond at tetrahedral site.The variation of Kt, Ko, R_A and R_B is shown in figure [4.12 & 4.13].

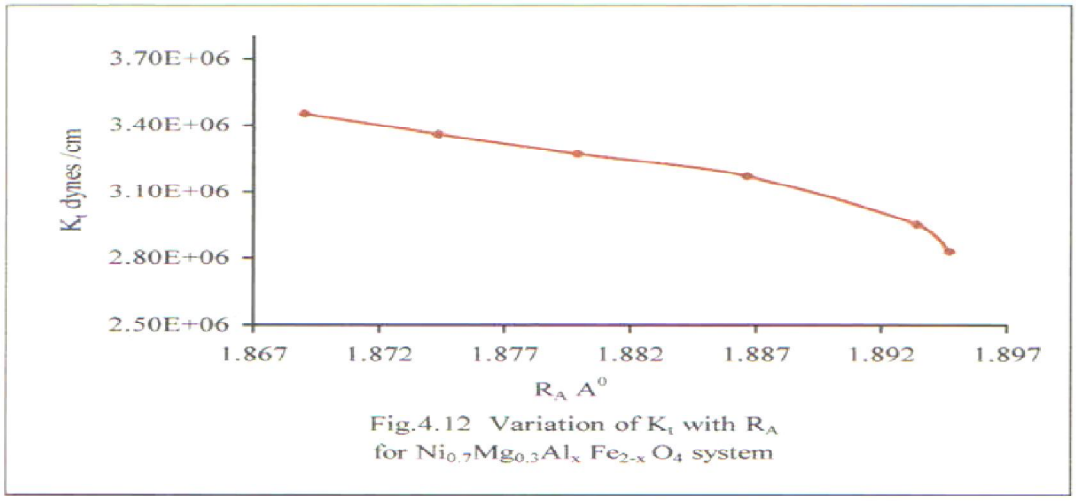

Fig.4.12 Variation of K_t with R_A for $Ni_{0.7}Mg_{0.3}Al_x Fe_{2-x} O_4$ system

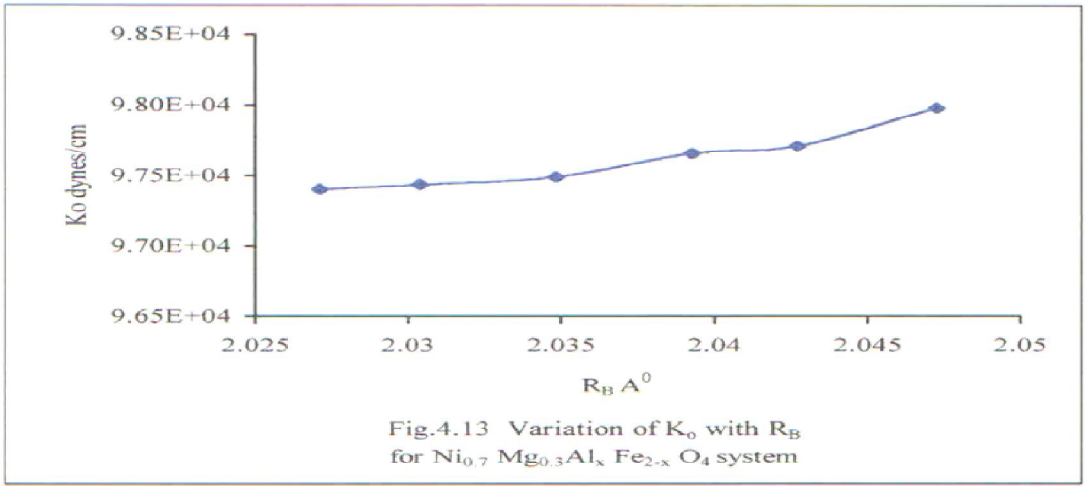

Fig.4.13 Variation of K_o with R_B for $Ni_{0.7}Mg_{0.3}Al_x Fe_{2-x} O_4$ system

(x)	Vibration Frequencies		Bond Lengths		Force Constants	
	$v_{1\ cm}^{-1}$	$v_{2\ cm}^{-1}$	R_A A^0	R_B A^0	$K_t x10^5$ dynes/cm	$K_0 x10^5$ dynes/cm
0.0	610	405	1.869042	2.047287	3.451148	0.97976
0.1	610	400	1.874365	2.042744	3.357251	0.97706
0.2	590	400	1.879911	2.039302	3.052872	0.97656
0.3	610	410	1.886672	2.034842	3.169458	0.97486
0.4	600	400	1.893429	2.030397	2.975550	0.97432
0.5	600	400	1.894719	2.027117	2.828725	0.97401

Table-4.4: Vibration frequency, Bond legths and force constants for $Ni_{0.7}Mg_{0.3}Al_xFe_{2-x}O_4$ system

4.3 Saturation magnetization

The values of saturation magnetization and Bohr magnetonnumber (the saturation magnetization per formula unit in Bohr magneton) at 300 °K were obtained from hysteresis loop technique for all the samples of the series (x = 0.0 to x = 0.5). The observed and calculated magnetic moments for all samples are listed in the table (4.5). All the samples show decrease in no with increasing Al^{3+} content in the composition. The saturation magnetization σ_s is calculated from hysteresis loop for all the six samples and magnetic moment per formula unit is calculated by using the following relation, [19]

$$\eta_B = \frac{\sigma_s}{5585} \times M_{wt} \quad \text{..... (4.5)}$$

where M_{wt} is molecular weight.

The decrease in the saturation magnetization with increase in Al^{3+} can be explained using Neel's [20] collinear model for ferrimagnetism.According to Neel's collinear model offerrimagnetism, the magnetic moment per formula unit is expressedas

$$\eta_B^N = M_B(\times) - M_A(\times) \quad \text{..... (4.6)}$$

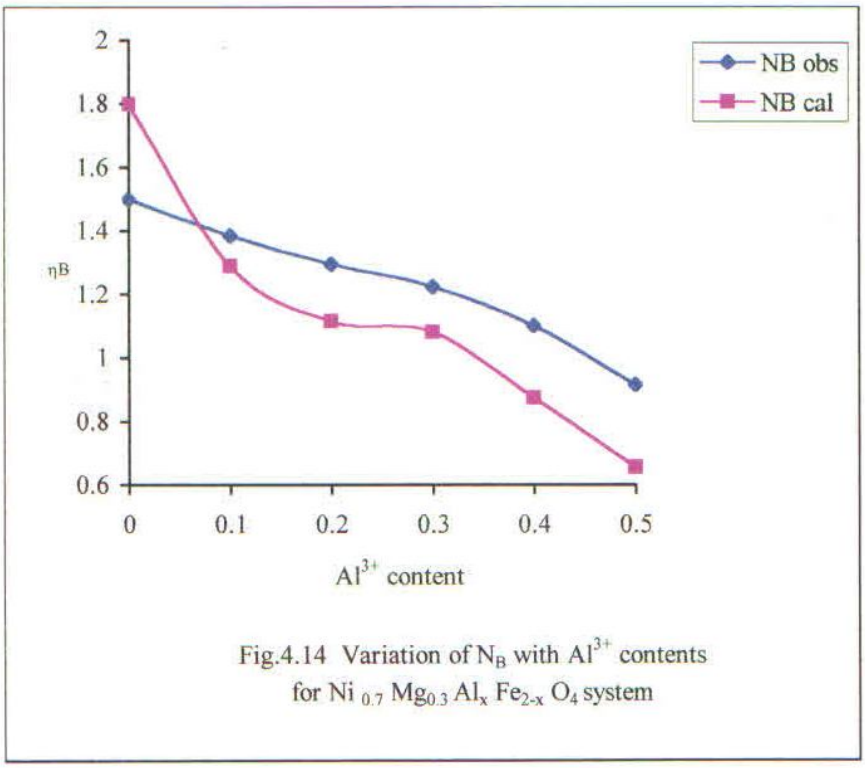

Fig.4.14 Variation of N_B with Al^{3+} contents for $Ni_{0.7}\ Mg_{0.3}\ Al_x\ Fe_{2-x}\ O_4$ system

where $M_A(x)$ and $M_B(x)$ are magnetic moments in of sub-lattice A and B respectively. The theoretical values of magnetic moment per formula unit in Bohr's magneton unit (η_B^N) have been estimated by using the cation distribution. The η_B^N values for $Ni_{0.7}Mg_{0.3}\ A1_x$, Fe_{2-x}, $O_4$with x = 0.0 to 0.5, were calculated by using the ionic magnetic moments of Fe^3, Ni^{2+}, Mg^{2+}, Al^{3+} with their respective values $5\mu_B$, $2\mu_B$,$0\mu_B$,and $0\mu_B$, The experimental and calculated values of η_B^N have been given in the table [4.5]. Thevariation of η_B^N with respect to the Al^{3+}concentration in the composition is shown in figure [4.14). The curves suggest the collinear spin order in the samples, which indicate a strong A-B interaction even though the non- magnetic cation is substituted [21-22].

4.4 A. C.Susceptibility

The temperature dependence of ac susceptibility χ_{ac} (T) for all the samples is as shown in the figure (4.15-4.16). The plots of relative low field ac susceptibility $\frac{\chi_T}{\chi_{RT}}$ (RT indicates roomtemperature) against temperature T, exhibit normal ferrimagnetic behavior. The nature of $\frac{\chi_T}{\chi_{RT}}$ curves suggests the magnetic domainstates in ferrite [23]. In all the $\frac{\chi_T}{\chi_{RT}}$ curves, there is peaking behavior near Curie temperature and just before Curie temperature it drops rapidly. The temperature corresponding to peak is called blocking temperature. The blocking temperature corresponds to the transition of magnetic particle from single domain to multi-domain [24]. This peak could be seen for a magnetic material in multi domain state if the material has a temperature at which magnetocrystalline an isotropy is zero. According to Been [25], the susceptibility is inversely proportional to the coercive force, therefore the increase in susceptibility after the isotropic peak is attributed to adecrease in coercive force. The peaking nature of the relative susceptibility indicates that samples contain the multi-domain structure. The addition of Al^{3+} reduces the coercive force. The Neel temperature decreases with increase in Al^3 content indicating reduction in ferromagnetic behavior, which

confirms the magnetization results. The Curie temperatures from ac susceptibility data are listed in the table (4.5). The decrease in Curie temperaturemay be attributed to decrease in super exchange linkages Fe^{3+}-O^{-2}-Fe^{3+} resulting from the replacement of Fe^{3+} by Al^{3+} in the present series.

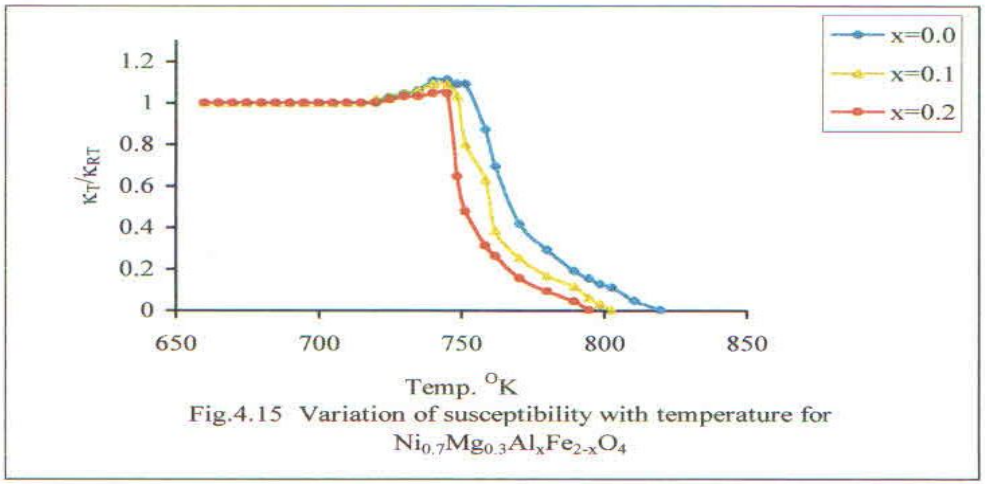

Fig.4.15 Variation of susceptibility with temperature for $Ni_{0.7}Mg_{0.3}Al_xFe_{2-x}O_4$

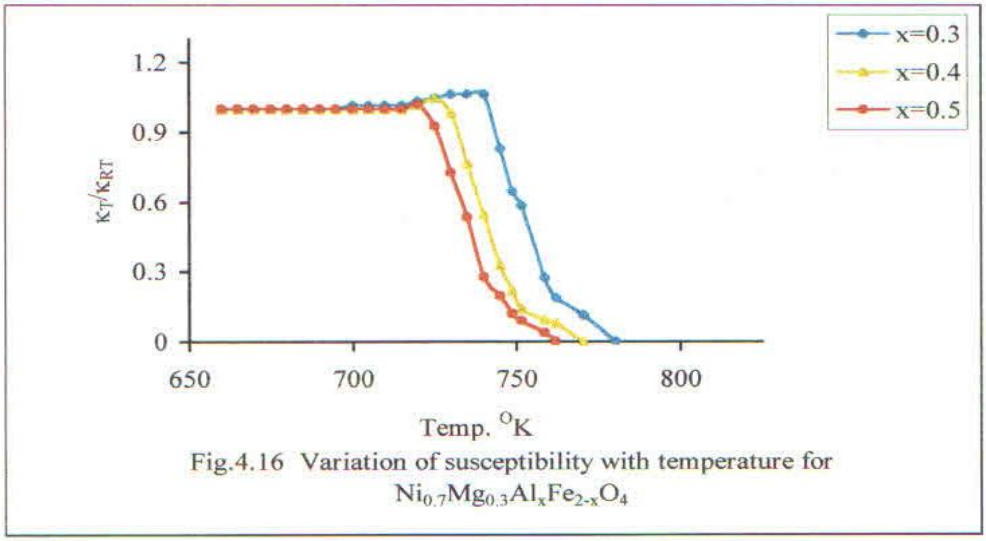

Fig.4.16 Variation of susceptibility with temperature for $Ni_{0.7}Mg_{0.3}Al_xFe_{2-x}O_4$

(x)	Saturation Magnetization σ_s (emu/gm)	Bond Lengths		Force Constants	
	$v_{1\ cm}^{-1}$	Cal	Obs.	From Susc.	From d.c. Resty.
0.0	37.294	1.55	1.496	819	809
0.1	34.882	1.40	1.381	802	790
0.2	33.11	1.32	1.294	794	780
0.3	31.7024	1.24	1.222	780	750
0.4	31.334	1.22	1.1	770	740
0.5	26.852	1.02	0.913	762	720

Table-4.5: Satration Magnetization, Bohrs magneton and Curie temperature for $Ni_{0.7}Mg_{0.3}Al_xFe_{2-x}O_4$ system

4.5 D.C. Resistivity

The variation of d. c. resistivity with respect to temperature has been studied for all the samples. The plots of log $\rho_{d.c.}$ Versus1000/T as shown in figure (4.17-18) indicate the variation in d. c. resistivity. The d. c. resistivity of all the six samples decreases with increase in temperature and obey the Arrhenius [26] relation

$$\rho_{dc} = \rho_0 exp\left(\frac{\Delta E}{K_B T}\right) \quad \text{..... (4.7.)}$$

The plots of log $\rho_{d.c.}$ Versus 1000/T show kinks near the Curie temperature where the magnetic phase changes from ferrimagnetic region to the paramagnetic region due to thermal energy. The activation energy, in ferrimagnetic and paramagnetic region, has been calculated using above relation (4.7) and is tabulated in the table (4.6). The ionization energy for Fe^{2+} to $Fe^{3+}$is 0.1eV. The activation energy values greater than 0.1eV indicate that there exists the hopping type of conduction mechanism. The activation energy inferrimagnetic region is lower than that of in paramagnetic region.The polarons in ferrites do not significantly introduce a strain in theionic lattice, as in the case of other ionic solids, due to the fact that d- electrons contribute the polaron. The co-operative behavior would be characteristics of such polar on, giving rise to lower activation energy.The conduction in ferrites can be explained on the basis of hopping mechanism. The cations occupy A-site and B-site in ferrites and electrons are localized due to ionic type of bonding. The distance between two inter metal ions in B-sites is smaller than that between intra metal ions (i.e. at B-site and another metal ion at A-site.). It is observed that under the normal conditions the electron hopping between B-A sites has very small as compared to that of B Bhopping. Hopping between A-A sites does not exist because most ofthe Fe^{3+} ions occupy A site and Fe^{2+}ions, which are formed during sintering process, preferentially occupy B-site only. The hopping probability depends upon the separation between the ions involved and the activation energy [28-29]. The conduction mechanism for present system may be given as

$$Ni^{2+} + Fe^{3+} \leftrightarrow Ni^{3+} + Fe^{2+}$$

$$Ni^{3+} + Al^{2+} \leftrightarrow Ni^{2+} + Al^{3+}$$

$$Fe^{2+} + Al^{3+} \leftrightarrow Fe^{3+} + Al^{2+}$$

$$Fe^{2+} \leftrightarrow Fe^{3+}$$

The AI^{3+} prefers to occupy B-site and replaces Fe^{3+} there by reduces the population of Fe^{3+} at B-site. This reduction of Fe^{3+} B -site causes consider able increase in the resistivity. Therefore, the d.c.resistivity is observed increasing with increase in Al^{3+} concentration.The observed high resistivity is up to 10^7 Ω.cm suggests that the d-band is very narrow and the carriers have low mobility (effective masses or holes). The probability of localized stable pair formation (pairs of different valence cations) is also one of the reasons to increase in de resistivity [30-31].

Composition (x)	ρ_{dc} at 600^0K x 10^6 Ω-cm^{-1}	Activation energy	
		Ferri-magnetic region (eV)	Paramagnetic region (eV)
0.0	1.2163	0.31	0.36
0.1	1.4130	0.33	0.39
0.2	2.0994	0.35	0.46
0.3	2.2026	0.38	0.49
0.4	3.2026	0.42	0.52
0.5	6.8600	0.43	0.54

Table-4.6: ρ_{dc} at fixed temperature and activation energy with composition for $Ni_{0.7}Mg_{0.3}Al_xFe_{2-x}O_4$ system

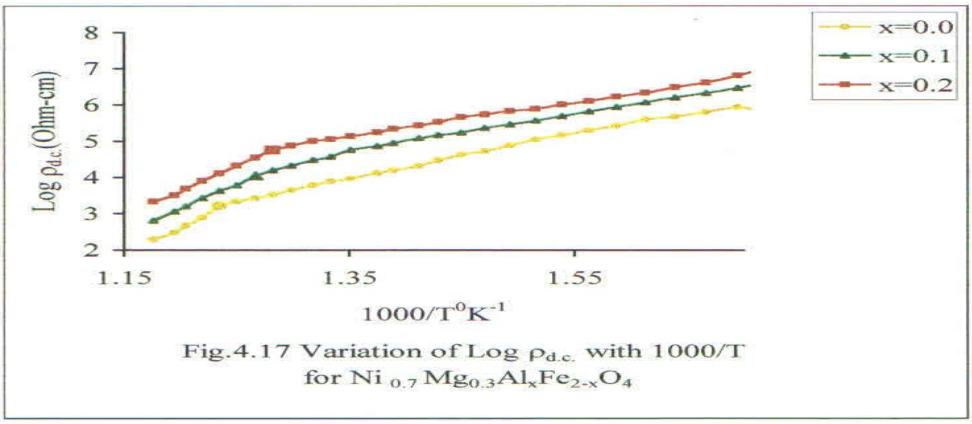

Fig.4.17 Variation of Log $\rho_{d.c.}$ with 1000/T for $Ni_{0.7}Mg_{0.3}Al_xFe_{2-x}O_4$

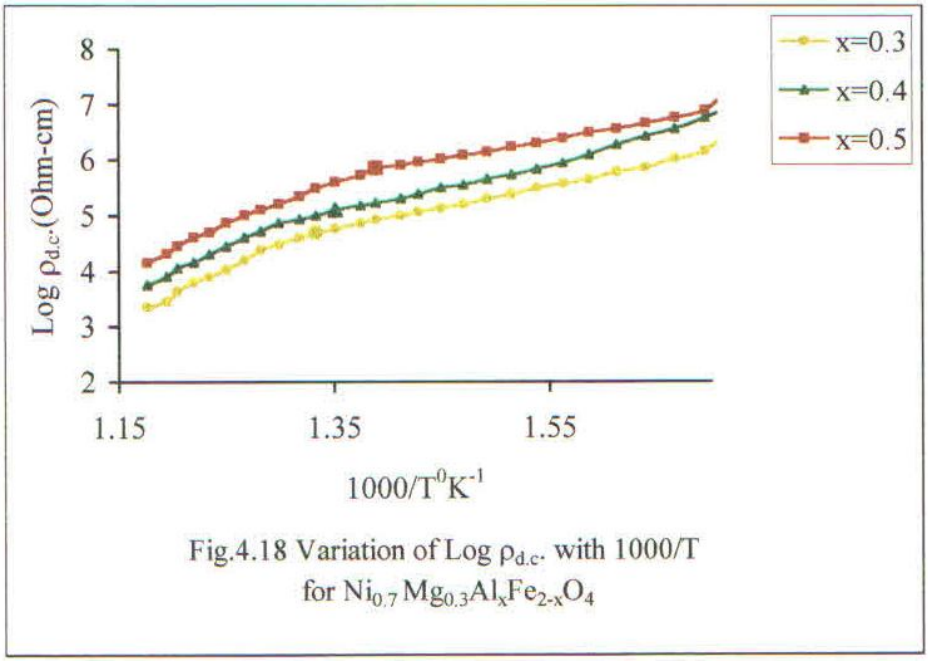

Fig.4.18 Variation of Log $\rho_{d.c.}$ with 1000/T for $Ni_{0.7}Mg_{0.3}Al_xFe_{2-x}O_4$

4.6 Thermoelectric power

The thermoelectric power measurement of all the samples have been carried out from room temperature to 850°K temperature. The values of Seebeck coefficient (a) have been determined by using the following relation,

$$\alpha = \frac{Thermo\ emf}{Temperature\ difference\ across\ the\ sample} \quad \text{..... (4.8)}$$

The plots of Seebeck coefficient as a function of temperature areshown in the fig (4.19-4.20).

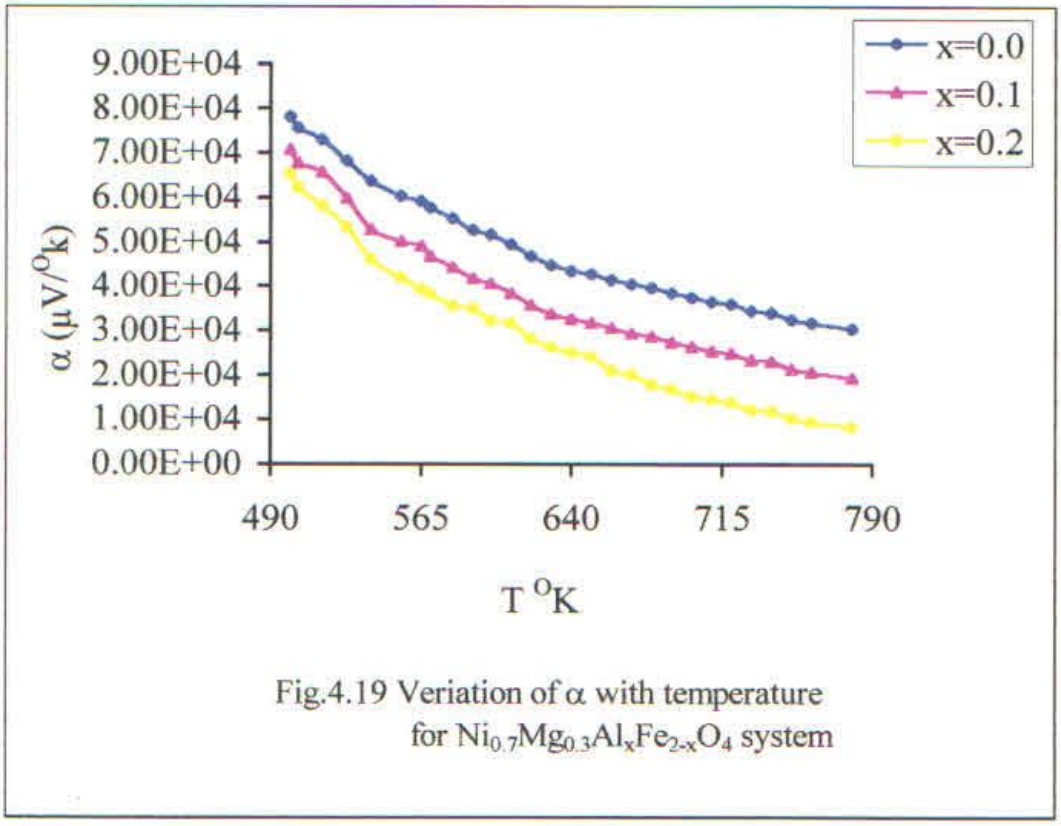

Fig.4.19 Veriation of α with temperature for $Ni_{0.7}Mg_{0.3}Al_xFe_{2-x}O_4$ system

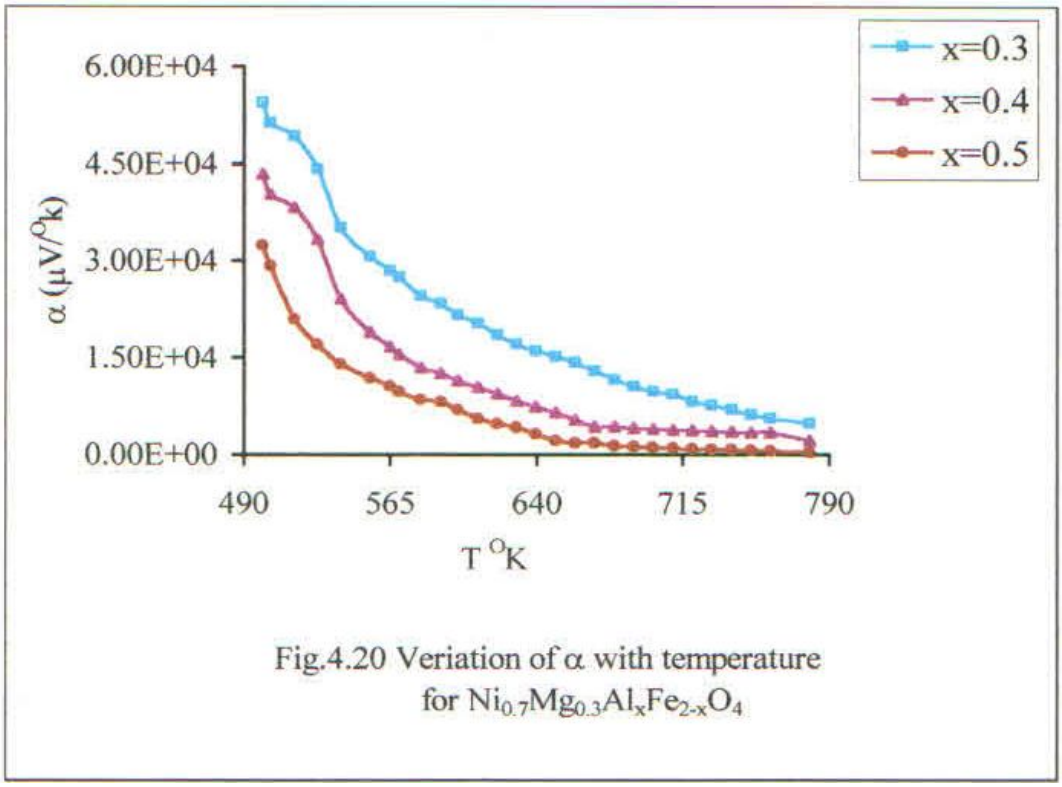

Fig.4.20 Veriation of α with temperature for $Ni_{0.7}Mg_{0.3}Al_xFe_{2-x}O_4$

The Seebeck coefficients have beenobserved to be negative upto 530°K and later on positive for higher temperature for all samples. This indicates that both types of charge carriers are present in the system. The decreases nonlinearly with increase in temperature, at high temperature number of holes hopping between Ni^{2+} to Ni^{3+} may increase which give rise topositive Seebeck coefficient [32]. The charge carrier concentration has been determined by using the following relation,

$$n = N\exp\left(\frac{-\alpha}{k}\right) \quad \ldots\ldots\ldots\ldots\ldots\ldots\ldots\ldots\ldots\ldots\ldots\ldots \quad (4.9)$$

where N is the density of the state and k is Boltzmann constant. Thevariation of concentration of charge carrier with temperature is asshown in figure (4.21-4.22). The concentration of the charge carriers increases with theincrease in temperature. The mobility for all the samples has beencalculated by the following relation,

$$\mu_d = \frac{\sigma}{ne} 4.10$$

where μ is de conductivity ,n is concentration of charge carriers andeis electronic charge. The variation of drift mobility with temperature is as shown in figure (4.23-4.24). The drift mobility increases with increase in temperature and decreases with Al^{3+}content. This clearly indicates that the conduction in the systemsdepends on the temperature dependent drift mobility and not on the temperature dependent charge carrier concentration. The Seebeck coefficient for the present series show that initially n type of charge carriers are predominant later on after 500°K to onwards, p-type of charge carriers are predominant. The conduction in n-type region isdue to electron hopping Fe^{2+} <-→ Fe^{3+} and that in p-type region is due to hole transfer between the two different valence states of the cation. Both Al^{3+} and Ni^{2+} may be playing certain role in controlling the resistivity along with Fe^{2+}- Fe^{3+}pair. From the thermoelectric power, the conduction is observed depending on the temperature dependent drift mobility and not on the temperature dependent charge carrier concentration. [33]

4.7 Dielectric properties

The variation of dielectric constant as a function of temperature at 1KHz frequency for all the six samples, with different Al^{3+} content in the compositions(i.e. x = 0.0 to 0.5) has been shown in the figure (4.25-4.26). The dielectric constant varies slowly at the beginning and after the temperature 650^0 K it increases rapidly

with increase in temperature. This behavior of $\varepsilon^{/}$ can be explained onthe basis of Maxwell Wagner interfacial polarization. The origin ofthe interfacial polarization is attributed to the distribution of electrical resistivity's in the ferrites which is considered to be caused by the non- uniform distribution of oxygen ions induced by the sintering process. The variation of & can be understood with the mechanisms of dielectric polarization and the electronic exchange which results in the displacement of the electrons in the direction of the electric field that determines the polarization in the ferrites [34].

The exchange of electron in conduction mechanism may be responsible for space polarization. Thus mechanism of dielectric polarization is similar to that of conduction [35-36]. As the conductivity increases with increase in temperature, the dielectric constant also increases with increase in temperature. With the rise in temperature the number of carriers increases resulting in an enhanced build up of space charge polarivation and hence increase in the dielectric constant. As an increase in concentration of Al^{3+} decreasesthe conductivity, the dielectric constant obviously increase with Increase inAl^{3+}, Figure (4.27-4.28) shown the variation of dielectric losstangent (tanδ) with temperature for all the samples. The loss tangent increases with increase in temperature. The variation of dielectric loss ($\varepsilon^{//}$) as a function of temperature for all the samples at frequency 1KHz is shown in the figures (4.29-4.30). The dielectric loss initiallyvaries very slowly up to 750°K temperature and later on it increases rapidly with the increase in temperature. The dielectric loss decreases with increase in Al^{3+} concentration in the system [37].

4.8 CONCLUSION

Thus from the above results and discussion the following conclusions can be drawn..

- $Ni_{0.7}\,Mg_{0.3}\,A1_x$, Fe_{2-x}, O_4 system has spinel structure
- The substitution of Al^{3+} decreases the lattice parameter
- The infrared spectra of the system consist of two bands, whichcorresponds tothe intrinsicvibrations of tetrahedral andoctahedral complexes.
- The force constant K_t decreases with increase in bond length R_A.
- The force constant K_o decreases with decrease in bond length R_B.
- The saturation magnetization decreases withincreaseinAl^{3+} content in the composition. The variation of the saturationmagnetization obeys the Neel's two sublattice collinear model forferrimagnetism The substitution of nonmagnetic Al^{3+}ion does notdisturb theA-B interaction. But it decreases the pair ofinteractionFe^{3+}-0- Fe^{3+}atBsite modulatesaturationmagnetization by occupying more at B-site as compared to that atA-site.
- The variation of ac susceptibility with increase in temperatureindicates the normal ferrimagnetic behavior of the system. Thesystem has multidomain structure.
- The Curie temperature decreases with increase in the Al^{3+} in the composition.
- The dc resistivity increases with increase inAl^{3+} content in thecomposition.
- The behavior of the system changes from ferrimagnetic toparamagnetic at a particular temperature.
- Thermoelectric power study exhibits that both n-types and p- types of charge carriers are responsible for charge transport andthe drift mobility causes the conduction.
- The dielectric constant increases withAl^{3+} content whereas thedielectric loss factor decreases with increase in the Al^{3+}content.

REFERENCES

1. Mazen S. A., Abdalla M.H., Nakhla R.I. , Zaki H. M. & Metawe F., Bull. For. Sci. Zagazig Uni. 13 (1991) 344.
2. Mazen S. A., Abdalla M.H, Sabrah B. A. & Hashem H. A. M. Phys. tatus. Solidi, A 134 (1992) 263
3. Dunitz J. D. , Orgel L. E. , J. Phys. Chem. Solids(1957)
4. Kunal B Modi et.al. , J. of Materials Sci. Letters 17 (1998)

5. Kunal B Modi et.al. , J. of Materials Sci. 31 (1996) 1311
6. Cullity B. D. , Elements of X-Ray Diffraction (Addison Wesley Press eading M. A. (1959)
7. Standley K. J. Oxide Magnetic Materials (Clerenden Press, Oxford, (1972)
8. Buerger M. J. , Crystal Structure Analysis., Wiley New York (1960)
9. R. K. Datta ,R. Roy J. Am. Cerm. Soc.50(1967) 578
10. R. W. G. Wyckoff, Crystal structure,Vol.2 p. 75 Interscience, New York (1964)
11. E. W. Gorter Philips Res. Rep. 9,295(1954)
12. E. F. Bertaut, C. r. hebd Seanc. Acad. Sci. Paris 230, 213 (1950)
13. E. F. Bertaut, J. Phys. Rad. 12,252 (1951)
14. Ohnishi & Teranishi T. J. Phys. Soc. Jpn.,16(1961) 36
15. Preudhomme J. & P. Tarte, Spectrochim Acta 28 A(1972) 69
16. P. Tarte, Spectrochim Acta 19 (1965) 49
17. R. D. Waldron Phys. Rev. 99 (1955) 1727
18. S. T. Hafner Z. Fur Krist 115, (1961) 331
19. J. N. Smith , Magnetic properties of material Mc Graw-Hill, New York.
20. L. Neel, Ann. Phys. 3 (1948)137
21. Urvi V. Chhaya , Bimal S. Trivedi et al. Physica B. 262 (1999) 5-12
22. K.B. Modi et al J. of Material Science 34 (1996) 1311-1317
23. C. R. K. Murthy, S. D. Likhite , Earth PlaneSci. Lett. 7 (1970)
24. C. Radha Krishnamurthy & N. G. NanadikarB Pramana J.Physics 13 (1979) 419
25. C. P. Been , J. Appl. Phys. 26 (1955) 1981
26. E. L. W. Verwey, P.W. Haajman F. C. Romeijn, LChem. Phys. 15 (1947) 181-187
27. L. G. Van Uitert, Proc. IRE, 44, (1956) 1294
28. G. H. Jonkar J. Phys. And chem. Of solids , 9 (1959) 165
29. W. Haubenreisses Phys. State. Solid. 21 (1956) 3905
30. G. Srinivasan & C.M. Srivastav,Phys. Stat. Solidi, 108 (1981)
31. B. Viswanathan, V. R. K. MurthyFerrite material science and TechnologyNarosa publ. House, New Delhi (1990)
32. D. Ravinder , G. Ranga Mohan,Material letters 44 (2000) 139-143
33. P. V. Reddi and T.S.Rao, Phys. Stat. Soli statsol (a) 92 , 303(1985)
34. C. G. Koops Phys. Rev. 83 (1951) 121
35. K. Iwauchi J. Appl. Phys. 10 (1971) 520
36. Rezlescu N. and Rezlescu E. Phys. Status Solidi (a). 23, (1974)
37. L. I. Rabin , Z. I. Novikova ,Ferrites , Mansik,(1960) 146.

CHAPTER - 5

RESULTS AND DISCUSSION FOR $Ni_{0.7}Mg_{0.3}Cr_xFe_{2-x}O_4$ SYSTEM

5.1 X-ray Diffraction

The single-phase formation of all the samples was confirmed from X- ray diffraction pattern as shown in fig (5.1). The X-ray diffraction patterns show reflections from the planes, which indicate spinel structure [1]. The values of the lattice parameter 'a' have been determined using X-ray data with an accuracy of ± 0.002A^0 for all the samples, which are listed in Table (5.1). The variation of lattice parameter with increase of Cr^{3+}concentration in the composition is as shown in figure (5.2). There is co-relation between the ionic radius and the lattice parameter [2]. The ionic radii r_A and r_B have been estimated by considering the cation distribution. The values of theoretical lattice parameters have been determined by using the following relation, [3]

$$a_{th} = \frac{8}{3\times\sqrt{3}}[(r_A + R_0) + \sqrt{3}(r_B + R_0)] \quad \text{(5.1)}$$

where r_A and a_B are ionic radii of tetrahedral site and octahedral site respectively and R_0 is the radius of the oxygen ion [4].

The decrease in r_B with increase in Cr^{3+} suggests the replacement of larger Fe^{3+}(0.64 A^0) by smaller Cr^{3+} (0.63A^0) [5] on B- site. The octahedral site plays a dominant role rather than the tetrahedral site in influencing the values of lattice parameter. The average ionic radii decrease slowly with increasing Cr^{3+} content,which is reflected in the decrease in lattice parameter with (x). Thus the decrease in lattice parameter may be attributed to the replacement of larger ion Fe^{3+}(0.64A^0) by smaller ions Cr^{3+} (0.63A°) [6]. The values of the theoretical lattice parameter and the observed lattice parameter are listed in the table (5.2). The values of lattice parameterare found to be comparable with reported values in the literature.

The x-ray densities of all the samples were calculated using the formula, [7]

$$dx = \left(\frac{8M}{Na^3}\right) gm.cm^{-3} \quad \text{(5.2)}$$

where a is lattice parameter, M is the molecular weight of the sample N is the Avagadro's number . All the values of x-ray density are listed in the table (5.1). X-ray density is found to be slightly increasing with increase of Cr^{3+} in the system and bulk density reflects the same trend. This small increase in density may be ascribed to the density and atomic weight of Cr^{3+} (51.996,7.19 gm-cm^{-3}) which is almost equal to that of Fe^{3+} (55.8,7.87gm-cm^{-3}).

The particle size (t) of all the samples was determined byScherr's formula, [8]

$$t = \frac{0.9\lambda}{BCos\theta} \quad \text{(5.3)}$$

where, λ is the wavelength of the target used (here Cukα=1.5418),B is the full width at half maximum of diffracted intensity line whichis obtained by resolving (311) reflectionline of X-ray diffraction pattern. The resolved peaks for all the samples are depicted in the fig. (5.1-5.6), the values of particle size for the samples are listed in the table (5.1). The particle size is observed to be in the range 300A^o to400Ao and the mean particle size is 317.6385 A^o. The observedvalues are appreciably comparable with that observed in ceramicallyprepared powders.

The percentage porosity (% P) of all samples have been determined with the help of following relation,

$$P = \left|1 - \frac{d}{dx}\right| \times 100\% \quad \text{(5.4)}$$

where d is bulk density and dx is X-ray density . The values of percentage porosity (% P) are listed in the table (5.1) the porosity level is found to be 15 % to 32%.

The x-ray intensities have been calculated by using theformula given by Burger [9]

$$I_{hkl} = |F_{hkl}|2\, P.L_P \quad \text{(5.5)}$$

where F_{hkl} is structure factor , P is multiplicity and L_p is Lorentz polarization .The cation distributions are determined by considering the ratios of intensities for the structure sensitive planes [11-13]. According to Ohnishi and Teranshi [14] the intensity ratios of the planes I(220)/I(400)and I(422)/I(400) are considered to

be sensitive.The ratios I_{220} /I_{440} and I_{422}/I_{400} have been taken into consideration todetermine cation distribution be sides the saturation magnetization.The intensity ratios are listed in the table (5.3). The cation distribution based on the X-ray intensity ratio has been estimated and is given in table (5.3).

Composition (x)	**Lattice parameter**		**X-ray density dx.gm/cm^3**	**Particle Size t.A^0**	**Porosity %**
	a.$_{obs.}$A^0	**a.cal A^0**			
0.0	8.3330	8.3344	5.142	315.61	32
0.1	8.3264	8.3240	5.144	325.95	21
0.2	8.3257	8.3180	5.146	331.29	19
0.3	8.3250	8.3129	5.148	380.10	15
0.4	8.3160	8.3072	5.151	320.69	20
0.5	8.3076	8.2920	5.156	256.71	15

Table-5.1: Variation of lattice parameter, X-ray density, particle size and porosity for $Ni_{0.7}\ Mg_{0.3}\ Cr_x\ Fe_{2-x}\ O_4$ System

Composition (x)	**r_A A^0**	**r_B A^0**	**a_AA^0**	**a_{obs} A^0**
0.0	0.64015	0.6694	8.3344	8.3330
0.1	0.64210	0.6566	8.3240	8.3264
0.2	0.64183	0.6677	8.3180	8.3257
0.3	0.64156	0.6674	8.3129	8.3250
0.4	0.64129	0.6670	8.3072	8.3160
0.5	0.64102	0.6942	8.2920	8.3076

Table-5.2: Variation of ionic radii and lattice parameter [Thoretical and observed] for $Ni_{0.7}\ Mg_{0.3}\ Cr_x\ Fe_{2-x}\ O_4$ System

(x)	**Cation distribution**		**Intenisity Ratios**					
	A-Sites	**B-Sites**	**I_{220}/I_{400}**		**I_{422}/I_{400}**		**I_{440}/I_{422}**	
			Cal.	**Obs.**	**Cal.**	**Obs.**	**Cal**	**Obs.**
0.0	$(Mg^{2+}_{0.015}\ Fe^{3+}_{0.985})$	$[Ni^{2+}_{0.7}\ Mg^{2+}_{0.285}\ Fe^{3+}_{1.015}]$	1.32	1.10	0.50	0.27	4.97	5.66
0.1	$(Mg^{2+}_{0.018}\ Ni^{2+}_{0.024}\ Fe^{3+}_{0.958})$	$[Ni^{2+}_{0.676}Mg^{2+}_{0.282}Cr^{3+}_{0.1}\ Fe^{3+}_{0.942}]$	1.40	1.00	0.53	0.40	4.23	3.85
0.2	$(Mg^{2+}_{0.015}\ Ni^{2+}_{0.021}\ Fe^{3+}_{0.964})$	$[Ni^{2+}_{0.679}Mg^{2+}_{0.285}Cr^{3+}_{0.2}\ Fe^{3+}_{0.836}]$	1.37	1.44	0.52	0.46	4.30	4.00
0.3	$(Mg^{2+}_{0.015}\ Ni^{3+}_{0.018}\ Fe^{3+}_{0.967})$	$[Ni^{2+}_{0.682}Mg^{2+}_{0.285}Cr^{3+}_{0.3}\ Fe^{3+}_{0.733}]$	1.39	1.50	0.52	0.50	4.26	3.43
0.4	$(Mg^{2+}_{0.009}\ Ni^{2+}_{0.015}\ Fe^{3+}_{0.976})$	$[Ni^{2+}_{0.685}Mg^{2+}_{0.291}Cr^{3+}_{0.4}\ Fe^{3+}_{0.624}]$	1.42	1.38	0.53	0.26	4.24	5.88
0.5	$(Mg^{2+}_{0.006}\ Ni^{2+}_{0.012}\ Fe^{3+}_{0.982})$	$[Ni^{2+}_{0.688}Mg^{2+}_{0.294}Cr^{3+}_{0.5}\ Fe^{3+}_{0.518}]$	1.32	1.29	0.50	0.37	4.39	4.59

Table-5.3: Cation distribution and intensity ratios for $Ni_{0.7}Mg_{0.3}Cr_xFe_{2-x}O_4$ system

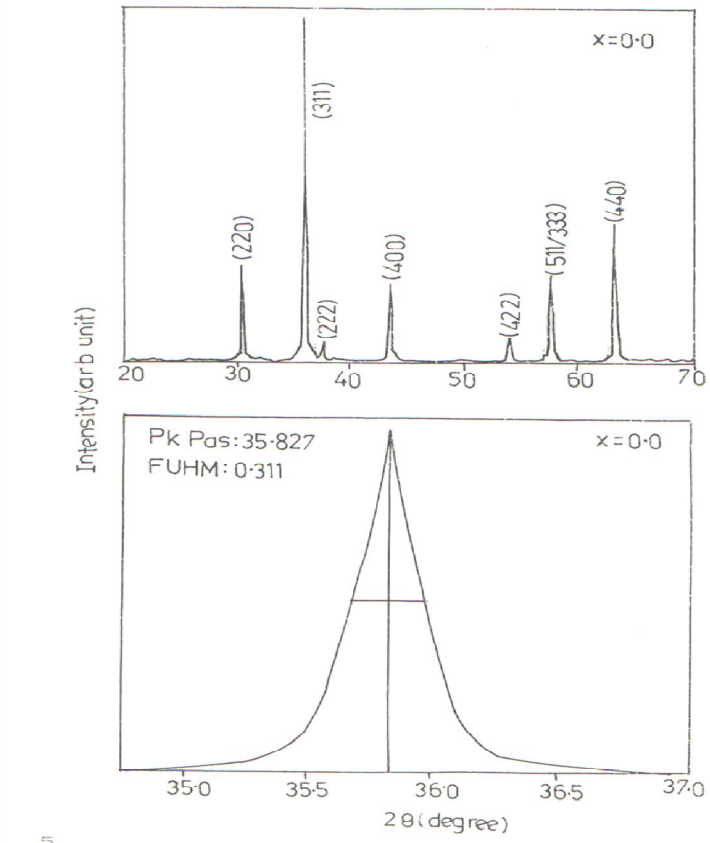

Fig.4.1 Typical X-ray diffractograms of $Ni_{0.7}Mg_{0.3}Cr_xFe_{2-x}O_4$ for x = 0.0

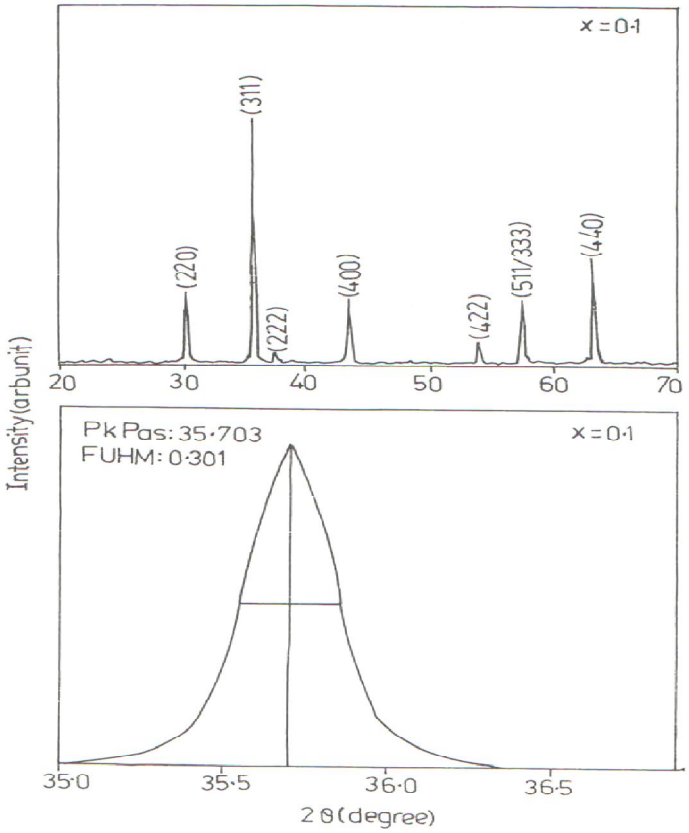

Fig.5.2 Typical X-ray diffractograms of $Ni_{0.7}Mg_{0.3}Cr_xFe_{2-x}O_4$ for x = 0.1

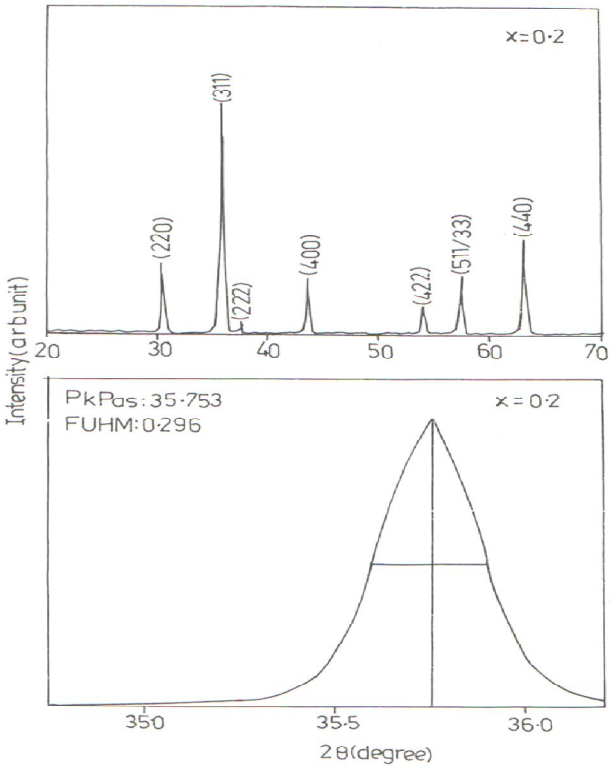

Fig. 5.3 Typical X-ray diffractograms of $Ni_{0.7}Mg_{0.3}Cr_xFe_{2-x}O_4$ for x = 0.2

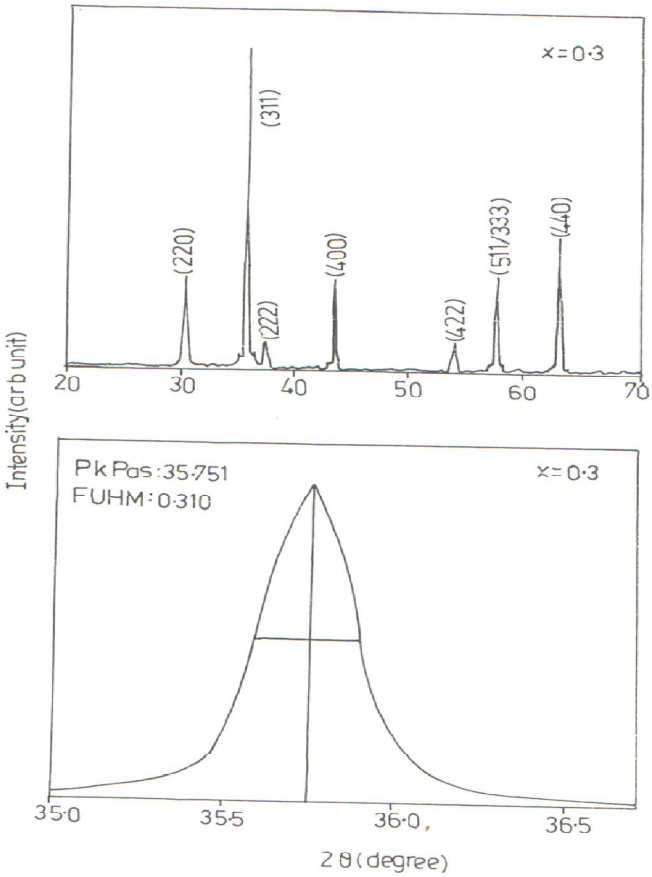

Fig. 5.4 Typical X-ray diffractograms of $Ni_{0.7}Mg_{0.3}Cr_xFe_{2-x}O_4$ for x = 0.3

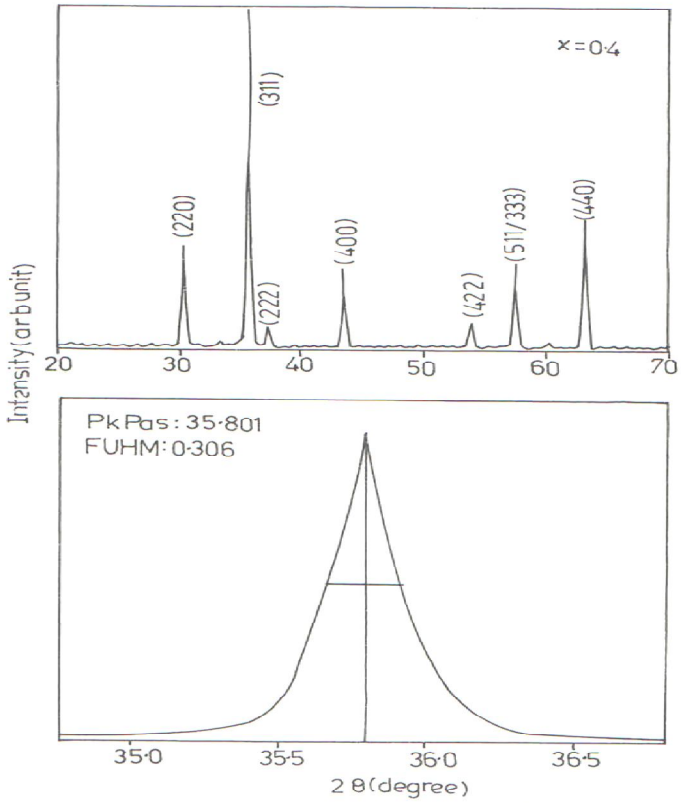

Fig.5.5 Typical X-ray diffractograms of $Ni_{0.7}Mg_{0.3}Cr_xFe_{2-x}O_4$ for x = 0.4

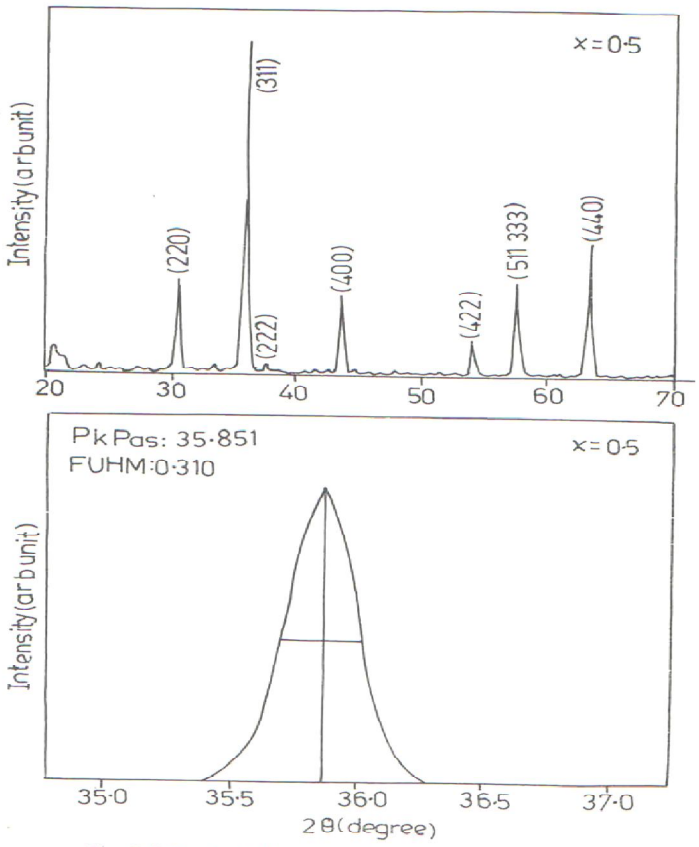

Fig.5.6 Typical X-ray diffractograms of $Ni_{0.7}Mg_{0.3}Cr_xFe_{2-x}O_4$ for x = 0.5

5.2 IR spectra

The infrared spectra of the present system at room temperature for the typical samples with x = 0.0 to 0.5 are shown in the (5.9-5.11). The absorption band positions are located on infrared spectra for all the six samples and are given in the table (5.4). TheI.R. spectra of the samples show that the absorption of lower frequency band (v_2) lies in the range 400-430 cm^{-1} and that of the higher frequency band (v_1) lies in the range 590-610 cm^{-1} [15]. The absorption bands for all the six samples are found to be in the expected range. Preudhomme and Tarte [16] have assigned the absorption of lower frequency band (v_2) to octahedral complex andthe absorption of higher frequency band (v_1) band to the tetrahedral complex. The difference in the band position is attributed to the difference in Fe-O distances for octahedral and tetrahedral site [17].The peak intensity changes with chromium content. The broadening of the low frequency band is observed and it is increasing with the increase in the chromium content.This broadening of the low frequency band may be due to chromium clustering and its different valence states.

The splitting in the band around lower frequency indicates the presence of Fe^{2+} in the octahedral site. The observed shoulders inthe I.R. spectra also present the ordering of the cations. The force constants and bond lengths for tetrahedral and octahedral sites have been calculated by using the method suggested by Smith J. N. [18] and are tabulated in table (5.4). The stretching bond at tetrahedral sites would lead to higher force constant than that of the octahedral sites. The decrease in the bond lengths is attributed to the decrease in the lattice parameter and indicates the increase in the covalent natureof the bonds. The force constants for both the sites decrease with increase in chromium content in the sample. The variations in the force constants and in the bond lengths with chromium content are shown in the figure (5.12-5.13).There are small decrease in thelattice parameter. The chromium occupies octahedral site and replaces Fe^{3+}. This replacement of Fe^{3+} by chromium results in the slight decrease in ionic radii which is due to very small difference intheir ionic radii.(Fe^{3+}=0.64^{0}A &Cr^{3+} = 0.63°A). From the I.R. studyit seems that the chromium modifies the cation ordering in the system. The molecular weight at tetrahedral (M_1) and that at octahedral (M_0) site have been calculated using the cation distribution obtained from X-ray diffraction and magnetization measurements. The values of v_1, v_2, K_t, K_0, R_A and R_B are found tobe in good agreement with reported ones. The force constant K_t decreases with the increase in R_A and the force constant K_0 decreases with decrease in the R_B. The slight variations in V_1 and V_2 indicate that the method of preparation, grain size, and sintering temperaturecan influence the band positions. The decrease in bond lengths is attributed to the decrease in lattice parameters. A slight splitting ofsome bands indicates valence variations of Fe^{2+} (i. e. presence ofFe^{2+} ion). Normally stretching bond of tetrahedral complex leads the higher force constant for tetrahedral site than that for octahedral site.

(x)	Vibration Frequencies		Bond Lengths		Force Constants	
	$v_{1\ cm}^{-1}$	$v_{2\ cm}^{-1}$	R_A A^0	R_B A^0	$K_t x10^5$ dynes/cm	$K_0 x10^5$ dynes/cm
0.0	610	405	1.869042	2.046439	3.479	0.9793
0.1	610	400	1.873597	2.044280	3.444	0.9860
0.2	600	420	1.874680	2.042540	3.410	0.9920
0.3	600	400	1.875180	2.040200	3.388	1.0000
0.4	610	400	1.876160	2.037471	3.350	1.0300
0.5	600	410	1.877150	2.034618	3.306	1.0600

Table-5.4: Vibration frequency, Bond legths and force constants for $Ni_{0.7}Mg_{0.3}Cr_xFe_{2-x}O_4$ system

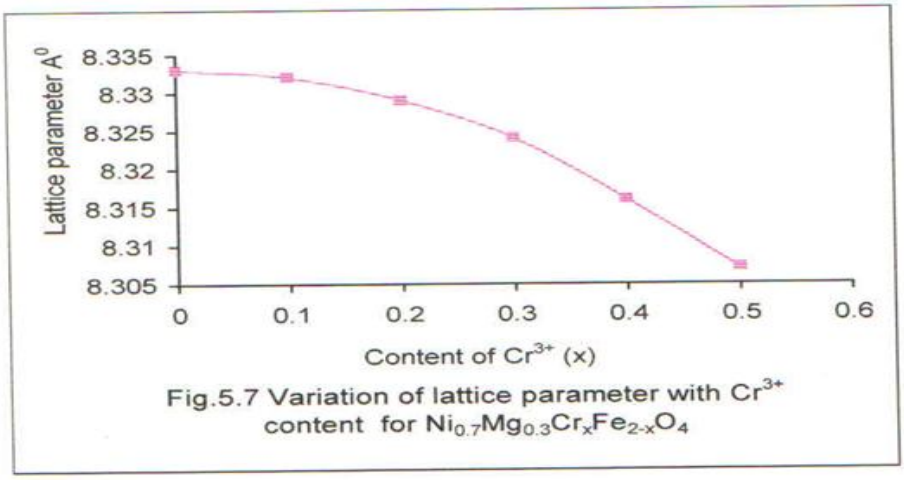

Fig.5.7 Variation of lattice parameter with Cr^{3+} content for $Ni_{0.7}Mg_{0.3}Cr_xFe_{2-x}O_4$

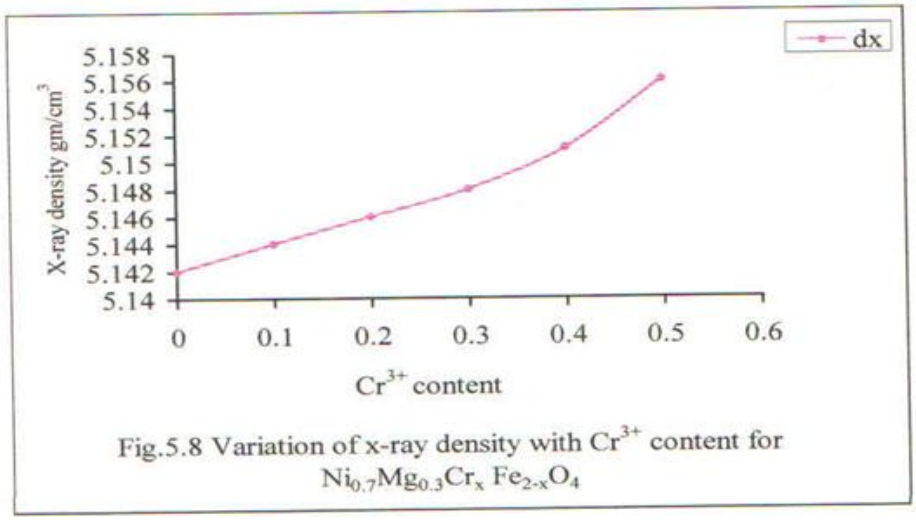

Fig.5.8 Variation of x-ray density with Cr^{3+} content for $Ni_{0.7}Mg_{0.3}Cr_x\ Fe_{2-x}O_4$

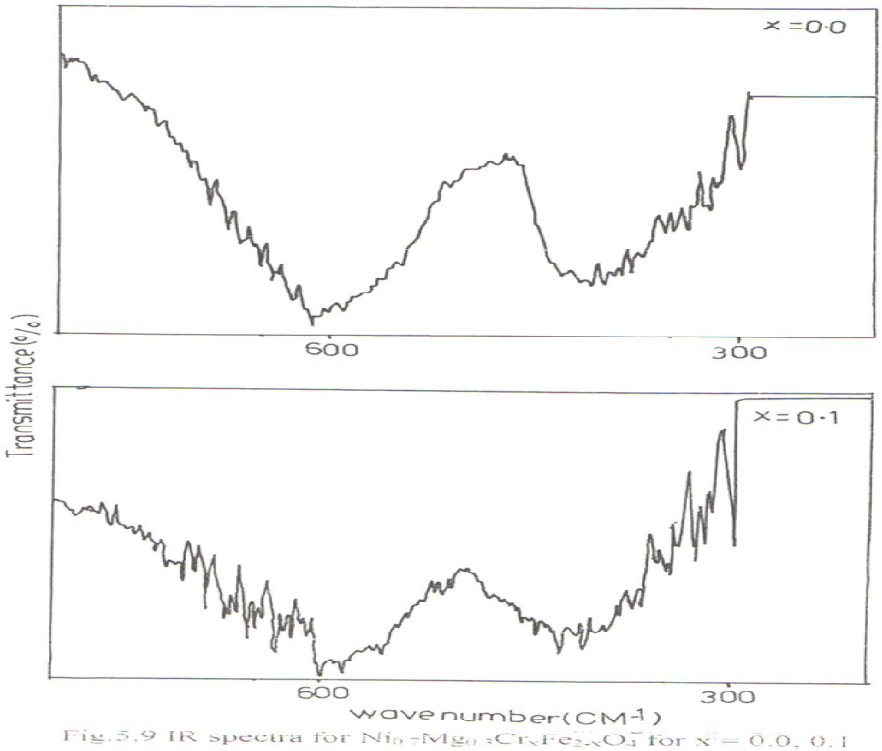

Fig.5.9 IR spectra for $Ni_{0.7}Mg_{0.3}Cr_xFe_{2-x}O_4$ for x = 0.0, 0.1

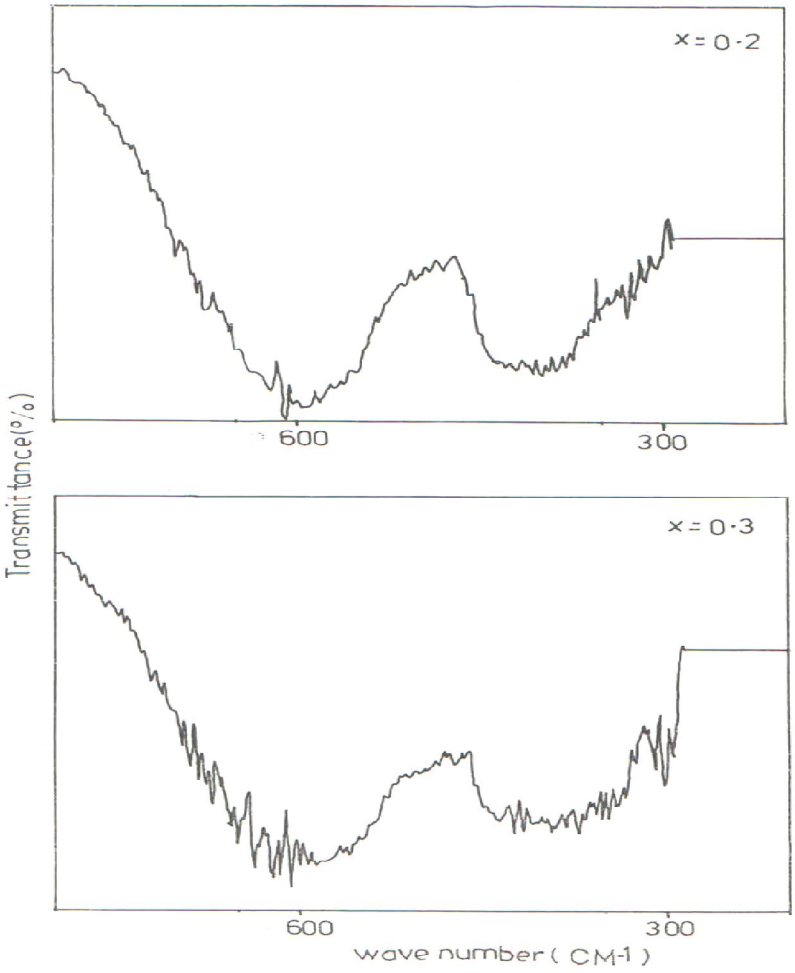

Fig.5.10 IR spectra for $Ni_{0.7}Mg_{0.3}Cr_xFe_{2-x}O_4$ for x = 0.2, 0.3

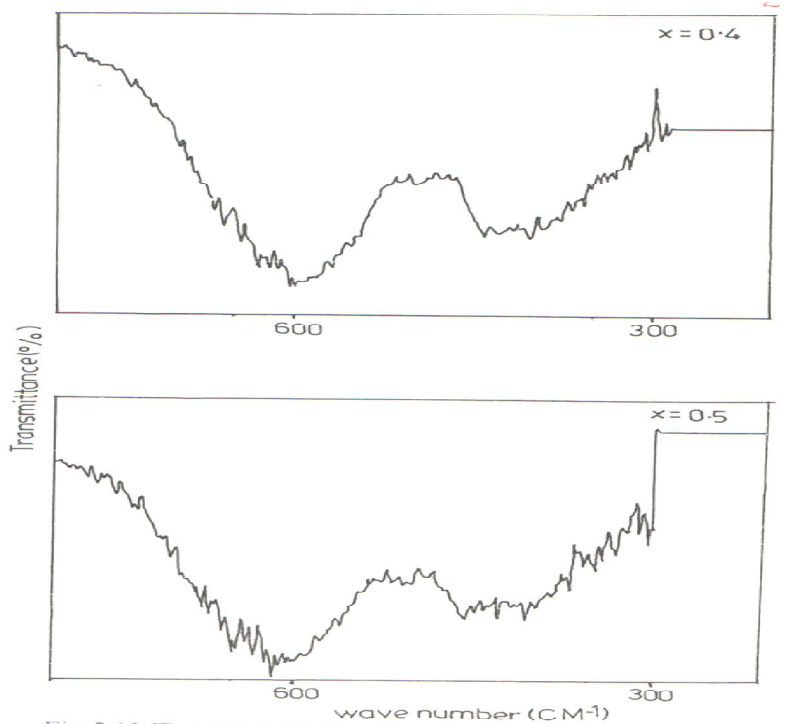

Fig.5.11 IR spectra for $Ni_{0.7}Mg_{0.3}Cr_xFe_{2-x}O_4$ for x = 0.4, 0.5

5.3 Saturation magnetization

The values of saturation magnetization (σ_s) and Bohr magneton number (η_B i.e.the saturation magnetization per formulaunit in Bohr magneton) at 300 °K were obtained from hysteresis loop technique for all the samples of the series. The values of σ_s and η_B are presented in table (5.5). From field dependence of magnetization and observed magnetic moment decreases with increase in chromium content. As chromium (Cr^{3+} has η_B=3) has strong B-site preference itreplaces Fe^{3+} (η_B = 5) decreases the magnetization at B-site therefore there is decrease in the magnetization with increasing Cr^{3+} content inthe composition. However the change in magnetization with increasein Cr^{3+} content in the composition is slower as compared to that of the first system. The saturation magnetization $\sigma_s$is calculated from hysteresis loop for all the six samples and magnetic moment performula unit (η_B) is calculated by using the following relation, [18]

$$\eta_B = \frac{\sigma_s}{5585} \times M_{wt} \quad \text{.....(5.6)}$$

where M_{wt} is molecular weight, $\sigma_s$is saturation magnetization. The decrease in the saturation magnetization with increase in Cr^{3+} can be explained by using Neel's two sub-lattice collinear model for ferrimagnetism upto x = 0.4. According to Neel's collinear model offerrimagnetism, the magnetic moment per formula unit is expressedas [19]

$$\eta_B^N = M_B(\times) - M_A(\times) \quad \text{..... (5.7)}$$

where $M_A(x)$ and $M_B(x)$ are magnetic moments in of sublattice Aand B respectively. The η_B^N values for $Ni_{0.7}Mg_{0.3}Cr_xFe_{2-x}O_4$ with x = 0.0 to 0.5 ,were calculated using the ionic magnetic moments of Fe^{3+}, Ni^{2+}, Mg^{2+}, $Cr^{3+}$with their respective values $5\mu_B$, $2\mu_B$, $0\mu_B$ and$3\mu_B$ .Chromium and nickel have strong B-site preference. The substituted chromium replaces Fe^{3+} and magnetic moment at B-site decreases. Thus the decrease in the saturation magnetization is due to occupation of B-site by Cr^{3+} which has less magnetic moment as compared to Fe^{3+} and reduction in Fe^{3+} content at B-site. The observed saturation magnetization for x = 0 to x = 0.4 can be explained by using Neel's collinear model for ferrimagnetism. However for larger chromium content, X = 0.5 the variation in the magnetization indicates the presence of canted spin arrangement on the B-site [20]. The experimental values of η_B^N are compared with those calculated ones by using cation distribution. The variations of η_B^N with respect to the Cr3+concentration in the composition, is shown in figure (5.14). The values of σ_s and η_B^N The curves suggest the existance of collinear spin order in the samples except sixth sample x > 0.4 as the higher Cr^{3+} concentration in the composition may affect the magnetic interactions. The larger quantity of Cr^{3+} may dilute the A-B interaction there by creating the canted spin structure. Thus the higher concentration of chromium makes magnetic structure to be non-collinear. The change of spin ordering from collinear to the non-collinear displays strong influence on the variation of the saturation magnetic moment.

(x)	**Saturation Magnetization σ_s (emu/gm)**	**η_B (μ_B)**		**Curie Temperaure T_c (^{0}K)**	
	$v_{1\ cm}^{-1}$	Cal	Obs.	From Susc.	From d.c. Resty.
0.0	37.294	1.55	1.496	820	809
0.1	36.781	1.524	1.381	790	790
0.2	34.430	1.276	1.295	775	785
0.3	33.550	1.058	1.222	760	780
0.4	32.630	0.78	1.190	765	778
0.5	31.700	0.532	1.007	750	765

Table-5.5: Satration Magnetization., Bohrs magneton and Curie temperature for $Ni_{0.7}Mg_{0.3}Cr_xFe_{2-x}O_4$ system

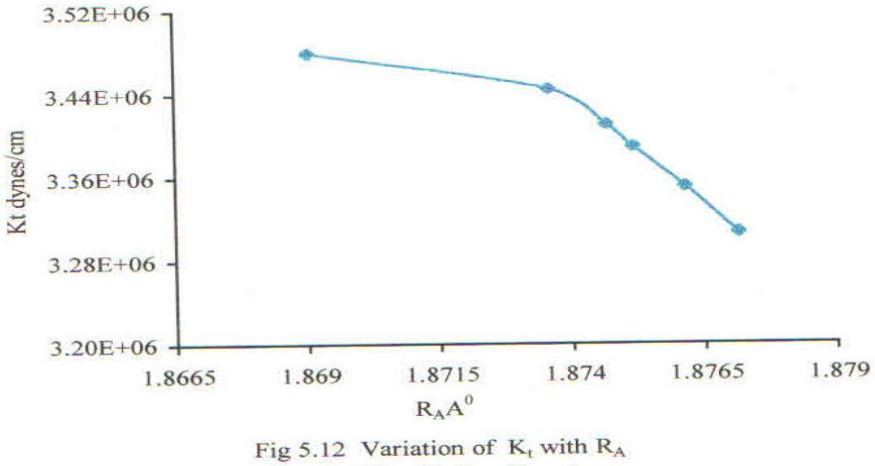

Fig 5.12 Variation of K_t with R_A for $Ni_{0.7}Mg_{0.3}Cr_xFe_{2-x}O_4$ system

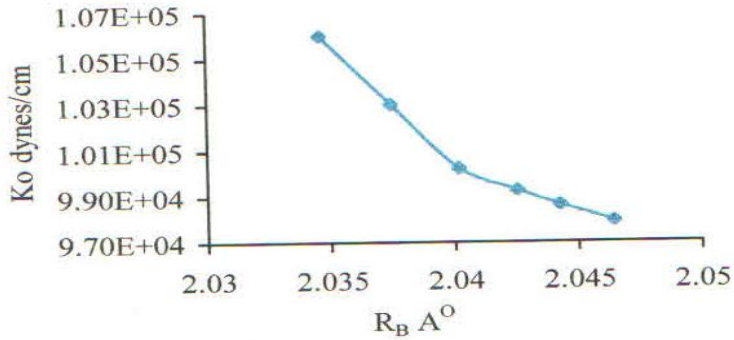

Fig. 5.13 Variation of K_o with R_B for $Ni_{0.7}Mg_{0.3}Cr_xFe_{2-x}O_4$

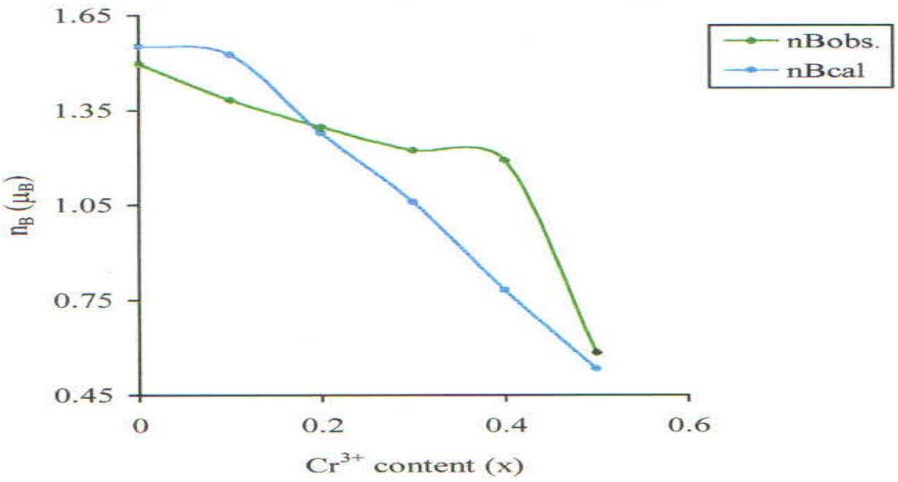

Fig.5.14 Variation of n_B with Cr^{3+} content for $Ni_{0.7}Mg_{0.3}Cr_xFe_{2-x}O_4$

5.4 A.C.Susceptibility

The plots of relative low field ac susceptibility $\frac{\chi_T}{\chi_{RT}}$ indicates room temperature) against temperature T, for all samples are shown in figure [5.15-5.16] which exhibit normal ferromagnetic behavior [21] . The nature of $\frac{\chi_T}{\chi_{RT}}$ curves suggests the magneticthan the domainstates in ferrites. The temperature variation of a.c.susceptibility shows that the samples contain multi-domain structure. The Curie temperature of $Ni_{0.7}Mg_{0.3}Cr_xFe_{2-x}O^{2-}_4$ system decreases with an increase of Cr^{3+}concentration in the composition. However, the rate of decrease of the curie temperatures for this is slower than that in case of the first system. The curie system temperatures of all the samples are considerably high which signify good stability of magnetic ordering at high temperature. In all the $\frac{\chi_T}{\chi_{RT}}$ curves, there is peaking behavior near Curie temperature and just before Curie temperature it drops rapidly. The temperature corresponding to peak is called blocking temperature. Near the blocking temperature, the transition of magnetic particle from single domain to multi-domain takes place [22]. This peak could be seen for a magnetic material in multi-domain state. According to Been [23], the susceptibility is inversely proportional to the coercive force, therefore the increase in susceptibility after the isotropic peak is attributed to a decrease incoercive force. The peaking nature of the relative susceptibility indicates that samples contain the multi-domain structure. The Fe-Fe interaction is stronger than the Cr-Cr or Fe-Cr interaction hence thereis decrease in magnetization which results in the decrease in the Curie temperature (T_c). The chromium substitution reduces the Fe-Fe linkages and the angels between them therefore the Curie temperature decreases with increase in Cr^{3+}. The decrease in Curie temperatures may also be attributed to decrease in A-B interaction.

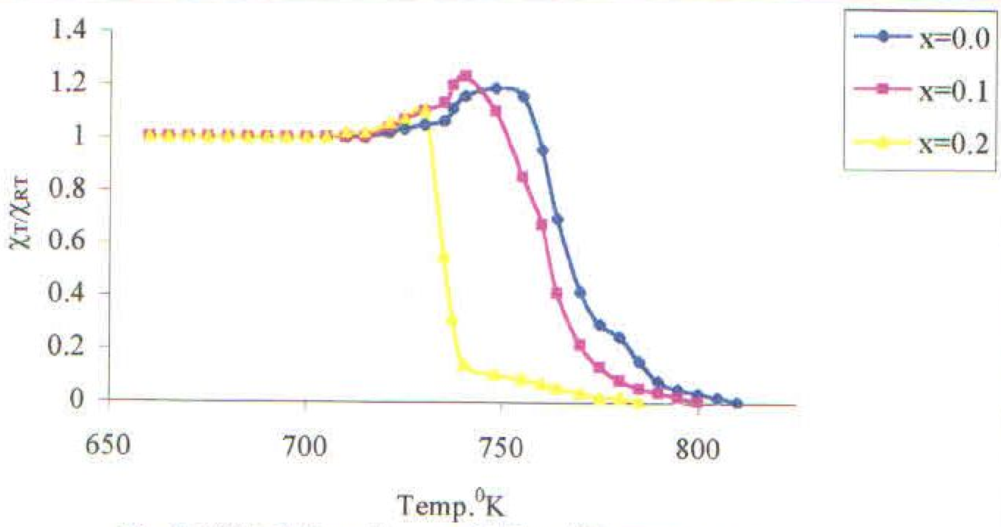

Fig. 5.15 Variation of susceptibility with temperature for $Ni_{0.7}Mg_{0.3}Cr_xFe_{2-x}O_4$system

5.5 D.C. Resistivity

The variation of d. c. resistivity with respect to temperature has been studied for all the samples.The d. c. resistivity of the system for all the samples decreases with increase in Cr^{3+}concentration in the compositions. The plots of log $\rho_{d.c}$. Versus1000/T as shown in figure (5.17-5.18) indicate the variation in d. c. resistivity. The d. c. resistivity of all the six samples decreases with increase in temperature and obey the Arrhenius relation [24]

$$\rho_{d.c.} = \rho_0 \exp\left(\frac{\Delta E}{k_B T}\right) \quad \ldots\ldots\ldots\ldots \quad (5.8)$$

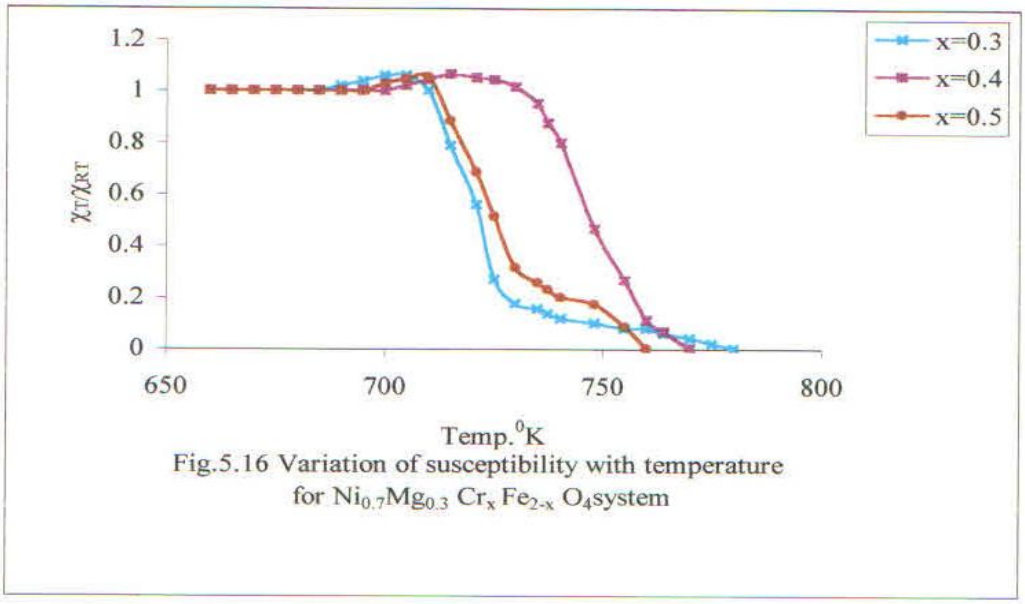

Fig.5.16 Variation of susceptibility with temperature for $Ni_{0.7}Mg_{0.3}$ Cr_x Fe_{2-x} O_4system

The plots of log $\rho_{d.c.}$ Versus 1000/T show kinks near the Curie temperature where the magnetic phase changes from ferrimagnetic region to the paramagnetic region due to thermal energy. The activation energy, in ferrimagnetic and paramagnetic region, has been calculated using above relation (4.7) and tabulated in the table (5.6). The activation energy values indicate that there exists the hopping type of conduction mechanism. The activationenergy in ferrimagnetic region is lower than that in paramagnetic region. The conduction in ferrites can be explained on the basis of hopping mechanism. It is observed that under the normal conditions the electron hopping between B-A sites is very small as compared tothat of B -B hopping. Hopping between A-A sites does not exist because most of the Fe^{3+} ions occupy A site and Fe^{2+} ions, which are formed during sintering process, preferentially occupy B-site only.The hopping probability depends upon the separation between the ions involved and the activation energy. The conduction mechanismfor the present system may be given as,

$$Fe^{3+} - Fe^{2+}$$

$$Ni^{3+} + Fe^{2+}$$

$$Ni^{2+} + Fe^{3+}$$

Both Ni and Fe ions having two different valances may be providing conductivity mechanism. The d. c. resistivity is observed to be decreasing with increase in Cr^{3+} concentration. The conduction in the ferrites is mainly due to the electron hopping among Fe^{2+} and Fe^{3+} on B-site [25] (phonon induced transfer mechanism). As the chromiumhas strong B-site preference it replaces $Fe^{3+}$from B-site which resultsin reducing the population of Fe^{3+}. This reduction of Fe^{3+}on B-site causes generally increase in the resistivity. The chromium ions do not participate in the conduction process but limit the degree of Fe^{2+}-Fe^{3+}conduction by blocking up the Fe^{2+}-Fe^{3+} pairs. The decrease in the resistivity can be attributed to following reason [26]. Fe^{2+} or Ni^{2+}may shift to tetrahedral site for higher concentration of chromium [27]. The conduction process between Fe^{2+}-Fe^{3+} takes place attetrahedral site, which results in an increase of conduction.Therefore, there is decrease in d. c. resistivity for higher Cr^{3+} ions content. The spin state in mixed magnetic oxides is also a cause for decrease in the resistivity the chromium ions exist in low spin state which cause the decrease in the resistivity (28-30).

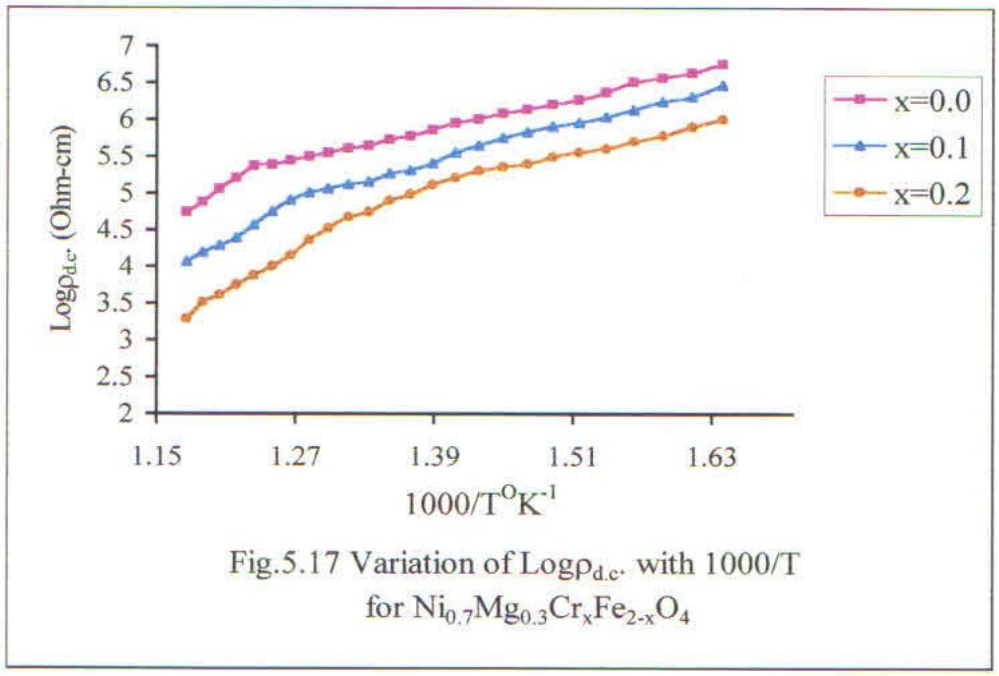

Fig.5.17 Variation of $Log\rho_{d.c.}$ with 1000/T for $Ni_{0.7}Mg_{0.3}Cr_xFe_{2-x}O_4$

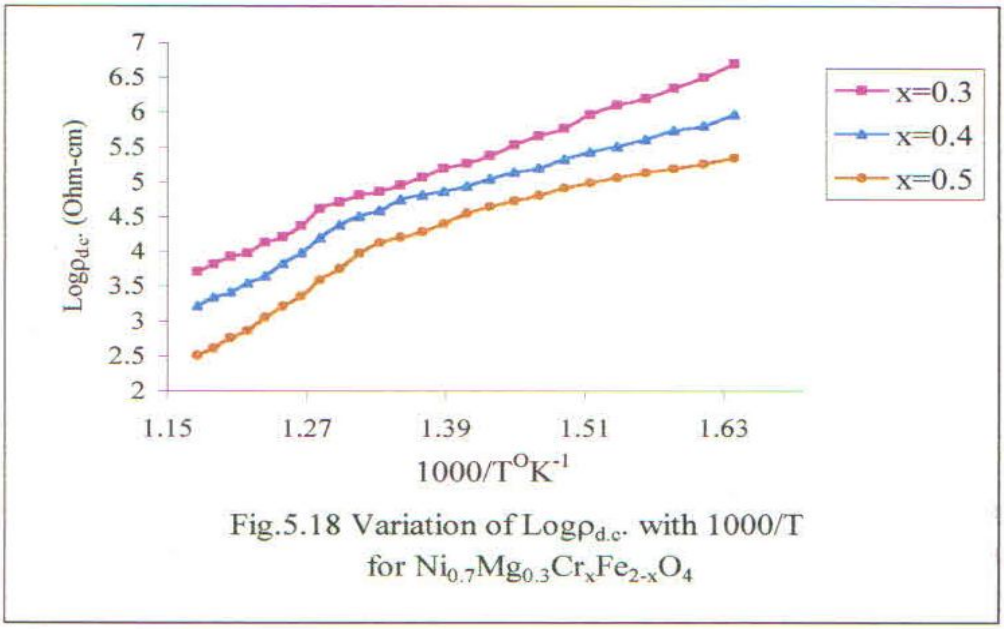

Fig.5.18 Variation of $Log\rho_{d.c.}$ with 1000/T for $Ni_{0.7}Mg_{0.3}Cr_xFe_{2-x}O_4$

5.6 Thermoelectric power

The thermoelectric power measurement of all the samples have been carried out from 350 ^{0}K to 850 ^{0}K temperature. The values of Seebeck coefficient (α) have been determined by using the following relation, [31]

$$\alpha = \frac{thermo\ emf}{Temperature\ difference\ across\ the\ sample} \quad \text{..... (5.9)}$$

The plots of Seebeck coefficient (α) against the temperature are shown in the fig.(5.19-5.20) The Seebeck coefficients have been observed to be negative upto 530°K and later on for highertemperature positive for all samples. This indicates that both types of charge carriers are present in the system. The α decreases nonlinearly with increase in temperature. The decrease of oxygen vacancies gives rise to decrease α [32]. The charge carrier concentration has beendetermined by using the following relation,

$$n = N\ exp(\frac{-\propto}{k}) \quad \text{..... (5.10)}$$

where N is the density of the state and k is Boltzmann constant. The concentration of the charge carriers increases with theincrease in temperature. The variation of charge concentration with temperature is shown in figure (5.21-5.22). The mobility for all the samples has been calculated by the following relation,

$$\mu_d = \frac{\sigma}{ne} \quad \text{..... (5.11)}$$

where σ is de conductivity ,n is the concentration of charge carriers and e is electronic charge. The variation of drift mobility with temperature is shown in figure (5.23-5.24). The drift mobility increases with increase in temperature and decreases with Cr^{3+}content. This clearly indicates that the conduction in the systems depends on the temperature dependent drift mobility and not on the temperature dependent charge carrier concentration. The decrease in dc resistivity with Cr^{3+}can also be explained on the basis of drift mobility. The Seebeck coefficient for the present series show that initially n type of charge carriers are predominant and later on from500°K onwards, p-type of charge carriers are predominant. The conduction in n-type region is due to electron hopping $Fe^{2+} \leftrightarrow Fe^{3+}$ and that in p-type region is due to hole transfer between the two different valence states of the cation [33]. The Ni^{2+} may be playing certain role in controlling the resistivity along with Fe^{2+}-Fe^{3+} pair.From the thermo electric power, the conduction is observed to be dependent on the temperature dependent drift mobility and not on the temperature dependent charge carrier concentration.

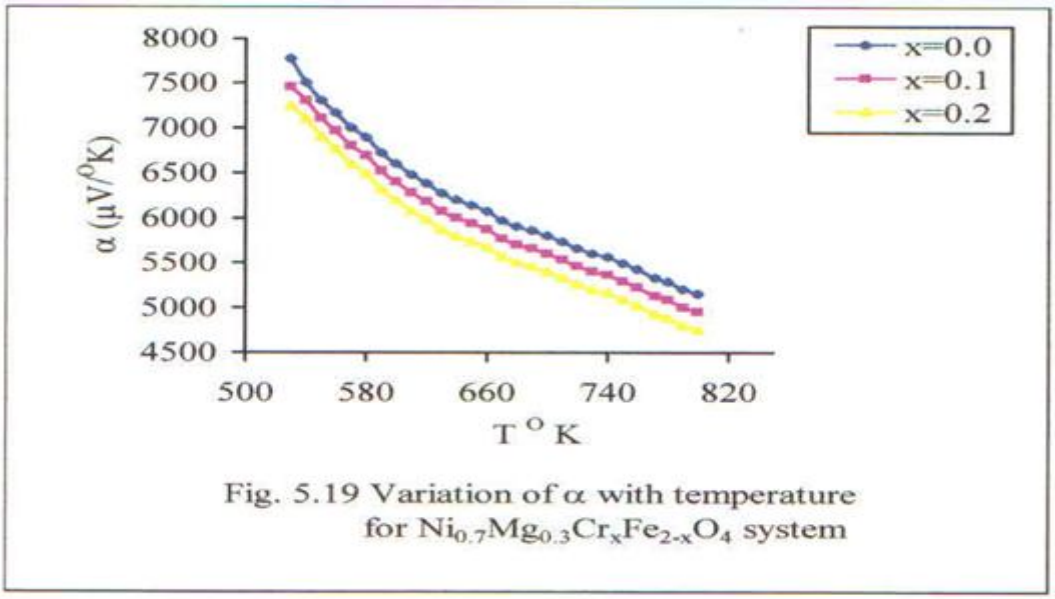

Fig. 5.19 Variation of α with temperature for $Ni_{0.7}Mg_{0.3}Cr_xFe_{2-x}O_4$ system

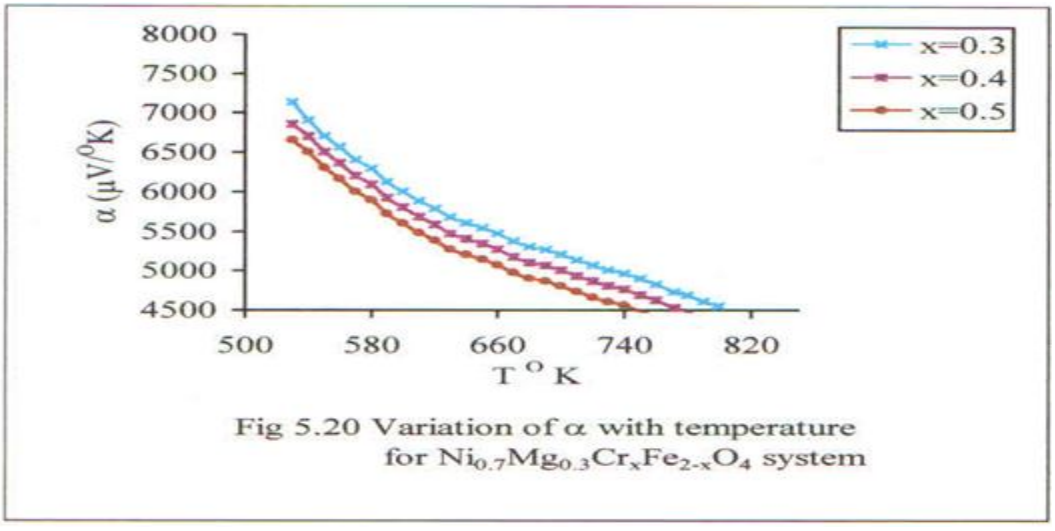

Fig 5.20 Variation of α with temperature for $Ni_{0.7}Mg_{0.3}Cr_xFe_{2-x}O_4$ system

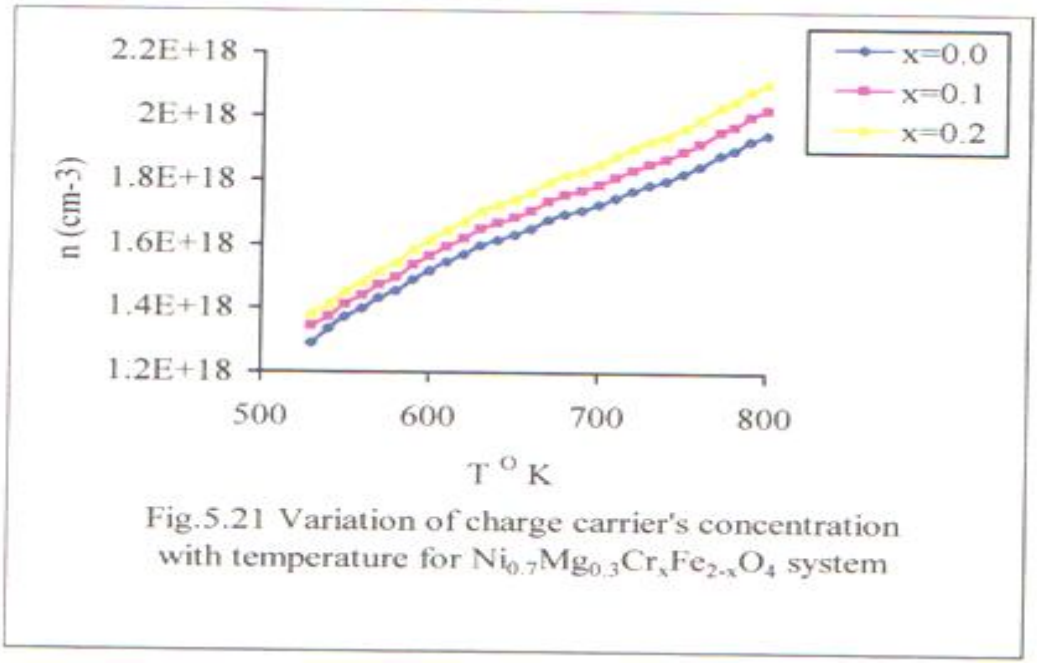

Fig.5.21 Variation of charge carrier's concentration with temperature for $Ni_{0.7}Mg_{0.3}Cr_xFe_{2-x}O_4$ system

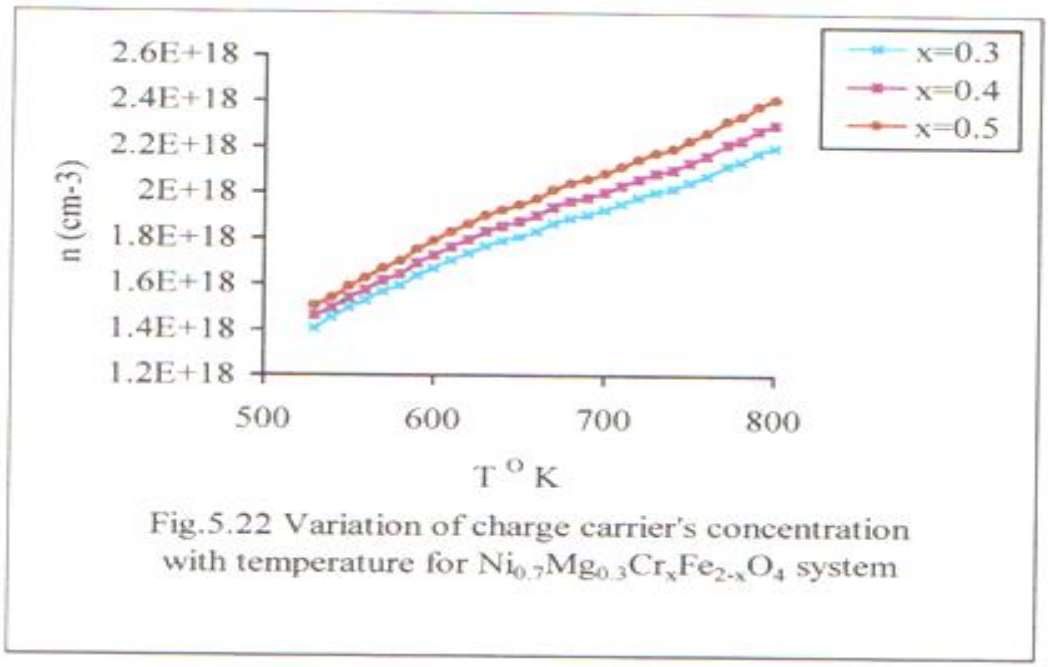

Fig.5.22 Variation of charge carrier's concentration with temperature for $Ni_{0.7}Mg_{0.3}Cr_xFe_{2-x}O_4$ system

5.7 Dielectric properties

The variation of dielectric constant as a function oftemperature at 1KHz frequency for all the six samples, containing different Cr^{3+} concentration, (i.e.for x = 0.0 to 0.5) has been shown in the figure (5.25-5.26). The dielectric constant varies slowly at the beginning and after the temperature 650° K it increases rapidly with increase in temperature. This behavior of the ε'could be explained on the basis of Maxwell Wagner interfacial polarization [34-36]. The origin of the interfacial polarization is attributed to the distribution of electical resistivities in the ferrites which is considered to be causedby the non- uniform distribution of oxygen ions induced by the sintering proces. The variation of ε' can be understood with the mechanisms of dielectric polarization and the electronic exchange which results in the displacement of the electrons in the direction of the electric field that determine the polarization in the ferrites [37].The exchange of electron in conduction mechanism may be responsible for space polarization. Thus mechanism of dielectric polarization is similar to that of conduction [38-40]. As the conductivity increases with increase in temperature, the dielectric constant also increases with increase in temperature [41]. With the rise in temperature the number

of carrier increases resulting in an enhanced build up of space charge polarization and hence increase in the dielectric constant. As the concentration of Cr^{3+} increases the conductivity, the dielectric constant obviously increases with increase in Cr^{3+}. Figure (5.27-5.28) shows the variation of dielectric loss tangent (tanδ) with temperature for all the samples. The loss tangent increases with increase in temperature. The compositional dependence shows that the dielectric loss tangent (tanδ) decreases with increase in the Cr^{3+} concentration. The variation of dielectric loss ($\varepsilon^{/}$) as a function of temperature for all the samples at frequency 1KHz is shown in the figures (5.29-5.30). The dielectric loss initially increases very slowly up to 750°K temperature and later on it increases rapidly with the increase in temperature. The dielectric loss decreases with increase in Cr^{3+} concentration in the system. Chromium minimizes the dielectric losses. The dielectric constant is found to be appreciably high.

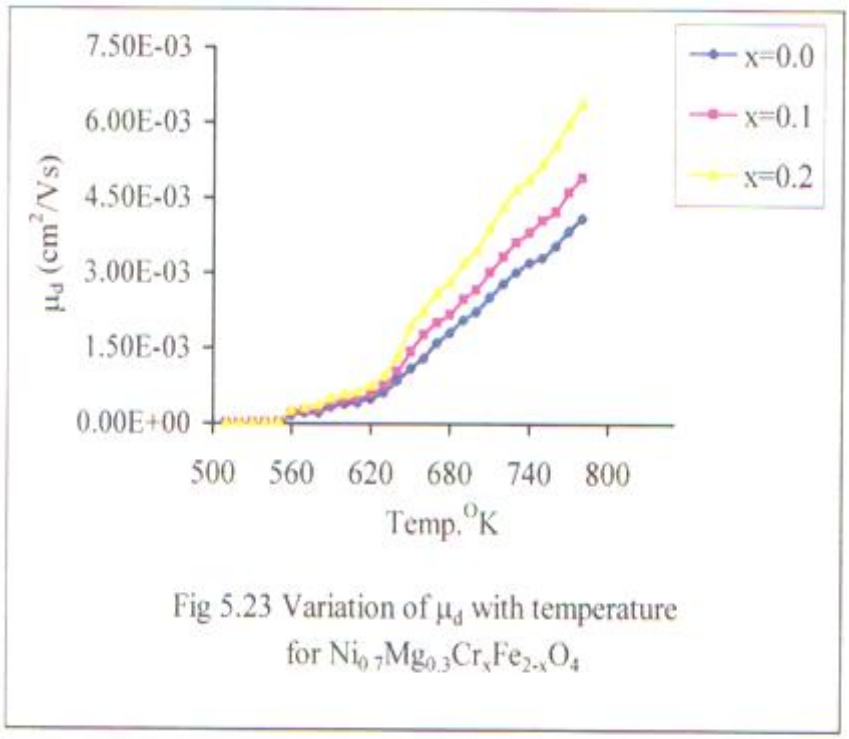

Fig 5.23 Variation of μ_d with temperature for $Ni_{0.7}Mg_{0.3}Cr_xFe_{2-x}O_4$

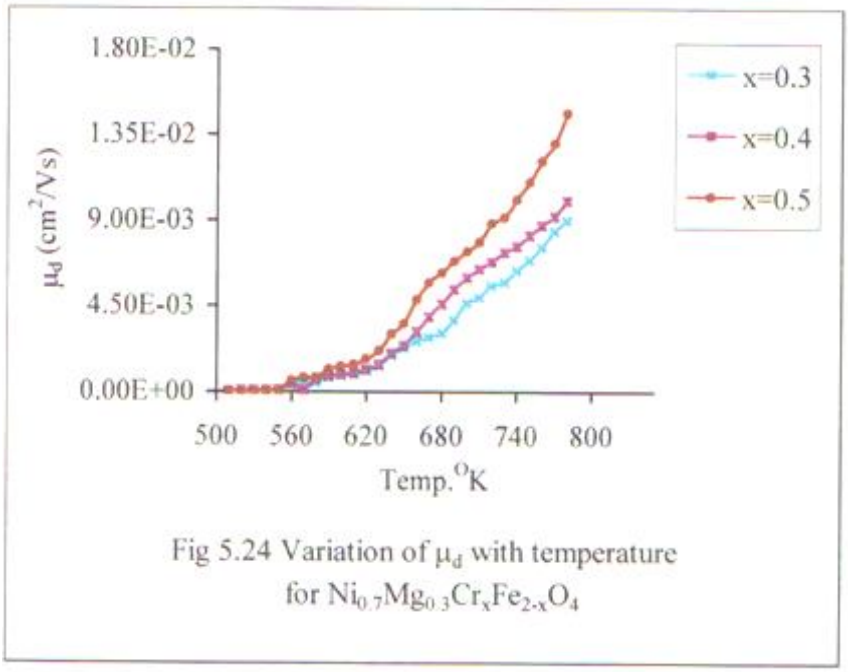

Fig 5.24 Variation of μ_d with temperature for $Ni_{0.7}Mg_{0.3}Cr_xFe_{2-x}O_4$

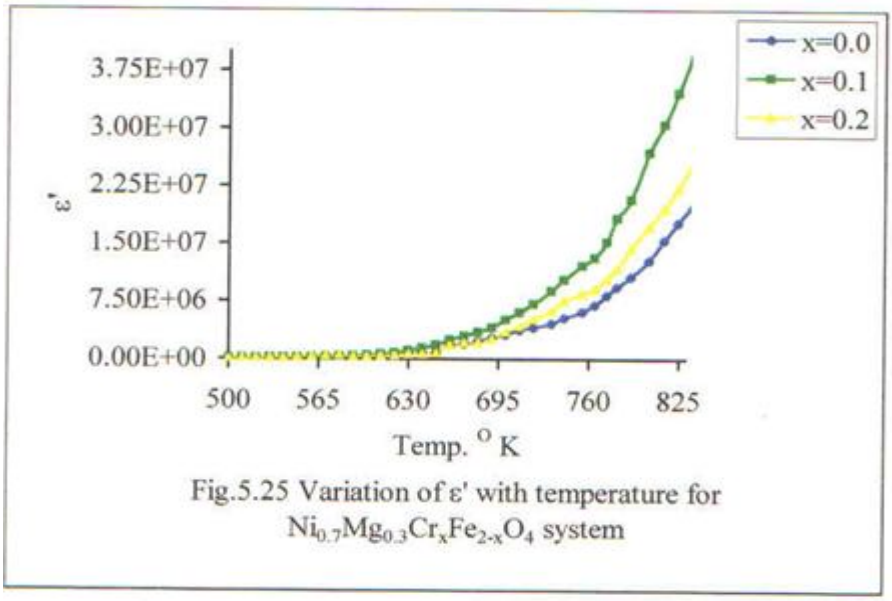

Fig.5.25 Variation of ε' with temperature for $Ni_{0.7}Mg_{0.3}Cr_xFe_{2-x}O_4$ system

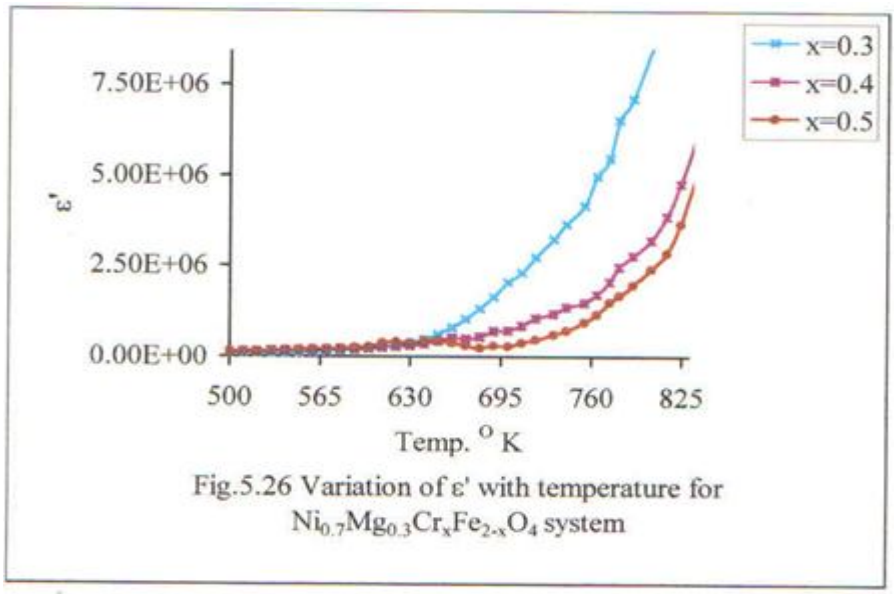

Fig.5.26 Variation of ε' with temperature for $Ni_{0.7}Mg_{0.3}Cr_xFe_{2-x}O_4$ system

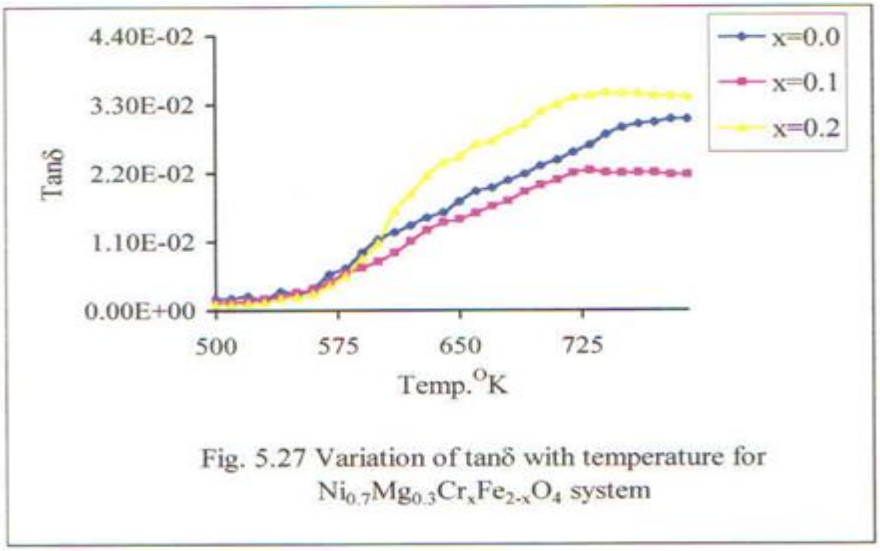

Fig. 5.27 Variation of tanδ with temperature for $Ni_{0.7}Mg_{0.3}Cr_xFe_{2-x}O_4$ system

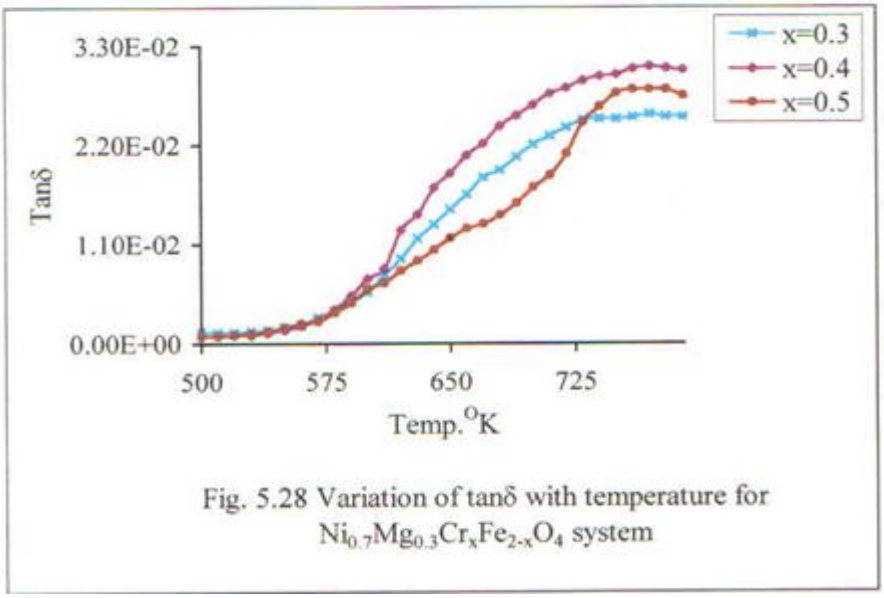

Fig. 5.28 Variation of tanδ with temperature for $Ni_{0.7}Mg_{0.3}Cr_xFe_{2-x}O_4$ system

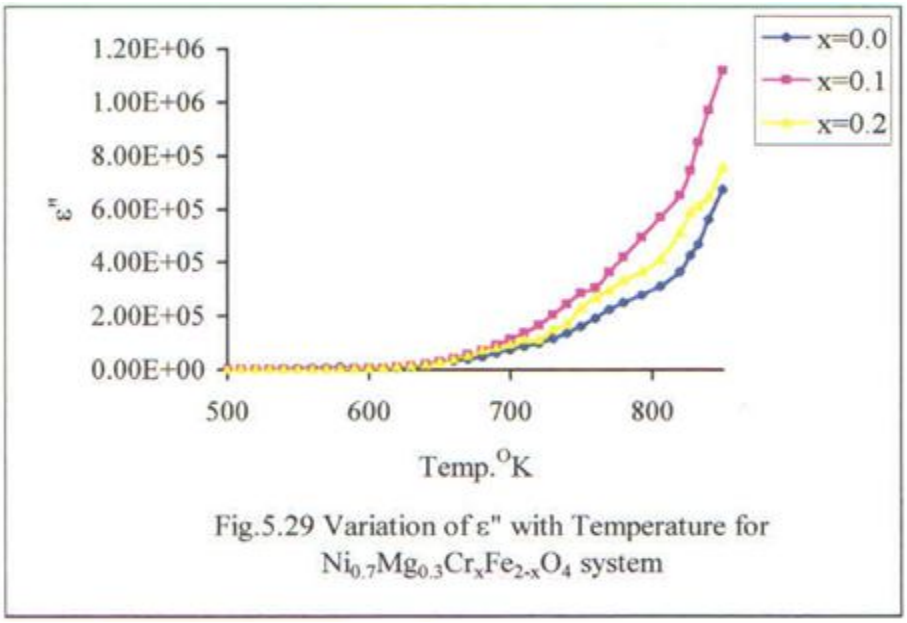

Fig.5.29 Variation of ε" with Temperature for $Ni_{0.7}Mg_{0.3}Cr_xFe_{2-x}O_4$ system

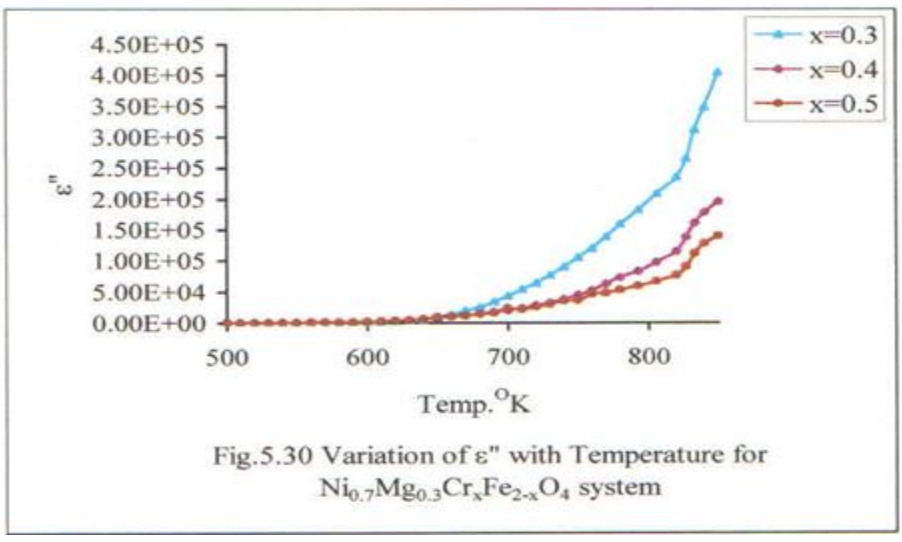

Fig.5.30 Variation of ε" with Temperature for $Ni_{0.7}Mg_{0.3}Cr_xFe_{2-x}O_4$ system

5.8 CONCLUSION

Thus from the above results and discussion the followingconclusions can be drawn.

- $Ni_{o.7}Mg_{0.3}Cr_xFe_{2-x}O_4$system has spinel structure
- The substitution of Cr^{3+} decreases the lattice parameter
- The infrared spectra of the system consist of two bands, which corresponds to the intrinsic vibrations of tetrahedral and octahedral complexes.
- The force constant K_t decreases with increase in bond length R_A
- The force constant K_0 increases with decrease in bond length R_B.
- The saturation magnetization decreases with increase inCr^{3+}content in the composition. The variation of the saturation magnetization obeys the Neel's two sublattice collinear model for ferrimagnetism upto x= 0.4 and later part indicates the canted spin
- The substitution of Cr^{3+} ion diluted the A-B interaction. The Cr^{3+}has strong B-site preference and replaces $Fe^{3+}$from B-site. The substitution of Cr^{3+} reduces the Fe-Fe linkages. Generally Fe-Feinter action is stronger than the interaction of Cr-Cr and Fe - Cr, Hence Cr^{3+} modulates the saturation magnetization.
- The variation of ac susceptibility with increase in temperature indicates the normal ferrimagnetic behavior of the system. The system has multidomain structure.
- The Curie temperature decreases with increase in the Cr^{3+} in the composition.
- The dc resistivity decreases with increase in Cr^{3+} content in the composition.
- The behavior of the system changes from ferrimagnetic to paramagnetic at a particular temperature.
- Thermoelectric - power study exhibits that both n-types and p-types of charge carriers are responsible for charge transport and the drift mobility causes the conduction.
- The dielectric constant increases with Cr^{3+}content initially and later on decreases where as the dielectric loss factor increases with increase in the Cr^{3+}content initially and decreases with increase in Cr^{3+}content. Both tanδ and dielectric loss increase with increase in the temperature.

REFERENCES

1. R. W. G. Wyckoff, crystal structure,Vol. 2 p. 75 Interscience, New York (1964)
2. G.M. Bhongale et al ,Bull. Mater.Sci.Vol. No2, (1992) PP 121-125
3. S. A. Mazen, M. H. Abdalla , R. I. Nakhla ,H. M. Zaki andF. Metawe , Bull. For sci. zagzig Uni. 13 (1991) 344
4. S. A. Mazen M. H. Abdulla , B. A. Sabrah andH.A.M.Hashem Phy. Status Solidi A134 (1992) 263
5. V. M. Goldschmidt, International Tobellen Zur Bestimmug Van Crystallstrukture.
6. A. K. Ghatage , S. C. Choudhari, S. A. Patil ,S. K.ParanjpeJ. Mate. Sci. Letters 15 (1996) 1548
7. B. D. Cullity, Element of x-ray diffraction(Addison Wesley Press reading Mass) (1959) p. 86
8. B. D. Cullity, Element of x-ray diffraction (Addison Wesley Press reading Mass) (1959) p. 99
9. M. J. Burger Crystal Structure Analysis, Wiley New York (1960)
10. H. Furuhashi et al ,J. inorg. Nucl. Chem. Vol.35 (1973)pp3009-3014 Pergamon Press, Printed in Great Britain.
11. E. F. Bertaut, C. r. hebd Seanc. Acad. Sci.Paris230, (1950) 213
12. E. F. Bertaut, J. Phys. Rad. 12,252 (1951)
13. R. K. Datta, R. Roy J.Am. Cerm. Soc. 56(1967) 578

14. Ohnishi & Teranishi, T. J. Phys. Soc. Jpn.16 (1961) 36
15. R.D.Waldron, Phys Rev. 99(1955) 1727
16. Preudhome J.P. Tarte, Spectrochim Acta. 28A(1972) 69
17. A.K.Ghatage et al. J. of Material Sci. Letters 15 (1996) 1548-1550
18. J.N.Smith, Magnetic properties of materialsMcGraw Hill, New York.
19. L. Neel, Ann. Phys. 3(1948) 137
20. Urvie , Chhaya, Bimal S. Trivedi, R. G. KulkarniPhysica B 262 (1999) 5-12
21. R. Satyanarayan and S. Raman Murthy,J. Mat. Sci. Lett. 4(1965)241
22. S.A.Plotinnikov and G.M.PrikhodkineSov. Phys. Solid State7(1965)241
23. C.P.Bean J. Appl. Phys. 26 (1955) 1381
24. L.G. Van Uitert, Proc. IRE,44(1956) 1294
25. EJ.W. Verwey and J.H.de Boer,Recl. Trav. Chim. Pays Bas. 55(1936) 53
26. E.W.Gorter, Philips Res. Rep. 9 (1954)4 27
27. F.C. Romeijn ibid 8 (1958) 304
28. A.Marais, T.Merceron, G. Maxim and M. Porte,C.R.Acd. Sci. B(France) 274 (1972) 8
29. M.A.Shamanev, P.P.Kirichok, N.D.Kazvini andD.E. Bondarev, Sov Phys.Dokl. 20(1975) 291
30. A.R.Mackintosh, Phys Rev. Lett. 9 (1962) 90
31. P. V. Reddy & T. S. Rao , Phys. Stat. Soli. Stat. Sol.9(a)92,303 (1985).
32. P. V. Reddy V. D. Reddi and D. RavinderPhy. Stat. Sol. (a) 127-439(19991)
33. Jonker, J. Phys. Chem. Solids , 9, 165(1959)
34. S.C.Watawe et al. J.of Mate. Sci. Magn. Mate.214 (2000) 55-60
35. K.J.Standley , Oxides Magnetic Materials,Clarendon Press Oxford (1972) p 140-147
36. B. Vishwanathan and V.R,K MurthyFerrite Materials Sci. and Technology, Springer-VerlagNarosa Publishing House (1990) p 58-64
37. K. Iwauchi J. Appl. Phys. 10 (1971) 520
38. N. Rezlescu and E. Rezlescu Phys. Stat.Solidi (a) 23 (1974)
39. L.I.Ranin , Z.i.Novikova, Ferrites Mansik, (1960) 146
40. C.G. Koops, Physical Rev. Vol.83, No.1 (1951)
41. R.P.Mahajan et al. Bull. of Material Sci. Vol. 23 NO 4(2000) pp 273-279

ABOUT THE BOOK

Finely tuned electrical and magnetic properties are the goal of all materials scientists. More energy efficient electronic devices, better performing hybrid electrical vehicles and smarter data storage devices are among potential applications for suitable material. Spinel ferrites possess the crystal structure of the natural spinel MgAl2O4. This structure is particularly stable, since there is an extremely large variety of oxide which adopt in fulfilling the conditions of overall cation to anion ratio of 3/4. Mixed magnetic oxides have fascinating properties with coexistence of ferrous and ferric cations in coordination with various cation combinations through stochiometric. The spnel structure is able to form an extremely wide variety of total solid solutions. It means the composition of a given ferrite can be strongly modified, while the basic crystalline structure remains the same. Present book introduces the method and techniques for synthesis and characterization of mixed magnetic oxides having spinel structure. Mixed magnetic oxides are basically spinel ferrites having specific stoichiometry and compositions of different cations, which is stable and has extremely large potential of variety of oxides depending on cations and cation distributions among octahedral and tetrahedral sites. The book presents study of two solid solutions, Ni0.7Mg0.3AlxFe2-xO4 and Ni0.7Mg0.3CrxFe2-xO4 .

The book has four chapters. First chapter introduces the basic structure and compositions sensitive properties of mixed magnetic oxides having spinel structure along with background of development in study of spinel ferrites. The second chapter presents information about spinel structure and ferrimagnetism. The third chapter is regarding experimental techniques and characterization of the mixed magnetic oxides. The last and fourth chapter gives systematic analysis of material properties achieved by the solid solutions under investigation. Thus the book is intended to introduce the most fundamental things required for the synthesis and characterization for solid solutions of mixed magnetic oxides in order to develop research interest. Hope the book will be useful for beginners, students, teachers and researchers.

Empyreal Publishing House

ISBN 978-81-944069-6-9